THE UNIVERSITY OF CALGARY

Physical and Rheological Characterization of Selected Paving Asphalts

by

Deepak Kumar Jhanwar

A THESIS

SUBMITTED TO THE FACULTY OF GRADUATE STUDIES

IN PARTIAL FULFILLMENT OF THE REQUIREMENTS FOR THE

DEGREE OF MASTER OF SCIENCE IN CHEMICAL ENGINEERING

DEPARTMENT OF CHEMICAL AND PETROLEUM ENGINEERING

CALGARY, ALBERTA

APRIL, 1998

Abstract

A study was performed to compare the current empirical test based Canadian specification and performance-based SUPERPAVE™ specification of paving asphalt. The compliance of currently used materials in Canada to the scenario when performance-based specification is implemented was also studied. Asphalts of varying consistency were derived from Cold Lake, Bow Valley and Redwater crude oils. The properties of prepared samples were compared with the present specification and SUPERPAVE™ requirements.

The results indicate that even the highest quality conventional asphalt can meet the 98% reliability requirements only in coastal areas of Canada. The 50% reliability requirements can be met by good quality conventional asphalts in the belt along the Canada-US border. In higher latitudes and extreme cold climate, modification of asphalt will be required.

The rheological characterizations of selected Cold Lake and Redwater asphalt samples were made from the dynamic mechanical analyses. Differences in their rheological behaviors were observed, which explain the differences in their performance as predicted by SUPERPAVE™ specification.

Acknowledgements

The author wishes to express his gratitude to Dr. Ludo Zanzotto for his support and encouragement in supervising the project. His contagious enthusiasm is responsible for much of this work.

Thanks also to Dr. J. Stastna for his guidance and assistance in the rheological work. His continuous interest in the project and for his suggestions and criticism during the course of the study is appreciated.

Special thanks goes to Dr. Peter Fransham for the preparation of the final project report. Thanks also to Susanna Ho for providing the chromatography data. The help of Zuzana Forgac and other colleagues at Bitumenous Material Laboratory in the testing of asphalts is also appreciated.

A special appreciation goes to Dr. Anil Kumar Mehrotra for his general advice and support.

I express a deep sense of gratitude to my parents, Shri Raghunath and Shrimati Suryakanta; to my brothers, Sushil and Venu; and to my love Tripti for their love, encouragement, support and sacrifice.

Also thanks to all friends and fellow graduate students, especially Amit Bhargava, Kunal Karan, Christie Liu, Priti Singh, Rajesh Jakher, Rajneesh Kumar, Simant Upreti, and Subobhsen Penamanu who made my stay here in Calgary lively and cheerful.

Financial Support by National Sciences and Engineering Research Council and Husky Oil is gratefully acknowledged.

Dedicated to My Beloved Country India

TABLE OF CONTENTS

LIST OF TABLES

LIST OF FIGURES

LIST OF SYMBOLS

a (T)	Time-Temperature Shift Factor
a_1	Parameters of Equation 5.1, °C/dmm
a_2	Parameters of Equation 5.1, °C
b_1	Parameters of Equation 5.3, Pa.s/dmm
b_2	Parameters of Equation 5.3
c_1	Parameters of Equation 5.4, Pa.s/dmm
c_2	Parameters of Equation 5.4
d_1	Parameters of Equation 5.5
d_2	Parameters of Equation 5.5
k	MWD Calibration Parameter
m-value	Rate of Change of Creep Stiffness, Pa/s
m, n	Number of Parameters in Equation 6.10
t	Time, sec
C_1	WLF Equation Parameter
C_2	WLF Equation Parameter, K
G'	Storage Modulus, Pa
G"	Loss Modulus, Pa
G*	Complex Modulus, Pa
E_a	Activation Energy, J/kmol
$Pen_{25°C}$	Penetration at 25°C, decimillimetre
R	Ideal Gas Constant, J/kmol-K
S	Stiffness, MPa
T_{high}	Highest Service Temperature, °C
T_{low}	Lowest Service Temperature, °C
T_d	Reference Temperature in WLF and Arrhenius Equation, K

Greek

α	MWD Calibration Parameter

η	Viscosity, Pa.s or mPa.s
$\eta_{60°C}$	Viscosity at 60°C, Pa.s
$\eta_{135°C}$	Viscosity at 135°C, mPa.s
η^*	Complex Viscosity, Pa.s
γ^*	Complex Shear Strain, 1/s
λ,μ	Relaxation Time, s
ν	Kinematic Viscosity, mm^2/s
τ^*	Complex Shear Stress, Pa
ω	Frequency, rad/s or Hz

Italic

i	Square Root of (-1)

Abbreviation

AET	Atmospheric Equivalent Temperature, °C
CL	Cold Lake
BV	Bow Valley
RW	Redwater

CHAPTER 1
Introduction

Asphalt is perhaps the first thermoplastic engineering material ever used. The area between Euphrates and Tigris rivers contains the earliest deposits of asphalt. Around circa 6,000 B.C., Sumerians were using asphalt as a waterproofing material in their shipbuilding industry. At the same time asphalt was used for road construction as well as a waterproofing sheet in temple baths and water cisterns. In the modern history, the first asphalt mastic pavement was laid at Pont Royal, Paris in 1835.

In modern times, travel by automobile using asphalt pavements has become by far the fastest growing means of transportation, giving an impetus to the economic development. It is estimated that the production of asphalt in the western world amounts to over 100,000,000 t/year. The total consumption of asphalt in Canada in 1992 amounted to 2.56 million tons. From these amounts, about 86 percent was used in road construction industry, the rest in roofing and other special applications. The demand for asphalt has been ever growing. Presently Canada has 880,000 km of roads, of which 280,000 km have paved surface. Annual expenditures on Canada's roadway infrastructure are currently about $10 billion. It is estimated that in order to maintain the existing infrastructure in an acceptable state, about twice that amount would be necessary (Zanzotto, 1996). The paving asphalt requirement in US is about ten times higher to that in Canada.

Asphalt is a complex material in its chemical composition as well as thermo-mechanical behavior. Even though it has contributed a lot to the advancement of the modern civilization, it did not get attention of researchers till the last quarter of the twentieth century and amount of research done in this field is relatively limited. The research on asphalt and its classification for commercial purposes in the first half of this century

relied exclusively on the system of conventional tests. Even though experienced engineers could, with the help of these tests, orient themselves in matters of the use and quality of asphalts, progress in the area of research after World War II contrasted more and more with the majority of conventional tests, both by methodology and insufficient empirical description of the required asphalt properties. It is interesting to note that most of the currently used grading systems for paving asphalt in North America as well other parts of world are based on the conventional and empirical tests which are inadequate in describing the property of asphalt and determining the expected performance of the pavements.

The currently used empirical tests are exposed to critique regarding their meaning and interpretation. As a result of this critique, there is a growing demand to classify asphalts by exact tests and to provide results in physical units. Both, paving asphalt manufacturers and users have felt the requirement for a rational system for the asphalt property evaluation as well as classification and selection.

Strategic Highway Research Program (SHRP), funded by US Federal Government, is the largest and most ambitious research effort on these lines. A primary area identified for research was asphalt and asphalt concrete due to an increasing number of premature pavement failures. The SUPERPAVE™ system is the ultimate final product of SHRP asphalt research program, in which new performance-based testing and classification method for asphalt has been developed. The property of asphalt is evaluated from the rheological measurements from which it is possible to determine the expected performance of the pavement when the asphalt is used. The asphalt is classified based on the performance achievable by asphalt sample and selected as per the required pavement performance for a location.

The SHRP performance graded specification system is still being studied and debated. The empirical based viscosity and penetration grading systems have been in place for many decades and while the performance based SHRP system is a fundamental improvement, there is resistance to embrace an unproven method. Since conventional asphalt binders manufactured from existing crude sources will essentially remain the same, the transition from currently used specification to the performance-based specification system entails a number of changes that need to be understood.

It is a matter of time when the SUPERPAVE™ system will be embraced by the Canadian Federal/Provincial Governments as well as the paving industry. This will change the picture of the asphalt use in Canada. The purpose of my study is to compare the present and SHRP specifications and to help in understanding the transition. The study will also help in understanding the impact of this switch over on Canadian paving industry.

CHAPTER 2

Objectives and Methodology

2.1 Objectives

The main objective of this study is to understand the transition from currently used empirical grading system of paving asphalt to the performance-based SUPERPAVE™ specification system and the compliance of the conventional asphalt in the new scenario for Canada. The study constitutes of the following two focus areas:

1. Empirical and Performance-Based Characterization (Chapter 3, 4 and 5)
2. Rheological Characterization (Chapter 6)

The objectives of each part are mentioned as follows :

2.1.1 Empirical and Performance-Based Characterization

- Evaluation of the SUPERPAVE™ Performance Grades requirement across Canada
- Expected SUPERPAVE™ Performance Grades from the currently used asphalt in Canada
- Transformation from empirical to performance-based specification system
- Compliance of the currently used material

2.1.2 Rheological Characterization

- Studying the rheological behavior of two asphalt samples graded as 'excellent' and 'poor' material by SUPERPAVE™ specification

- Explore the possible reasons for the difference in their service performances as reflected by SUPERPAVE™ testing
- Determination of molecular weight distribution from the rheological measurement to relate its performance with the internal structure

2.2 Methodology

The following methodology was used for the empirical and performance-based characterization of the paving asphalts used in this study. Each step is discussed in detail in its respective sections.

- Selection of crude oils for the preparation of asphalt samples
- Preparation of asphalt samples by distillation of crude oils
- Binder characterization and evaluation from empirical and performance-based tests
- Comparison of conventional and SHRP grades for the prepared asphalt samples
- Determination of expected SHRP grades of the asphalts derived from the studied crude oils from their Canadian General Standards Board (CGSB) grades
- Determination of the SHRP grades required for the various locations across Canada
- Comparison of the CGSB and SHRP grades
- Study the compliance of the asphalts derived from the crude oils used

The methodology used for the rheological characterization is mentioned in brief as follows:

- Selection of asphalt samples
- Measurement of complex modulus at different temperatures and frequencies
- Generation of master curve for the components of complex modulus
- Modeling of complex modulus

- Comparison of complex modulus
- Determination of the molecular weight distribution

CHAPTER 3
Asphalt Behavior and Grading System: A Background

3.1 Viscoelastic Behavior of Asphalt Binder

Asphalt binders are viscoelastic in nature, and hence their behavior depends on both temperature and rate of loading. In pavement service, the asphalt is subjected to the varying ambient temperature and loading pattern. The effects of time of loading and temperature on the deformation of asphalt are related; the behavior at high temperature over short time periods is equivalent to what occurs at lower temperatures and long loading time. This is often referred to as the time-temperature shift or superposition concept and has been discussed in detail in the latter part of this report. The behavior of asphalt at different temperatures is discussed in the following sections.

3.1.1 Low Temperature Behavior

In cold climates or under rapidly-applied loads, asphalt behaves like an elastic solid. Elastic solids deform when they are loaded, and when unloaded, they return to their original shape.

The elastic solid like behavior is shown in Figure 3.1a. On application of constant stress or creep load in between time t_0 and t_1, asphalt gets deformed and developed strain is directly proportional to stress. On removal of stress at time t_1, the material regains its initial shape instantaneously. If stressed beyond material capacity or strength, elastic solids may break. Asphalt as an elastic solid at low temperatures may become too brittle

and crack when excessively loaded. For this reason, low temperature cracking sometimes occurs in asphalt pavement during cold weather.

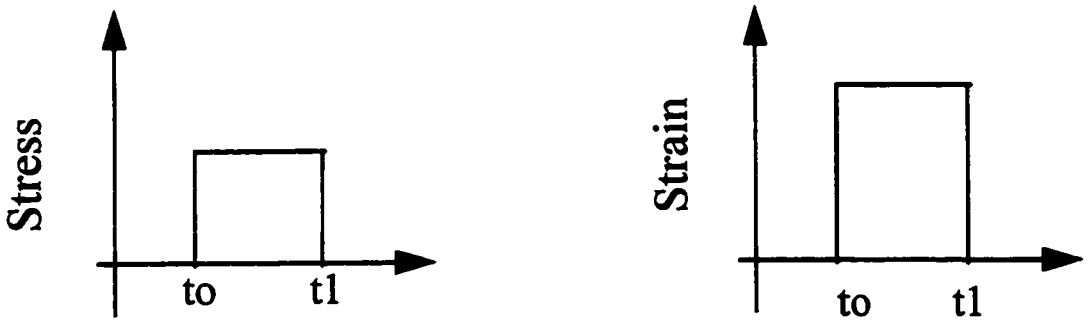

Figure 3.1a : Stress-Strain Relationship for Elastic Body

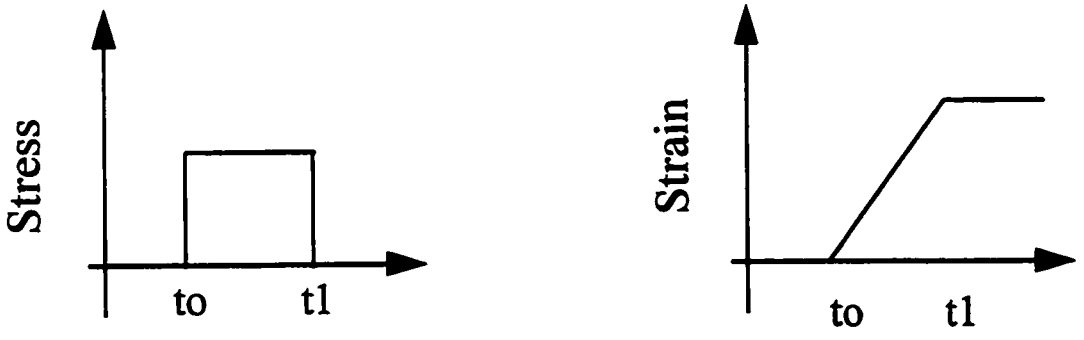

Figure 3.1b : Stress-Strain Relationship for Viscous Material

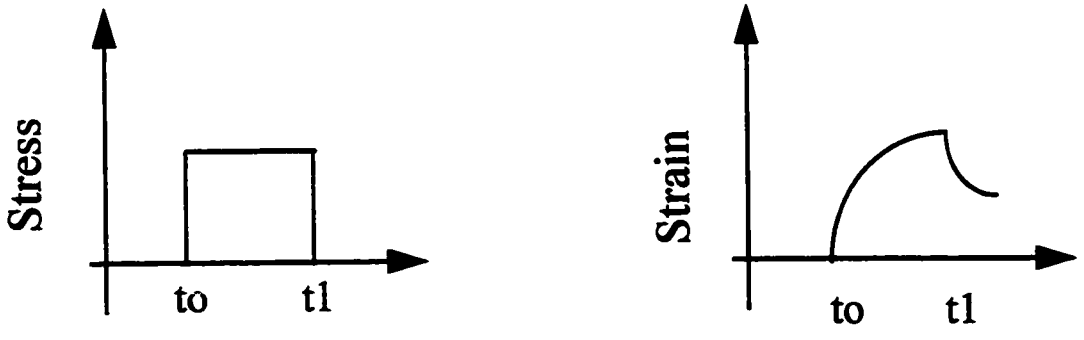

Figure 3.1c : Stress-Strain Relationship for Viscoelastic Material

3.1.2 High Temperature Behavior

At high temperature or under sustained loads, asphalt acts like a viscous liquid. In these conditions, asphalt will deform at a constant rate when the load is applied at t_0, and will continue to deform at that rate until the load is removed, at that point there is no further deformation. The viscous behavior of asphalt is shown in Figure 3.1b.

It is interesting to note that asphalt binder at high temperatures (approximately at temperatures higher than 60°C) can be characterized as newtonian fluid. The stress-strain relationship for the shear of a Newtonian fluid is defined as :

$$\text{Shear Stress} = \text{Coefficient of Viscosity} \times \text{Rate of Shear Strain} \qquad (3.1)$$

Viscous liquids like hot asphalt are sometimes called plastic because once they start flowing, they do not return to their original position. This is why in hot weather, some less stable hot mix asphalt pavements flow under repeated wheel loads and rutting in the pavement is caused.

3.1.3 Intermediate Temperature Behavior

Most environmental conditions lie between the extreme hot and cold situations. In these climates, asphalt binders exhibit the characteristics of both viscous liquids and elastic solids and hence their behavior is termed viscoelastic.

In this case, as shown in Figure 3.1c, the asphalt shows both elastic and viscous components of response. When loaded in creep, there is an immediate deformation, corresponding to the elastic response, followed by a gradual time-dependent deformation. This time-dependent deformation may further be divided into a purely viscous component

and a delayed elastic component. Upon removing the load at t_1, the viscous flow ceases and none of this deformation is recovered. The delayed elastic deformation is, however, recovered, but not immediately as with pure elastic deformation. Instead, once the load is removed, the delayed elastic deformation is slowly recovered, at a decreasing rate, as shown in Figure 3.1c.

On application of infinitesinal sinusoidal or oscillatory shear stress on asphalt binder, the resulting shear strain is also oscillatory (Figure 3.2). Both, the viscous and elastic behavior of the binder is characterized by measuring the complex shear modulus (|G*|) and the phase angle (δ). |G*| is a measure of the total resistance of a material to deformation when exposed to periodic sinusoidal shear stress and is calculated as the ratio of total shear stress to total shear strain. The phase angle is an indicator of the relative amount of recoverable and non-recoverable deformation, and is calculated from the time lag between the applied stress and resulting strain. The phase angle is zero for the elastic body and 90° for the viscous liquid.

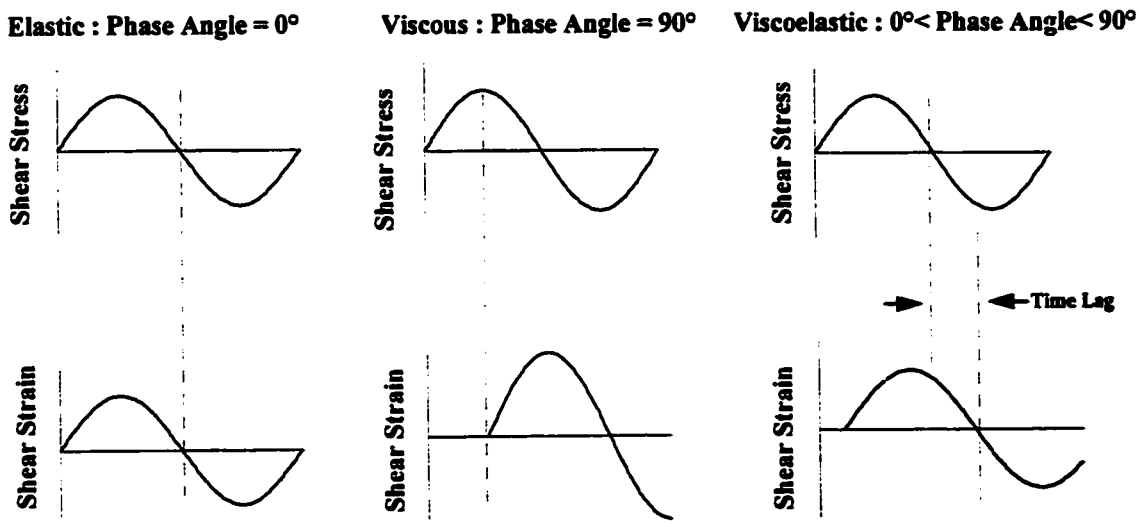

Figure 3.2 - Shear Stress-Strain Response in Oscillatory Experiment

As discussed in Section 3.1.1, pavement in the service is vulnerable to change in temperature and loading pattern. Age hardening of asphalt binder is another factor which is responsible for the deterioration in the performance of pavement. Age hardening is caused by the loss of volatile material during hot-mix operation and oxidation of asphalt by the oxidants present in environment during service in pavement.

For the characterization of asphalt, it is necessary to evaluate the properties which affect the performance of asphalt in pavement. The currently used specifications of asphalt in North America are based on the empirical tests which fail to describe the performance of asphalt and to predict its service life. The development of empirical specifications and their shotcomings are discussed in the next section.

3.2 Empirical Grading

The need for fundamental research on the properties of asphalt and classification of asphalt in different grades is not new and dates back to as early as beginning of this century. Specifications for asphalts were introduced around the year 1900. At the beginning, the specifications were on a local basis and there were broad differences between the requirements. The key parameter for specifying different grades of asphalt was penetration number, which is still found in almost all currently used specifications. In USA in 1923 there were 88 different penetration limits (Zanzotto 1996). In 1926, the producers and users agreed on 10 penetration grades of road asphalt. The selected grades included asphalts from the penetration 20 decimillimetre (dmm) to 200 dmm. This was the beginning of the system of classification of asphalt according to penetration. The specifications also included other tests like softening point, ductility etc.

In penetration based specifications, all asphalt grades were classified according to penetration and softening point. These values only represent characteristic data, indirectly derived from viscosity, which are determined under special empirical procedures and conditions. The penetration number gives an idea of hardness or consistency of asphalt. Ease of carrying out this test made it popular among producers and users.

As the results of test for penetration number do not represent any physical property, efforts were made to develop specification based on physical tests. Classification of asphalt based on viscosity was a major step towards this process and such specifications are still popular. Under these specifications, penetration of the sample is also measured but it is classified according to its viscosity at a specified temperature. Most of the currently used spacifications such as Canadian General Specifications Board (CGSB) specification, Alberta specification etc. characterize the asphalt binder on the basis of both penetration and viscosity. The limits of the grade in these specifications are determined by penetration.

Since much of the research on the asphalt and classification of the asphalt in the past has relied on tests such as penetration and capillary viscometry, and related temperature susceptibility parameters, it is desirable to review these methods. These methods are not adequate for fully defining the linear viscoelastic properties which are needed to relate asphalt chemistry, physical properties and performance with each other. More importantly, these empirical tests have failed to developed a performance-based specifications (Petersen et. al. 1994a, Superpave 1995).

Penetration-based, CGSB and Alberta specification for the paving asphalt are discussed in Appendix A. A review of the shortcomings of the tests involved in these specifications is presented in the following section.

3.2.1 Penetration Test

The penetration test indicates the stiffness of the asphalt, but any relationship between asphalt penetration and performance has to be gained by experience. A drawback of the empiricism is that the relationship between the test and performance may not be very good. Another limitation of penetration test is that it does not give information for the entire range of typical pavement temperatures. Penetration test at 25°C describes only consistency at a medium temperature, whereas the lower temperature elastic behavior cannot be realistically determined from these data to predict low temperature performance.

3.2.2 Viscosity Measurement

The rheological properties of asphalt vary significantly at the temperatures encountered during handling, mixing, paving, and in service. The external load of traffic also causes the deformation of asphalt and asphalt-aggregate mix. At the pavement service temperatures higher than 60°C, and at mixing and compaction temperatures, unaged asphalt generally behaves as a newtonian fluid (Superpave 1995, Anderson et. al. 1991, Van der Poel 1954). At these conditions the binder can be properly characterized by capillary viscometry. But the aged binder even at the higher range of pavement service temperatures, shows significant non-newtonian behavior, so capillary viscometry is less applicable in that case (Puzinauskas 1979).

Many researchers (Romberg et. al. 1947, Moavenzadeh et. al. 1965, Griffin et. al. 1956) have used steady-state creep measurements to calculate the coefficient of viscosity for asphalt at intermediate pavement service temperature, in the range of 0-25°C. To conduct such a measurement, it is necessary to apply a shear stress to the asphalt until the strain rate becomes constant. Time necessary for the delayed elasticity to be expended and for

steady-state to occur may be so long that very large strains will likely result, causing geometric non-linearity. At temperatures between ambient and 60°C, most paving grade asphalts, even when loaded in the linear range, exhibit significant delayed elasticity, and strain rate varies with loading time.

Delayed elasticity and geometric nonlinearity are often either confound or have gone unrecognized by many researchers, causing them to apply nonlinear representations to the stress-strain behavior of asphalt. The testing is generally conducted in the nonlinear region, and the delayed elastic response exhibited by the asphalt is either not considered or considered as a nonlinear effect. These problems advocate against the use of viscosity measurement to characterize asphalt.

3.2.3 Temperature Susceptibility Parameters

Temperature susceptibility is defined as the change in consistency, stiffness or viscosity of a material as a function of temperature and is usually quantified through parameters calculated from consistency measurement made at two different temperatures. Asphalt pavements, and hence asphalt binders, are subjected to a wide range of temperatures in the service. Because many of the problems observed in pavements clearly result from the large temperature dependent changes in consistency, temperature susceptibility parameters have been frequently proposed as a means of characterizing paving-grade asphalt. However, there are major problems in analyzing and interpreting such parameters.

The various temperature susceptibility parameters which have been used to classify asphalts are all empirically derived and are simply indicators of how rapidly the consistency of a given asphalt changes with temperature. The widely used temperature

susceptibility parameters are a) Penetration index (PI); b) Penetration-viscosity number (PVN); and c) Viscosity-temperature susceptibility (VTS).

The empirical methods which have received the most attention are perhaps the PI and PVN. The PI was first postulated by Pfeiffer and Van Doormaal (1936) and was later used by Van der Poel (1954) in the development of a nomogram for predicting the stiffness of asphalt using routine test data. The PI is calculated based on the change in penetration with temperature. These researchers recognized the confounding of time and temperature effects that was inherent in the calculation of PI or PVN. To further complicate the matters, the rheological properties and temperature dependence change with aging. Hence, the PI values change with aging, but the PVN parameter, developed by McCleod (1972) appears to remain unchange with aging. In the case of PVN, the penetration at 25°C is used along with viscosity data to calculate its value.

Viscosity-temperature susceptibility (VTS) was defined using capillary viscometry measurements at 60°C and 135°C. For unaged unmodified asphalt, flow behavior over this temperature range is essentially Newtonian and independent of time of loading, therefore the VTS will in many cases accurately characterize temperature dependence above 60°C. However this parameter cannot be extrapolated to describe behavior at lower temperatures, where the delayed elastic properties of the asphalt become significant.

As the rheological properties of asphalt are functions of both loading time and temperature, temperature-susceptibility parameters must be based on measurements at different temperatures but similar loading times. Unfortunately, no commonly used temperature-susceptibility parameter meets this criterion. Furthermore, the application of the results from the empirical tests for calculation of these parameters makes them questionable.

3.2.4 Nomographs and Their Inadequacies

The nomographs developed by various researchers offer a mean of calculating the stiffness of asphalt at various temperature and loading time. The first nomograph for this purpose was developed by Van der Poel in 1954 using PI which was later updated and revised by McCleod (1972) to accommodate penetration and viscosity measurement. These nomographs provide reasonable estimates of asphalt stiffness at temperature above ambient temperature but the estimates provided by these nomographs may be in considerable error at lower temperatures and longer loading times (Petersen 1994a). Given the poor reliability of these nomographs, a more direct measurement of low-temperature stiffness was sought.

3.2.5 Aging Index

The control of premature aging is an important specification function, and aging index, either directly or indirectly, have traditionally been used for this purpose. Commonly used single point aging index which is calculated by dividing aged by unaged viscosity, can effectively describe the increase in stiffness when the response is essentially viscous. Such single point aging index will not always accurately reflect changes in stiffness at low temperatures, where delayed elasticity is a significant portion of the response.

As with temperature susceptibility, a single point aging index is insufficient to characterize the rheological changes that occur with aging. An aging index based on stiffness at a selected temperature and loading time will vary with the temperature and loading time chosen and will differ numerically from an aging index based on viscosity. More properly, the effect of aging on hardness and temperature dependence should be described by direct measurement of the rheological properties.

3.2.6 Need for Performance Related Properties for Use as Specification Criteria

Traditional methods of rheological characterization of asphalts include capillary viscometry, penetration measurements, ductility test and the determination of the softening point temperature. The last three methods are unacceptable for a rational characterization of viscoelastic behavior as they are completely empirical. Capillary viscometry, although a rational test method, does not provide information on the time dependence of the properties of asphalt. Temperature-susceptibility parameters as they are calculated from penetration, softening-point and viscosity data, are not rational indicators of rheological behavior. These parameters have additional shortcoming of confounding time and temperature effects which makes a complete and accurate description of viscoelastic behavior impossible with their use. Rational measurements and parameters that accurately describe the time and temperature dependence of the stress-strain response of asphalt are needed to develop an effective performance based specification.

Moreover, the rheological properties of asphalt below 60°C cannot be described by either penetration test or the ductility test because the stress fields within the test specimens cannot be defined, the strains developed during the test are very large and vary within the test specimen and the stress and strain fields cannot be easily modeled or calculated. Thus the continued use of these tests in performance based specification is undesirable and need to be replaced by more fundamental tests that can be used to define a rational rheological model for temperature ranging from 60°C to as low as -40°C and sometime even lower.

Current specifications for asphalt used in the United States of America and Canada are based on either viscosity grading or penetration grading. Both specification methods are limited by the penetration test, an empirical test that provides limited rheological

information. The viscosity-grading system is also limited in its control over low-temperature properties, since the grading is done at 60°C. To fully control the potential performance of an asphalt, the mechanical properties over the entire range of temperatures to which pavements are subjected must be accurately measured and specified.

3.3 SHRP Grading Considerations

3.3.1 Development of New Test Methods and Specification

In the spring of 1987, the United States Congress passed legislation which provided $150 million (US) over five years for the Strategic Highway Research Program (SHRP), the largest and most ambitious highway research effort ever undertaken in the United States. A primary area identified for research was asphalt and asphalt concrete due to an increasing number of premature asphalt pavement failures. This created an awareness of the need for a well funded research effort to develop improved asphalt binder and asphalt-aggregate mixture specifications with an aim to remove the short-comings of current specifications as mentioned in previous section. Planning for this highly focused research effort began in 1983 and was developed under the guidance of the American Association of State Highway and Transportation Officials (AASHTO), the Transportation Research Board (TRB) and the Federal Highway Administration (FHWA) (Special Report 202 1984, SHRP 1986).

The authors of Transportation Research Board (TRB) Special Report 202 (1984) identified the objective of the SHRP asphalt program as:

"To improve pavement performance through a research program that will provide increased understanding of the chemical and physical properties of asphalts and asphalt concrete. The research results would be used to develop specifications, tests,.... needed to achieve and control the pavement performance desired".

In 1991, the term SUPERPAVE™ was coined to signify the integration of performance-based specifications, test methods, equipment, testing protocols and a mixture design system. As a result, the SUPERPAVE™ system became the ultimate final product of SHRP asphalt research program. The initial work plan (SHRP 1986) for the research program addressed the fundamental chemical and physical properties of asphalt and their relationships to asphalt-aggregate mixture performance. Specific research topics were identified for consideration. From this initial development, the program was expanded and contracting plans which combined similar research topics were prepared. The resulting research contracts are shown in Table3.1.

Table 3.1: Research Contracts for SHRP

CONTRACT NO.	TITLE
A-001	SHRP Asphalt Program: Technical Direction and Specification-AAMAS Development
A-002 A	Binder Characterization and Evaluation
A-002 B	Novel Approaches for Investigating Asphalt Binder
A-002 C	Nuclear Magnetic Resonance Investigation of Asphalt
A-003 A	Performance-Related Testing and Measuring of Asphalt - Aggregate Interaction and Mixtures
A-003 B	Fundamental Properties of Asphalt-Aggregate Interaction Including Adhesion and Absorption
A-004	Asphalt Modification Practices and Modifiers
A-005	Performance Models and Validation of Test Results

To satisfy the objectives of the A-002A project, the researchers were required to identify the distress mechanisms that are critical to field performance, select and develop material response parameters that relate to the critical distress mechanism and incorporate these response parameters into specification type test methods and specification criteria. The following distress modes were considered (Anderson et. al. 1990):

- Aging
- Plastic deformation or rutting
- Low-temperature thermal shrinkage cracking
- Thermal fatigue
- Load-associated fatigue cracking

3.3.2 Consideration of Aging in Specification

The criteria in a true performance-based specification must be representative of the material in the pavement. Aging or hardening of asphalt occurs during the mixing and laydown process and during service. The existing aging methods, the thin film oven test (TFOT) and the rolling thin film oven (RTFO) test can simulate the aging during construction only.

To simulate long-term field aging, the pressure-aging vessel (PAV) test was adopted. This test has been used by other researchers and has been modified for the new SHRP binder specification (Kim et. al. 1987). Unfortunately, no correlation between PAV and field aging has been yet developed and it is largely assumed that the PAV represents 5-10 years of aging in service.

3.3.3 Consideration of Rutting in Specification

Rutting in the upper pavement layers is caused by the accumulated plastic deformation in the mixture that results from the accumulation of non-recoverable component of the response to the repeated application of traffic loading at higher service temperatures. Although the rutting tendencies of a pavement are influenced primarily by aggregate and mixture properties, the properties of binder are also important. Because rutting is more prevalent at high temperatures than at the intermediate or low temperatures, the properties related to the rutting should be measured in the upper range of pavement service temperatures. The SUPERPAVE^{TM} specifications defines and places requirements on a rutting or deformation factor, $|G^*| / \sin \delta$ measured at a fixed frequency of 10 rad/s, which represents a measure of the high temperature stiffness or rutting resistance of the asphalt binder. The value of $|G^*| / \sin \delta$ must be minimum of 1.00 kPa for the original binder and 2.20 kPa after aging the binder using the RTFO procedure. The details of measurement of $|G^*| / \sin \delta$ for the asphalt binder will be discussed in the next chapter.

3.3.4 Consideration of Thermal Cracking in Specification

Thermal shrinkage cracking is a serious problem in much of the northern United States and in most of Canada. When the pavement temperature decreases asphalt concrete shrinks. Since friction against the lower pavement layer inhibits movement, tensile stresses build-up in the pavement. When these stresses exceed the tensile strength of the asphalt mix, a low temperature crack occurs. Cracking may result from a single temperature excursion to the critical cracking temperature or from repeated cycling to somewhat higher temperature. The concept of critical temperature below which cracking will occur as a result of a single cooling cycle has led to the definition of a limiting stiffness temperature (Haas et. al. 1969, Monismith et. al. 1965). According to this concept, when the asphalt binder reaches a critical stiffness value, cracking should result.

In SUPERPAVE™, the bending beam rheometer is used to apply a small creep load to a binder beam specimen and measure the creep stiffness. If the stiffness is too high, the asphalt will behave in a brittle manner, and the cracking is more likely to occur. To prevent this cracking, creep stiffness has a maximum limit of 300 MPa after 4 minutes of loading. Since low temperature cracking usually occurs after the pavement has been in service for quite some time, the sample of binder for testing is used after aging in RTFO and PAV. This method has been discussed in detail in the next chapter.

3.3.5 Consideration of Fatigue in Specification

The selection of specification criteria to ensure satisfactory resistance to fatigue cracking is perhaps the most difficult challenge presented by the new specification. Fatigue cracking generally occurs late in the life of a pavement, requiring the testing of asphalt that is appropriately aged to simulate the long term in situ properties of the binder.

The asphalt binder specification criteria for fatigue is the loss modulus ($G'' = |G^*| \sin\delta$) . Since fatigue generally occurs at low to moderate temperatures after the pavement has been in service for a period of time, the specification addresses these properties using binder aged in both, RTFO and Pressure Aging Vessel (PAV). The binder specification has a maximum value of 5000 kPa for $|G^*| \sin \delta$. Low values of $|G^*|$ and δ are considered desirable attributes from the standpoint of resistance to fatigue cracking. This criteria has been doubted by researchers and the fatigue parameter is now being revised.

3.4 SUPERPAVE™ Specification

The central theme of the Superpave binder specification is its reliance on testing asphalt binders in conditions that simulate the three critical stages during the binder's life. Tests

performed on the original asphalt represent the first stage of transportation, storage and handling. The second stage represents the asphalt during mix production and construction and is simulated for the specification by aging the binder in a Rolling Thin Film Oven. This procedure exposes thin binder films to heat and air and approximates the aging of the asphalt during mixing and construction. The third stage occurs as the binder ages over a long period as part of the hot mix asphalt pavement layer. This stage is simulated for the specification by the pressure aging vessel. This procedure exposes binder samples to heat and pressure in order to simulate years of in-service aging in a pavement.

The aging and test procedures are summarized in Table 3.2.

As per SUPERPAVE™ specification, the paving asphalt is graded on the basis of the highest and lowest temperatures up to which that material can be used. The highest temperature is determined by the dynamic shear test and the lowest temperature is determined by bending beam test. A unique feature of this specification is that the specified criteria remain constant for all of the performance grades (PG), but the temperature at which the criteria must be achieved changes with the grades. As an example, consider two construction projects - one at the equator and one at the Arctic Circle. Good asphalt performance is expected in both locations, but the temperature conditions under which specified binder properties must be achieved are vastly different. Performance graded binders are selected on the basis of the climate in which the pavement will serve. Table 3.3 lists the binder grades.

The distinction among various grades is the specified maximum and minimum temperatures at which requirements must be met. For example, a binder classified as PG 46-40 means that the binder will meet high temperature requirements up to a temperature of 46°C and the low temperature physical property requirement down to -40°C.

Table 3.2 : Aging and Test Procedures in SUPERPAVE™

Equipment	Sample Condition	Performance Property
Rotational Viscometer	Original	Handling and Pumpability
Flash Point	Original	Safety
Rolling Thin Film Oven	Original	Simulating binder aging characteristic
Pressure Aging Vessel	RTFO Aged	Simulating binder aging characteristic
Dynamic Shear Rheometer	- Original - RTFO Aged - PAV Aged	Binder properties at intermediate and high temperatures
Bending Beam Rheometer	PAV Aged	Binder properties at low temperatures
Direct Tension Tester	PAV Aged	Binder properties at low temperatures

Table 3.3 : Performance Grade

High Temperature Grades (°C)	Low Temperature Grades (°C)
PG 46	-34, -40, -46
PG 52	-10, -16, -22, -28, -34, -40, -46
PG 58	-16, -22, -28, -34, -40
PG 64	-10, -16, -22, -28, -34, -40
PG 70	-10, -16, -22, -28, -34, -40
PG 76	-10, -16, -22, -28, -34
PG 82	-10, -16, -22, -28, -34

The specifications of different SUPERPAVE™ binder grades are mentioned in Table 3.4. The table does not content all grades which can be found in Superpave (1995). The specifications are applied using pavement design temperature. Various models are available for the calculation of pavement temperatures which are developed by US Federal Highway Administration and Canadian SHR Program (C-SHRP). These models are discussed in Appendix C.

Table 3.4 : SUPERPAVE™ Grades

Performance Grade	PG-52					PG-58						
	-10	-16	-22	-28	-34	-40	-46	-16	-22	-28	-34	-40
Average 7-day Max. Pavement Design Temp.,°C	< 52					< 58						
Min. Pav. Design Temp., °C	>-10	>-16	>-22	>-28	>-34	>-40	>-46	>-16	>-22	>-28	>-34	>-40
Original Binder												
Flash Point Temp.,°C	230											
Viscosity, Max. 3.0 Pa.s, Test Temp.,°C	135											
Dynamic Shear, G*/sinδ, Min. kPa, Test Temp. @10 rad/s, °C	52					58						
Rolling Thin Film Oven Test Residue												
Mass Loss, Max. %	1.0											
Dynamic Shear, G*/sinδ, Min. 2.2 kPa,Test Temp. @10 rad/s, °C	52					58						
Pressure Aging Vessel Residue												
PAV Aging Temp.,°C	90					100						
Dynamic Shear, G*/sinδ, Max. 5000 kPa,Test Temp. @10 rad/s, °C	25	22	19	16	13	10	7	25	22	19	16	13
Creep stiffness, S, Max.,3x 10^5 Pa, m-value, Min, 0.30 Test Temp., 60 sec, °C	0	-6	-12	-18	-24	-30	-36	-6	-12	-18	-24	-30
Direct Tension ,Failure Strain, Min,1%, Test Temp,°C	0	-6	-12	-18	-24	-30	-36	-6	-12	-18	-24	-30

Table 3.4 : SUPERPAVE^{TM} Grades (Contd.)

Performance Grade	PG-64			PG-70					PG-76			
	-22	-28	-40	-16	-22	-28	-34	-40	-16	-22	-28	-34
Average 7-day Max. Pavement Design Temp.,°C	< 64			< 70					< 76			
Min. Pav. Design Temp., °C	>-22	>-28	>-40	>-16	>-22	>-28	>-34	>-40	>-16	>-22	>-28	>-34
Original Binder												
Flash Point Temp.,°C	230											
Viscosity, Max. 3 Pa.s, Test Temp.,°C	135											
Dynamic Shear, G*/sinδ, Min. 1kPa, Test Temp. @10 rad/s, °C	64			70					76			
Rolling Thin Film Oven Test Residue												
Mass Loss, Max. %	1.0											
Dynamic Shear, G*/sinδ, Min. 2.2 kPa,Test Temp. @10 rad/s, °C	64			70					76			
Pressure Aging Vessel Residue												
PAV Aging Temp.,°C	100			100					100			
Dynamic Shear, G*/sinδ, Max. 5000 kPa,Test Temp. @10 rad/s, °C	25	22	16	31	28	25	22	19	34	31	28	22
Creep stiffness, S, Max.,3 x 10^5 kPa, m-value, Min, 0.30 Test Temp., @60 sec, °C	-12	-18	-30	-6	-12	-18	-24	-30	-6	-12	-18	-24
Direct Tension ,Failure Strain, Min,1%, Test Temp,°C	-12	-18	-30	-6	-12	-18	-24	-30	-6	-12	-18	-24

CHAPTER 4

Empirical and Performance-Based Characterization : Experimental Work

In this chapter, the rationale behind the selection of crude oils, experimental work for the preparation of paving asphalts from these oils, and testing procedure for asphalts are discussed in detail.

4.1 Selection Of Crude Oil

For characterization of paving asphalt, vacuum distillation residues of various stiffness (penetration @ 25°C) were prepared from three Canadian crude oils - Cold Lake; Bow Valley; and Redwater oils. Cold Lake crude oil is known to have high asphaltic content where as Redwater is a paraffinic crude oil. Asphalt derived from Cold Lake crude oil is considered to have good temperature susceptibility whereas Redwater crude gives one of the worst paving asphalt. The performance of asphalt obtained from Bow Valley crude lies in between these two extremes. These observations are based on the industrial experiences. Thus three crude oil were selects with an objective to prepare paving asphalts of 'good', 'average' and 'poor' qualities.

4.2 Distillation of Crude Oil

The residue obtained after vacuum distillation of crude oil finds application as paving asphalt. In this experimental work 5-6 specimens of the asphalts with penetration number ranging between 40-400 decimillimetre (dmm) were prepared from each crude oil. The details of the experimental set-up and procedure are given in this section.

4.2.1 Equipments and Instrumentation

The schematic diagram of the distillation unit has been shown in Figure 4.1. This unit can be divided into 3 sections:

4.2.1.1 Distillation Kettle and Column

Distillation kettle The brass distillation kettle in which crude oil is charged has a capacity of approx. 10 litres. The kettle is electrically heated with a mantel. A temperature probe measures the temperature inside the kettle.

Distillation column A glass distillation column of diameter 8 cm and height 24 cm is mounted on the kettle. A temperature probe measures the vapor temperature at the top of the column.

Electrical heating mantel The mantel is provided for the heating of kettle. The heating is controlled by temperature controller.

Electrical heating jacket The heating jackets are provided for column and upper part of kettle to prevent the condensation of vapor. The jackets also provide required insulation.

4.2.1.2 Condenser and Distillate Collection System

Main Condenser This condenser (Condenser 1) has maximum heat transfer area and it condenses most of vapor. The condensate is collected as distillate. The condenser has two co-axial cylinders. A schematic diagram has been given in Figure 4.2. Isopropyl alcohol (IPA) is filled in the inner cylinder and dry ice is added to that which acts as medium for

the heat removal. Vapors pass through the outer cylinder and are condensed on the outer wall of inner cylinder.

Auxiliary Condensers There are three auxiliary glass condensers, placed on the top of column (Condenser 2), at downstream of main condenser (Condenser 3) and upstream of vacuum pump (Condenser 4). Condenser 2 prevents the accumulation of vapors in the dead-end above column and protects the pressure transducers. Condenser 3 and 4 help in lowering the load on vacuum pump. All of these condensers use dry-ice in IPA as condensing media. Condenser 2 and 3 are similar in design to that of main condenser but have much lower heat transfer area. In Condenser 4, a helical coil which carries the vapor is placed in a cylinder filled with IPA.

Distillate Flask & Graduated Receivers The distillate from Condenser 1 flows through the distillate flask and is collected in a train of 6 graduated glass receivers of 500 ml. capacity each. The flask can be rotated to direct the flow of distillate into the desired receiver.

4.2.1.3 Vacuum Generation System

Caustic Scrubber A bed of caustic placed in a glass flask works as caustic scrubber. The purpose of scrubber is to prevent corrosion of vacuum pump from corrosive gases by scrubbing them out.

Vacuum Pump E2M2 series vacuum pump supplied by Edwards High Vacuum International which is a rotor vane type pump has been used in the distillation unit. The pump comprise two-stage direct drive, oil sealed outfit. Direct drive is provided, via a flexible coupling, from a 3-phase motor. The motor fitted is totally enclosed with fan cooling. The swept volume of pump is 3.4 m^3/h. The ultimate vacuum of 1×10^{-3} mbar is achievable with this pump.

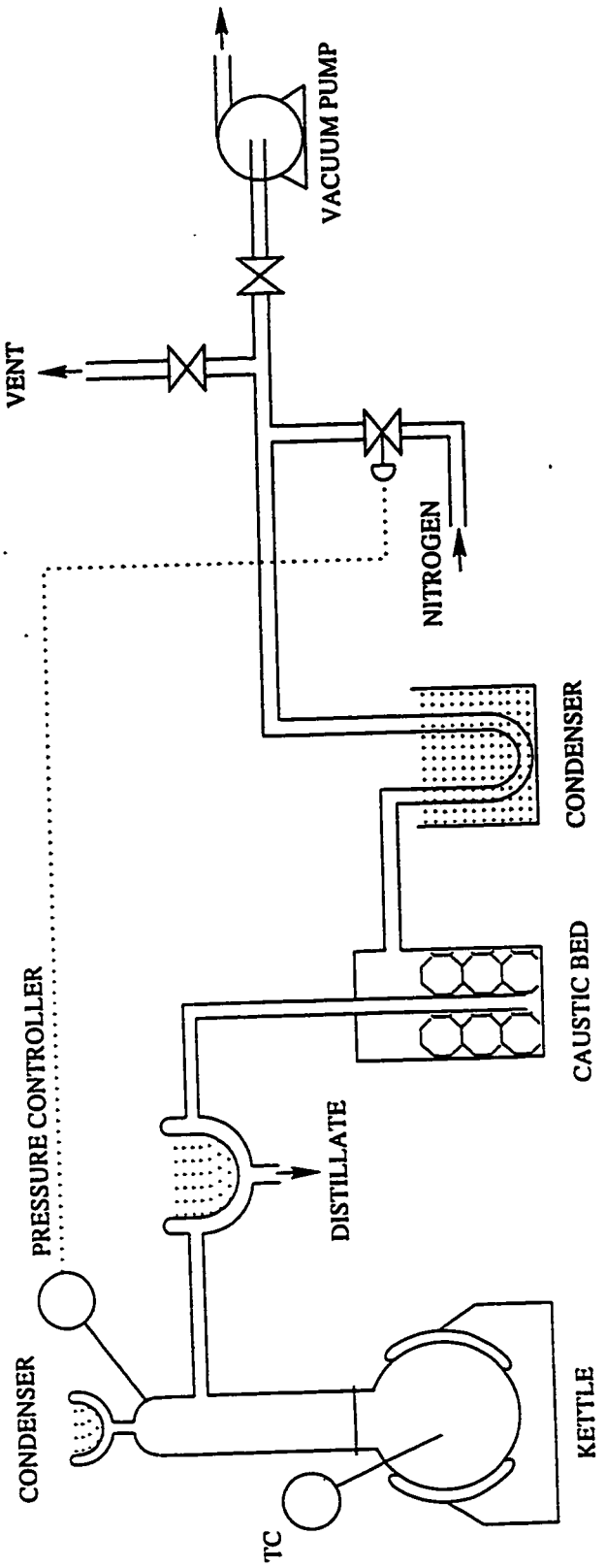

Figure 4.1: Schematic Diagram of Distillation Unit

Nitrogen Bleeding System Nitrogen bleeding system regulates the vacuum of the distillation unit and pressures the system when distillation is over. Nitrogen is supplied to the system from a cylinder through a valve which is regulated by vacuum controller.

Temperature Controller : A user-friendly temperature controller - 'Powers Process Controller 545' regulates the kettle temperature. With two independent full feature control loops, the 545 can work like two PID controllers. Additionally pre-programmed functions can be called for cascade, ratio and feed forward applications. In our case, we are using 545 for only one loop - with PID algorithm and the kettle temperature as the process variable. The controller output controls the heating by mantel.

Resistance Temperature Detector (RTD) : Two RTDs, one each for the kettle and the column are provided for the measurement of temperature of material in kettle and vapor in column. The output from RTDs are sent to the LCD displays of controller. The least count of temperature measurement is 0.1°C.

Pressure Gauge : MKS Baratron® Type 220C pressure gauge measures the vapor pressure at the top of column. The Type 220C pressure gauge is a self-contained unit with the sensor, associated electronics and power supply mounted in a dust proof box. The input to pressure gauge is 115/220 VAC and the output is 0-10 VDC. The output from pressure gauge goes to a vacuum controller. There are two pressure gauges connected in parallel. One can measure vacuum from 10-1000 Torrs whereas another senses vacuum less than 10 Torrs. The selection between these gauges can be made from controller.

Vacuum Controller : H.S. Martin vacuum controller prevents excessive vacuum formation by controlling nitrogen bleed valve which is an 'on-off' valve. After termination of distillation, the bleed valve is actuated by this controller for pressurizing of system.

4.2.2 Procedure

The distillation of crude oil is carried out in two steps, the first is atmospheric distillation followed by vacuum distillation. Atmospheric distillation is performed to remove the maximum possible lighter components from the crude oil prior to vacuum distillation. It is otherwise difficult to control the distillation of crude oil with a high percentage of low boiling fractions in this apparatus after introduction of vacuum. Moreover, atmospheric distillation also reduces the load on the vacuum pump. Vacuum distillation is performed to obtain residue of desired consistency.

The crude oil is poured in the kettle to approximately 80% of capacity. Maximum 8 liter of oil can be charged to the kettle. The charge weight is recorded and is used for the calculation of recovery of residue.

The charged kettle is placed on the heating mantel and the joint between kettle and column is sealed with the vacuum seal grease. Other joints and connections of the distillation unit are also sealed. The temperature probes (RTDs) of kettle and column are connected to the temperature controller. The heating jackets are wrapped around the kettle and column.

The distillation is started by selecting the desired final temperature in the temperature controller and turning it on. During atmospheric distillation, the downstream of condenser 4 is connected to vent. The set-point is selected around 220-240°C to ensure that at any instance temperature remains lower than the flash point in the kettle. Isopropyl alcohol is filed in the condenser traps and dry ice is added.

The distillation starts when the temperature in kettle reaches around 60°C. The vapor start generating and is condensed and collected in the distillate receivers. Dry ice has to be

added periodically to ensure proper condensation. The temperature controller is turned off when set point is achieved. The kettle is allowed to cool down.

The down-stream of condenser 4 is then connected to the suction port of the vacuum pump. After the temperature of material in the kettle has dropped to 100°C, the vacuum pump is turned on and the pressure reduced to 2-3 mm Hg. The set-point of the temperature controller is raised according to the desired atmospheric equivalent temperature (400-600°C) and the heating is again started. The estimation of atmospheric equivalent temperature has been discussed in Appendix B. The heavier distillate tends to condense rapidly and plug the condenser. To avoid this, the distillate is heated with an infra-red lamp until it flows through the flask into the graduated receivers. The vacuum controller regulates the vacuum by bleeding nitrogen into the system. When the desired end temperature is achieved, distillation is terminated by increasing the pressure and shutting off the heating elements. The pressure is increased by bleeding nitrogen gas. Nitrogen also prevents the hot residue from being altered by oxidation. The residue is cooled to a temperature lower than its flash point before exposing it to atmosphere. The residue is removed from the kettle and weighed. The procedure is then repeated for a fresh charge of oil to get residue of another desired penetration.

4.3 Binder Characterization and Evaluation : Test Methods

4.3.1 Conventional Tests and Aging Procedures

In this sections, the tests and the aging procedures required for grading of the paving asphalt as per existing specification, Penetration based ASTM specification, Alberta and CGSB specifications are discussed.

4.3.1.1 Penetration Test

Penetration is defined as consistency of a bituminous material expressed as the distance in tenth of a millimeter that a standard needle vertically penetrates a sample of the material under known conditions of loading, time, and temperature.

The sample is melted and poured in a metal or glass cylindrical, flat-bottom container and then cooled under controlled condition in a water bath. The penetration is measured with a penetrometer by means of which a standard needle is applied to the sample under specific load and loading time. In most of the conventional specifications, the temperature, load and time are taken as 25°C, 100 g and 5 sec. respectively. Other conditions which are mentioned in Table 4.1 may be used for special testing.

Table 4.1 : Conditions for Penetration Test

Temperature, °C	Loading, g	Time, s
0	200	60
4	200	60
46.1	50	5

The detailed procedure for penetration test is given in ASTM Designation D 5.

4.3.1.2 Viscosity Measurement by Capillary Viscometer

This test method is used for determination of the kinematic viscosity of asphalt. The kinematic viscosity, the ratio of the dynamic viscosity to the density, characterizes flow behavior of a material.

In this test the time is measured for a fixed volume of the liquid asphalt to flow through capillary of a calibrated glass capillary viscometer under an accurately reproducible head and at a closely controlled temperature. The kinematic viscosity is then calculated by multiplying the efflux time in seconds by the viscometer calibration factor. The tests are carried out usually at 60° and 135°C and the results are customarily reported in the mm^2/s unit. Results of this test method can be used to calculate viscosity when the density of the test material at the test temperature is known.

The detailed procedure for this test is given in ASTM Designation D 2170.

4.3.1.3 Ductility

The ductility of a bituminous material is measured by the distance to which it will elongate before breaking when two ends of a briquette specimen of the material are pulled apart at a specified temperature and speed. This test method indirectly provides one measure of tensile properties of the material.

In this test, the sample is melted and poured in a brass mold and allowed to cool first at room temperature, then at the specified test temperature in a water bath. In most of the conventional specifications, the test is carried out at 25°C. The two ends of the test specimen are pulled apart at the speed of 5 cm/min. The distance in centimeters through which the specimen has been pulled to produce rupture is measured and reported.

The detailed procedure for this test is given in ASTM Designation D 113.

4.3.1.4 Flash Point

The flash point of paving asphalt is determined to estimate the temperature up to which the material can be handled safely. The flash point in this study was measured by Cleveland open cup apparatus.. The test cup is filled to a specified level with the sample. The temperature of the sample is increased rapidly at first and then at a slow constant rate as the flash point is approached. At specified intervals a small test flame is passed across the cup. The lowest temperature at which application of the test flame causes the vapor above the surface of the sample to ignite is taken as the flash point.

The detailed procedure for this test is given in ASTM Designation D 92.

4.3.1.5 Aging Procedures

Asphalt binders are aged primarily due to two different mechanisms: oxidation and volatilization of light oils present in the asphalt during hot-mix operation, and oxidation by reacting with the oxygen in the environment when asphalt pavement is in service. In conventional specifications, the thin film oven (TFO) or the rolling thin film oven (RTFO) procedures simulate aging during hot-mix operation. There is no procedure in these specifications to simulate in-service aging.

Thin Film Oven (TFO) Procedure

The TFO procedure serves two purposes. One is to provide an aged asphalt binder that can be used for further testing. The second is to determine the mass quantity of volatiles lost from the asphalt during the process. Volatile mass loss, besides the change in viscosity, is an indication of the aging that may occur in the asphalt during the TFO procedure. The aging of sample in TFO is aimed to simulate the aging of asphalt binder

when it is subjected to high temperature in the hot-mix operation. The effect of aging is determined from measurements of selected asphalt properties before and after the test. Penetration, viscosity at 60°C and ductility tests are carried out on TFO aged samples.

The TFO procedure requires an electrically-heated convection oven. The oven contains a circular horizontal rotating shelf. Four pans of the sample are placed on the shelf. To prepare for TFO aging, a binder sample is heated until fluid and 50 grams of sample is charged in each pan. The oven is preheated to the aging temperature, 163°C. The sample pans are placed on the shelf and rotated at a rate of 5.5 revolutions per minute for the aging time of 5 hrs. After aging, the mass loss is calculated and the aged asphalt binder is collected for further testing.

The detailed procedure for this test is given in ASTM Designation D 1754.

Rolling Thin Film Oven (RTFO) Procedure

The RTFO procedure also requires an electrically-heated convection oven. The oven contains a circular, vertical carriage that holds 8 sample bottles and rotates about center. An air jet blows air into each sample bottle at its lowest position as it circulates in the carriage. While the bottle is rotating, a film of asphalt which is formed on the wall of bottle gets oxidized.

To prepare for RTFO aging, a binder sample is heated until fluid and 35 grams of sample is charged in each bottle. The oven is preheated to the aging temperature, 135°C. The sample bottles are placed in the carriage and rotated at a rate of 15 revolutions per minute. The air flow is set at a rate of 4000 ml/min., and the samples are subjected to these conditions for 85 minutes. After aging, the mass loss is calculated for 2 sample bottles and the aged asphalt binder from other bottles is collected for further testing.

The detailed procedure for this test is given in ASTM Designation D 2872.

4.3.2 SUPERPAVE™ Aging Procedures and Tests

The tests and the aging procedure included in the SHRP specifications simulate the performance of the paving asphalts. These procedures are discussed in detail in this section. The SHRP specification uses the rolling thin film oven (RTFO) procedures to simulate aging during hot-mix operation. Pressure aging vessel (PAV) procedure is used to simulate in-service aging. RTFO procedure is mentioned in the previous section.

4.3.2.1 Pressure Aging Vessel (PAV) Procedure

The effect of long term in-service aging of asphalt were not incorporated in specifications for asphalt binders prior to the SUPERPAVE™ specification. The PAV, used for many years in asphalt research, was modified by SHRP and a new procedure was developed to simulate in-service aging. The PAV exposes the RTFO-aged binder to high pressure and temperature for 20 hours to simulate the effects of long term aging. Consequently, PAV residue simulates binder that has been exposed to the environmental conditions to which binders are subjected during production and service.

The pressure aging apparatus consists of the pressure aging vessel and a forced draft oven. Air pressure is provided by a cylinder of clean, dry compressed air with a pressure regulator. The aging is carried out at 2070 kPa and at either 90°, 100° or 110°C, depending on the asphalt consistency.

To prepare for the PAV, RTFO-aged binder is heated until fluid and stirred to ensure homogeneity and 50 g sample is poured in different sample pans. The PAV pans are placed in the sample rack which is placed in unpressurized, preheated pressure vessel.

When the vessel temperature is within 2°C of the required temperature, the pressure is applied and the timing for the aging period begins. After 20 hours, the pressure is gradually released and the pans are taken out of vessel. The pans are weighed to determine weight gain due to oxidation and the sample is collected for further testing.

The detailed procedure for this test is given in ASTM Designation PS 36.

4.3.2.2 Dynamic Shear Rheometry

Since asphalt behavior depends on both loading time and temperature, the realistic test for asphalt binders should include both factors. Fortunately, testing equipment with this capability already exists and is generically known as dynamic shear rheometer. In SHRP testing, the DSR is used to measure the magnitude of complex modulus and the phase angle between stress and strain of asphalt binders at intermediate to upper pavement service temperatures and a frequency of 10 rad/s.

There are two types of dynamic shear rheometers: controlled stress and controlled strain. Controlled stress rheometers work by applying a fixed torque to move the oscillating plate in which asphalt sample is 'sandwiched'. Controlled strain rheometers work by moving the oscillating plate at the specified amplitude and measuring the torque required. SUPERPAVE^{TM} binder tests are conducted in the controlled stress mode.

The DSR is used to characterize both viscous and elastic behavior by measuring the magnitude of complex shear modulus ($|G^*|$) and phase angle (δ) of asphalt binder. $|G^*|$ is a measure of the total resistance of a material to deformation when exposed to repeated pulses of shear stress. It consists of two components : elastic or recoverable ($G' = |G^*| \cos \delta$) and viscous or non-recoverable ($G'' = |G^*| \sin \delta$). The phase angle is an indicator of the relative amounts of recoverable and non-recoverable deformation. The value of

$|G^*|$ and δ for asphalt are highly dependent on the temperature and frequency of loading. By measuring both $|G^*|$ and δ, the DSR provides a more complete picture of behavior of asphalt at pavement service temperature. These measurements are made for infinitesimal strains only so that we are in linear visco-elastic region.

Test Procedure

A disk-shaped asphalt specimen with diameter equal to the oscillating plate of the DSR is required for testing. The thickness of the asphalt between the oscillating plate and the fixed plate must be carefully controlled. Two different diameter oscillating plates, each with a corresponding gap thickness, are used in binder tests. The plate diameter and gap thickness used depends upon the aged state of the asphalt being tested. Original and RTFO aged binders are tested with a 25 mm diameter plate and 1000 micron gap; PAV-aged binder is tested with an 8 mm diameter plate and 2000 micron gap.

To prepare the test specimen, the asphalt binder is heated until fluid, stirring occasionally to remove air bubbles and achieve a homogeneous sample. Then it is poured directly onto the base plate to provide the appropriate thickness of material. A mold may also be used for the same purpose. After the asphalt is in place, the specimen is trimmed flush with parallel plates.

After the test specimen is in place, the sample temperature is controlled by a circulating fluid bath. Fluid baths typically use water which is circulated through a temperature controller that precisely adjusts and maintains the desired sample temperature.

Testing consists of setting the DSR to apply a constant oscillating stress and recording the resulting strain and time lag, δ. The shear strain is set between about one to 12 percent, depending on the aged state of the binder being tested. Original binders and RTFO aged

binders are tested at strain values of approximately 2-12 %. PAV-aged binders are tested at strain values of about 1%.

Prior to beginning the test, the sample is first conditioned by loading the specimen for 10 cycles. During this conditioning period, the rheometer measures the stress required to achieve the set shear strain and then precisely maintains this stress during the test. After the 10 conditioning cycles, ten additional cycles are applied to obtain test data. The rheometer software automatically computes and reports |G*| and δ, using the relationship between the applied stress and the resulting strain.

Data Analysis

Two parameters formed from |G*| and δ at fixed frequency, are used in the binder specification. Permanent deformation is governed by limiting |G*| /sin δ at the test temperatures to values greater than 1.00 kPa for original binder and 2.20 kPa after RTFO aging. Fatigue cracking is governed by limiting |G*| sin δ of pressure aged material to values less than 5000 kPa at the test temperature.

4.3.2.3 Bending Beam Rheometry

Asphalt binders at low temperatures are too stiff to reliably measure their properties using the parallel plate geometry of the DSR. So SHRP researchers introduced the Bending Beam Rheometer (BBR) to evaluate binder properties at low pavement temperatures.

The BBR is used to measure how much a binder deflects or creeps under a constant load at a constant temperature. The BBR test temperatures are related to the lowest service temperature of a pavement. Furthermore, the test is performed on binders that have been aged in both RTFO and PAV.

The test method uses beam theory to calculate the stiffness of an asphalt beam sample under a creep load. By applying a constant load to the asphalt beam and measuring the center deflection of the beam throughout the four-minute test procedure, the creep stiffness (S) and creep rate (m) can be calculated. Creep stiffness is the resistance of the binder to creep loading and the m-value is the change in asphalt stiffness with time during loading.

Test Procedure

The BBR consists of fluid bath, load cell, loading frame support and deflection transducer. A rectangular beam of asphalt of dimension 6.25 mm x 125 mm x 12.5 mm is prepared using an aluminum mold and conditioned at test temperature in the bath. The deflection transducer and load cell are calibrated, and the compliance of the loading frame is checked with a rigid stainless steel reference beam. Most of the system calibration is controlled by the BBR software and user-friendly instructions.

After the 60 minute thermal conditioning period in the bath, the asphalt beam is placed on the support. A 980 mN load is applied to the beam for a total of 240 seconds. The deflection is measured with the deflection transducer. During the test, the graphs of load and deflection versus time are continuously generated on the computer screen for observation. After 240 seconds, the test load is automatically removed and the rheometer software calculates creep stiffness and creep rate.

Data Analysis

Beam theory is used to obtain creep stiffness of the asphalt in this test. The equation for calculating creep stiffness, S(t), is

$$S(t) = \frac{PL^3}{4bh^3D(t)} \qquad (4.1)$$

S(t) = creep stiffness (MPa) at time t

P = applied constant load, N

L = distance between beam supports, 102 mm

b = beam width, 12.5 mm

h = beam thickness, 6.25 mm

D(t) = deflection (mm) at time t

The BBR software makes this calculation using deflection versus time. The desired value of creep stiffness is when the asphalt has been loaded for two hours at the minimum pavement design temperature. However, using the concept of time-temperature superposition, SHRP researchers confirmed that by raising the test temperature by 10°C (Superpave 1995), an equal creep stiffness in most conventional asphalts can be obtained after only a 60 seconds loading. The SHRP specification requires that the creep stiffness not exceed 300 MPa at 60 seconds. However, if the creep stiffness is between 300 and 600 MPa, the direct tension failure strain requirement can be used in lieu of the creep stiffness requirement. The direct tension test is described in the next section.

The second parameter determined from the results of the bending beam test is the m-value. The m-value represents the rate of change in the creep stiffness, S(t), versus time. This value is also calculated automatically by the bending beam software. The m-value is the slope of the log stiffness versus log time curve at any time, t. The SHRP specification requires that m-value be greater than or equal to 0.300 at 60 seconds.

4.3.2.4 Direct Tension (DT) Test

Numerous studies (Petersen and Anderson, 1994a) of low temperature asphalt binder behavior have shown that there is a strong relationship between stiffness of asphalt binder and the amount of stretching it undergoes before breaking. It is important that an asphalt binder be capable of a minimal amount of stretching or elongation.

Creep stiffness as measured by the BBR is not adequate to completely characterize the capacity of asphalts to stretch before breaking. For example, some binders exhibit high creep stiffness but can also stretch further before breaking. Consequently, SHRP researchers developed a specification system to accommodate these stiff-but-ductile binders. These binders are allowed to have relatively high creep stiffness if they can also display reasonably ductile behavior at low temperatures. This additional requirement applies only to binders that have a BBR creep stiffness between 300-600 MPa. If the stiffness is below 300 MPa, the additional testing is not required.

The equipment that measures the amount of binder strain before failure at very low temperatures is the direct tension tester (DTT). The test is performed on the RTFO and PAV aged sample at the temperature range 0° to -36°C.

Test Procedure

The direct tension test is carried out on "dog bone" shaped asphalt specimens, formed in an aluminum mold. The DT tester consists of three components : testing machine to apply load, an elongation measurement system and an environmental control system. The key feature of the testing machine is the gripping system used to attach specimens to the alignment rods that apply the tensile load. Because the direct tension test is performed at such low temperatures, the failure strains are relatively small. The environmental

chamber includes a mechanical refrigeration unit capable of producing and precisely maintaining chamber temperatures as low as -40°C.

The test is carried out on four specimens which are tested individually. A tensile load is applied by pulling one end of the specimen at starting speed of 1 mm/min. The test is designed to maintain constant rate of elongation, the pulling speed is increased to compensate for decreasing cross-section of the tested sample. The test is carried out until specimen fails.

Data Analysis

A single test result consists of the average strain to failure of the four specimens, reported to the nearest 0.01%. Also in this test, the shift factor of 10°C is used, even though it is not absolutely clear that the same shifting applies (Zanzotto, 1996). The low temperature task force of Expert Tar Group (ETG) at FHWA is working on this matter as well as on the issue of combining results of BBR and DT.

4.3.2.5 Rotational Viscometer

The measurement of viscosity performed in rotational viscometer is used to determine the flow characteristics of the asphalt binder to provide some assurance that it can be pumped and handled at the hot mixing facility. In SHRP specification, the viscosity is measured at 135°C.

The rotational viscometer consists of cylindrical sample chamber, spindle and torque measuring device. The viscosity is determined by measuring the torque required to maintain a constant speed of the cylindrical spindle while submerged in the asphalt binder

sample at a constant temperature. The torque is directly related to the binder viscosity, which is calculated automatically by the viscometer.

In this study, Mettler RM 260 and Contraves RM 115 viscometers were used for measurement of viscosity at 60°C and 135°C respectively.

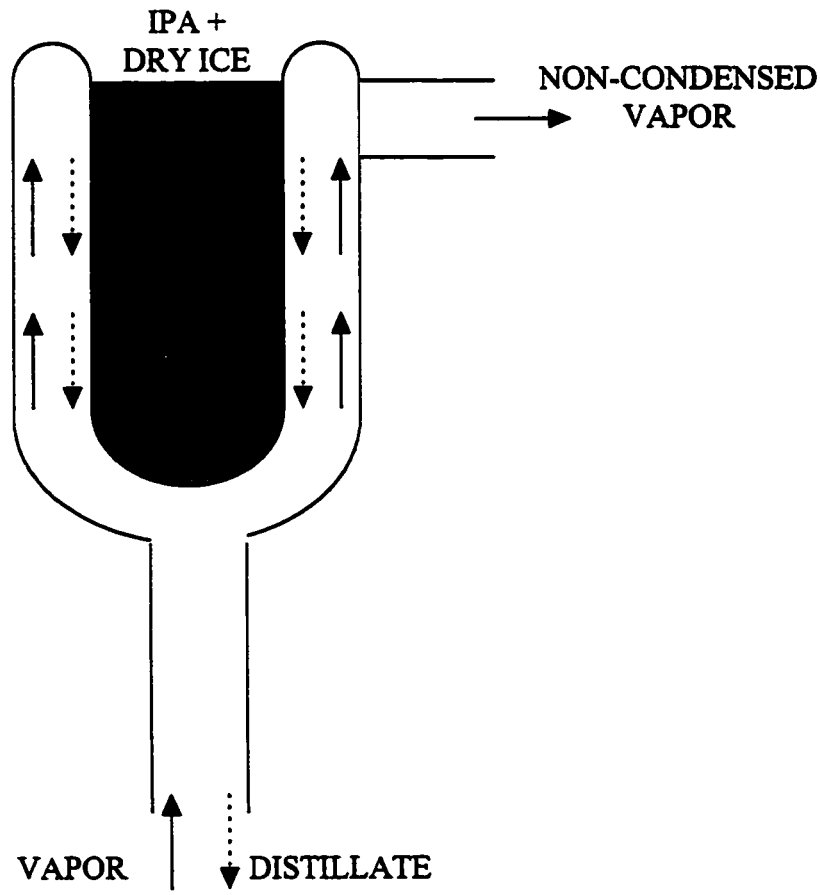

Figure 4.2 : Main Condenser

CHAPTER 5

Empirical and Performance-Based Characterization : Results and Discussion

5.1 Preparation of Asphalt

To prepare the residues of different penetrations, Cold Lake (CL), Bow Valley (BV) and Redwater (RW) crude oils were distilled under vacuum. Prior to the distillation of these oils, the process parameters for obtaining residue of the desired penetration were not known. Hence, the atmospheric equivalent temperatures (AETs) for the termination of different runs of vacuum distillation were arbitralily chosen. The AETs set as the termination temperatures and penetration at 25°C ($Pen_{25°C}$) of the materials prepared are plotted in Figure 5.1. It can be observed from the plot that there is practically a linear relationship between AET and $Pen_{25°C}$. The relationship is dependent on the crude source. From the regression of AET- $Pen_{25°C}$ data, the following correlation was developed,

$$AET = a_1 (Pen_{25°C}) + a_2 \qquad (5.1)$$

where a_1 is the slope and a_2 is the intercept of AET-$Pen_{25°C}$ plot. The values of a_1 and a_2 for differnt crude oils are reported in Table 5.1.

Table 5.1 : Correlation Parameters of AET

Crude Oil	a_1	a_2	r^2
Cold Lake	- 0.2578	501.99	0.96
Bow Valley	- 0.1989	560.06	0.94
Redwater	- 0.0903	571.90	0.94

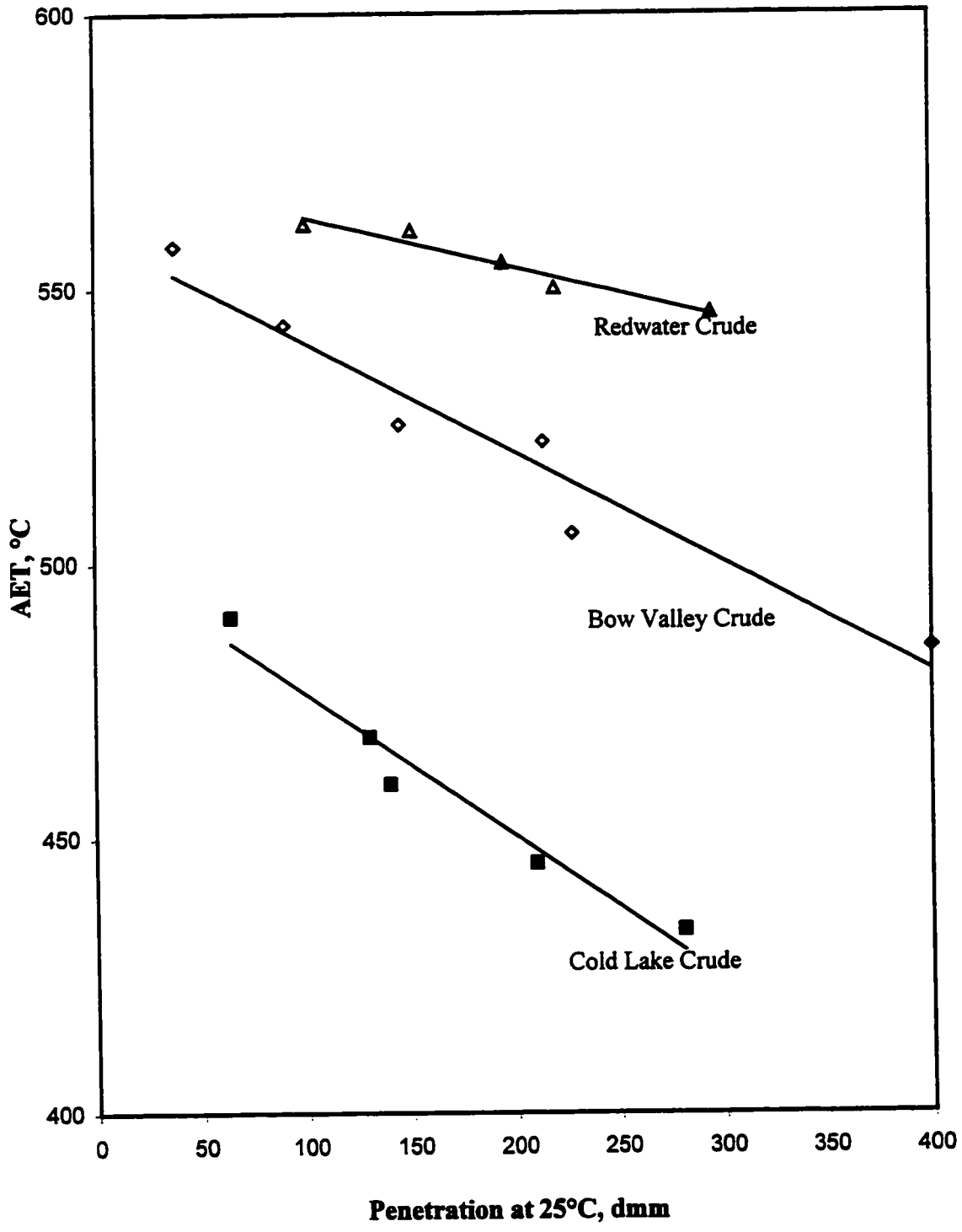

Figure 5.1 - Atmospheric Equivalent Temperature vs. Penetration at 25°C

One of the simple measures of the goodness of a correlation is the correlation coefficient r^2, which is defined as,

$$r^2 = 1 - \frac{\sum (y_i - \hat{y}_i)^2}{\sum y_i^2 - \left(\sum y_i\right)^2 / n} \qquad (5.2)$$

where y_i and $\hat{y}_i$ are actual and correlated quantities and n is the sample size. Generally, for the correlations, the values for r^2 greater than 0.9 are considered to be acceptable. For detailed statistical analysis, it is recommended to use the measures like standard deviation, sensitivity analysis etc.

AET at which distillation was terminated is minimum for CL crude whereas it is maximum for RW crude. To prepare the asphalt binders of the penetration at 25°C ranging between 100-300, the range of AET up to which distillation should be carried out is 440-480°C for CL, 510-540°C for BV and 550-560°C for RW. The lower severity of distillation for Cold Lake crude is because of its higher asphaltic content. The slope of AET vs. $Pen_{25°C}$ is maximum for CL crude and minimum for RW crude. The proposed correlations represented by Equation 5.1, will facilitate in the selection of required AET for the preparation of asphalt from these oils.

The weight percentage of crude oil residue obtained from the vacuum distillation are plotted against the $Pen_{25°C}$ of the residue in Figure 5.2. There appears to be a linear relationship between Wt.% Residue and $Pen_{25°C}$. This relationship is also crude source specific. The quantity of asphalt obtained from RW crude is minimum whereas it is maximum for CL crude. About 20% residue is obtained from RW crude which has $Pen_{25°C}$ in the range of 100-300 whereas 40-45% residue is prepared from BV crude and 58-68% from CL crude for the same penetration range. This indicates that among crude

oils studied experimentally, CL crude has the maximum asphaltic content while RW crude has the minimum.

5.2 Penetration and Viscosity Measurement of Original Samples

The following tests, carried out on the original asphalt samples, are discussed in this section:

- Penetration at 25°C
- Viscosity at 60°C ($\eta_{60°C}$) by rotational viscometer
- Viscosity at 135°C ($\eta_{135°C}$) by rotational viscometer
- Kinematic Viscosity at 135°C ($\nu_{135°C}$) by capillary viscometer

The results of these tests are reported in Table 5.2.

The viscosity at 60°C has been plotted against $Pen_{25°C}$ in Figure 5.3 . The plots show that the viscosity and the penetration exhibit a power law relationship which is well supported by other researchers (Corbett et. al. 1973). As expected, the viscosity of the asphalt decreases with the increase in its penetration. The correlation for viscosity can be written as,

$$\eta_{60°C} = b_1 (Pen_{25°C})^{b_2} \qquad (5.3)$$

The parameters of Equation 5.3 are reported in Table 5.3. The value of r^2 is higher than 0.97 which shows that the fits are very good.

Table 5.2 : Penetration and Viscosity Data of Samples

Asphalt	$Pen_{25°C}$	$\eta_{60°C}$, Pa.s	$\eta_{135°C}$, mPa.s	$\nu_{135°C}$, mm^2/s
Cold Lake (CL1)	64	315	461	459
Cold Lake (CL2)	130	118	280	296
Cold Lake (CL3)	140	97	267	253
Cold Lake (CL4)	210	58	208	208
Cold Lake (CL5)	281	37	165	167
Bow Valley (BV 1)	38	489	572	573
Bow Valley (BV 2)	90	157	340	334
Bow Valley (BV 3)	145	83	243	241
Bow Valley (BV 4)	214	51	203	198
Bow Valley (BV 5)	228	42	184	177
Bow Valley (BV 6)	400	20	124	122
Redwater (RW 1)	100	94	209	194
Redwater (RW 2)	151	53	155	161
Redwater (RW 3)	195	41	138	156
Redwater (RW 4)	220	29	123	130
Redwater (RW 5)	295	28	110	120

Table 5.3 : Correlation Parameters of Viscosity at 60°C

Asphalt	b_1	b_2	r^2
Cold Lake	126,951	-1.4422	0.99
Bow Valley	73,651	-1.3698	0.99
Redwater	18,348	-1.1573	0.97

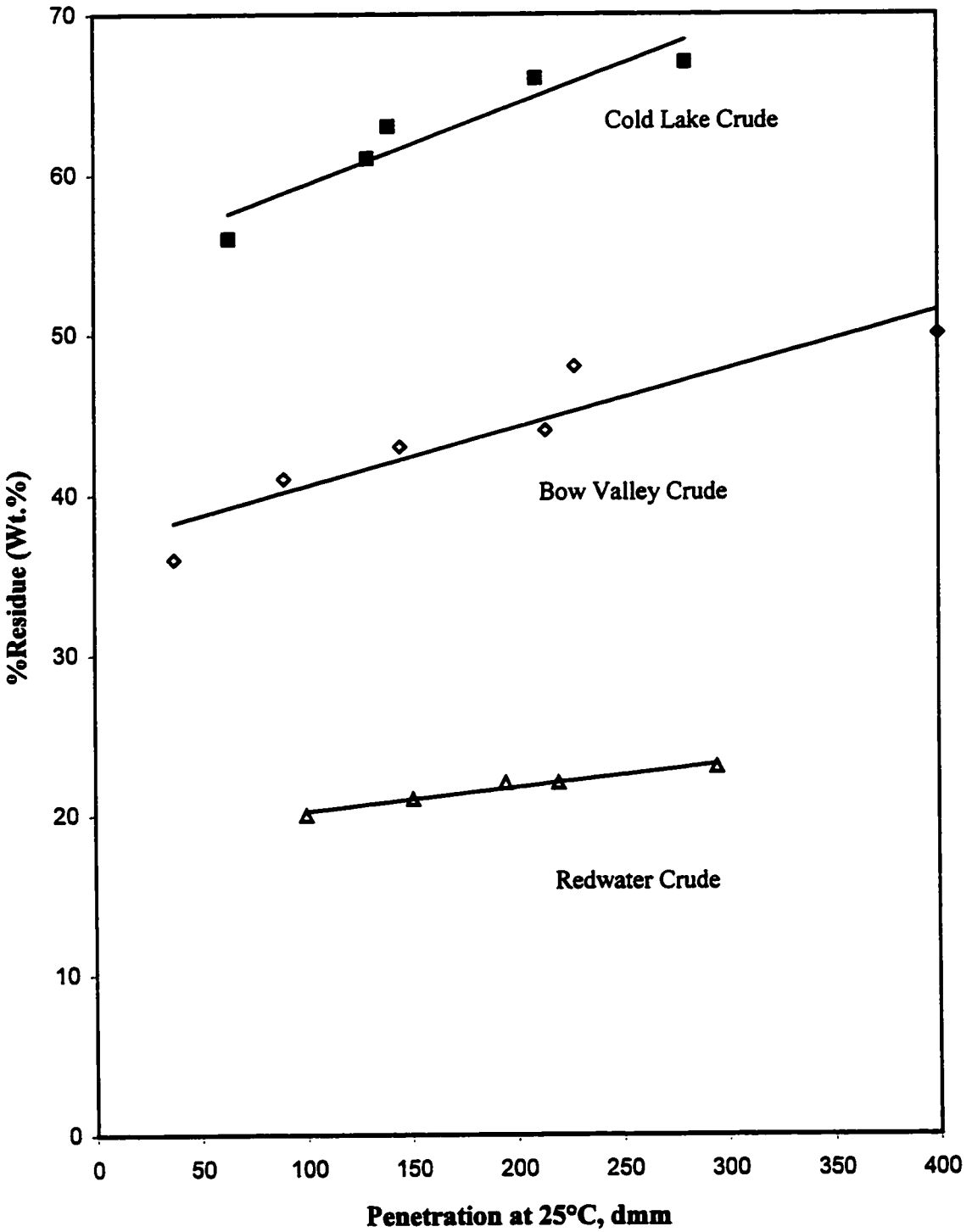

Figure 5.2 - Vacuum Distillation Residue vs. Penetration at 25°C

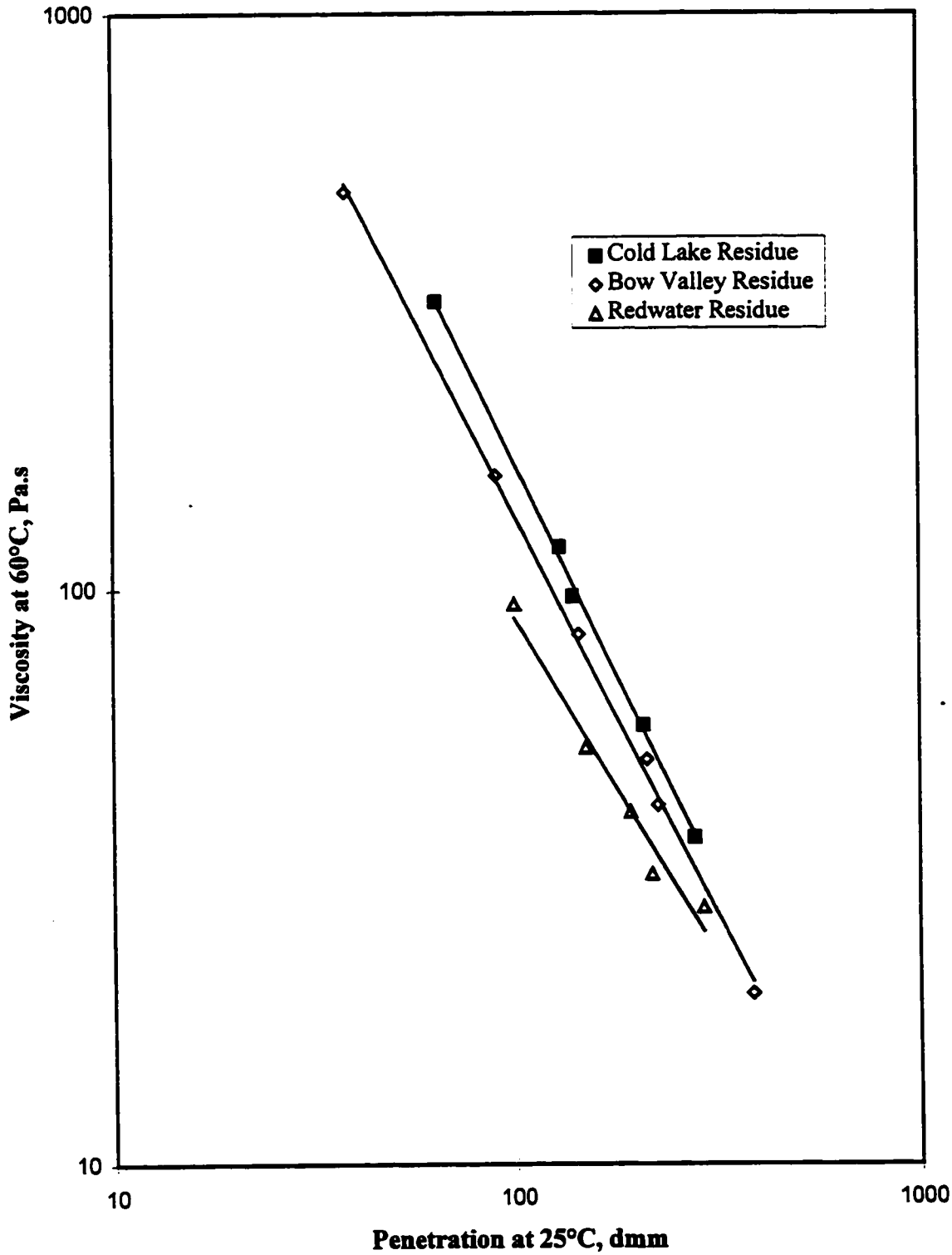

Figure 5.3 - Viscosity at 60°C vs. Penetration at 25°C

The viscosity at 135°C measured by rotational viscometer has been plotted against $Pen_{25°C}$ in Figure 5.4. It is evident from the plot that $\eta_{135°C}$ for asphalt also exhibits a power law relationship with $Pen_{25°C}$, similar to that observed for $\eta_{60°C}$ - $Pen_{25°C}$. The power law relationship can be expressed as,

$$\eta_{135°C} = c_1 (Pen_{25°C})^{c_2} \qquad (5.4)$$

The values of c_1 and c_2 were determined by regressing the $\eta_{135°C}$ - $Pen_{25°C}$ data. It was found from the regression that CL and BV asphalt can be characterized by the same correlation where c_1 and c_2 are 6638.2 and -0.6564, respectively. The values of c_1 and c_2 for the correlation for RW asphalt are 3222.6 and -0.5991, respectively. RW asphalt sample has a lower viscosity at 135°C compared to that of CL and BV asphalts for the sample of same penetration.

It has been reported in the literature that conventional paving asphalt behaves as a newtonian fluid at temperature higher than 60°C (Superpave 1995). The experiments were carried out to investigate the shear stress - shear rate relationship for the asphalt samples prepared in this study. CL4, BV4 and RW4 samples were selected as they have approximately same penetration at 25°C. The expriments were performed at 40°C and 60°C. The results are plotted in Figure 5.5 and Figure 5.6 for 40°C and 60°C respectively. It is interesting to observe from these figures that the samples chosen seem to behave as newtonian fluids even at temperature as low as 40°C. Redwater residue which has high wax content also exhibits this behavior. The zero shear rate viscosity obtained from the extrpolation of data for CL4, BV4 and RW4 are 1637.8, 918.73 and 381.06 Pa.s respectively at 40°C and 93.11, 59.97 and 24.65 Pa.s respectively at 60°C. These measurements were made at shear rate higher than 0.01 s^{-1}. It is difficult to comment upon the behavior of samples for the lower shear rates. The sample will not necessarily exhibit Newtonian bhavior in that region.

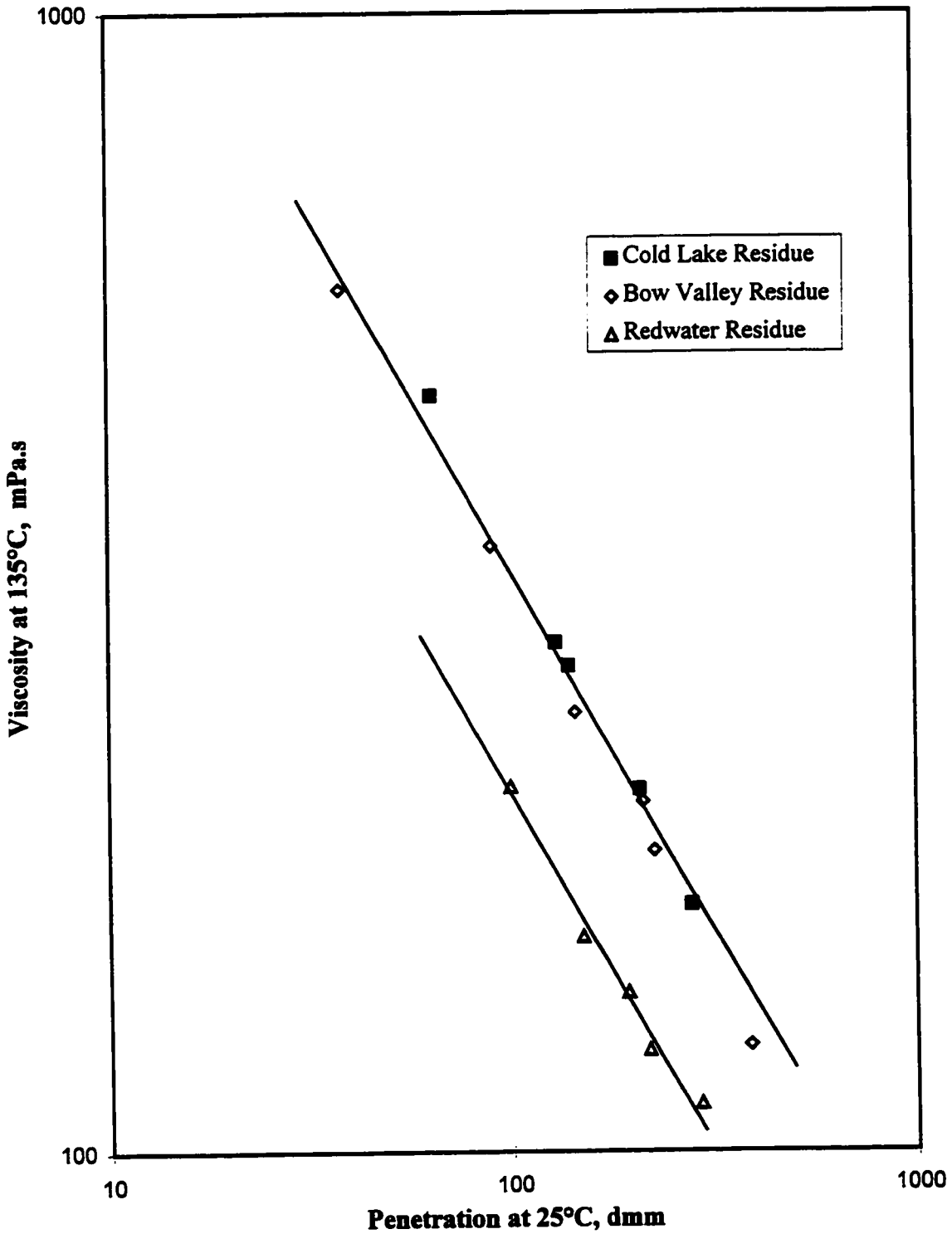

Figure 5.4 - Viscosity at 135°C vs. Penetration at 25°C

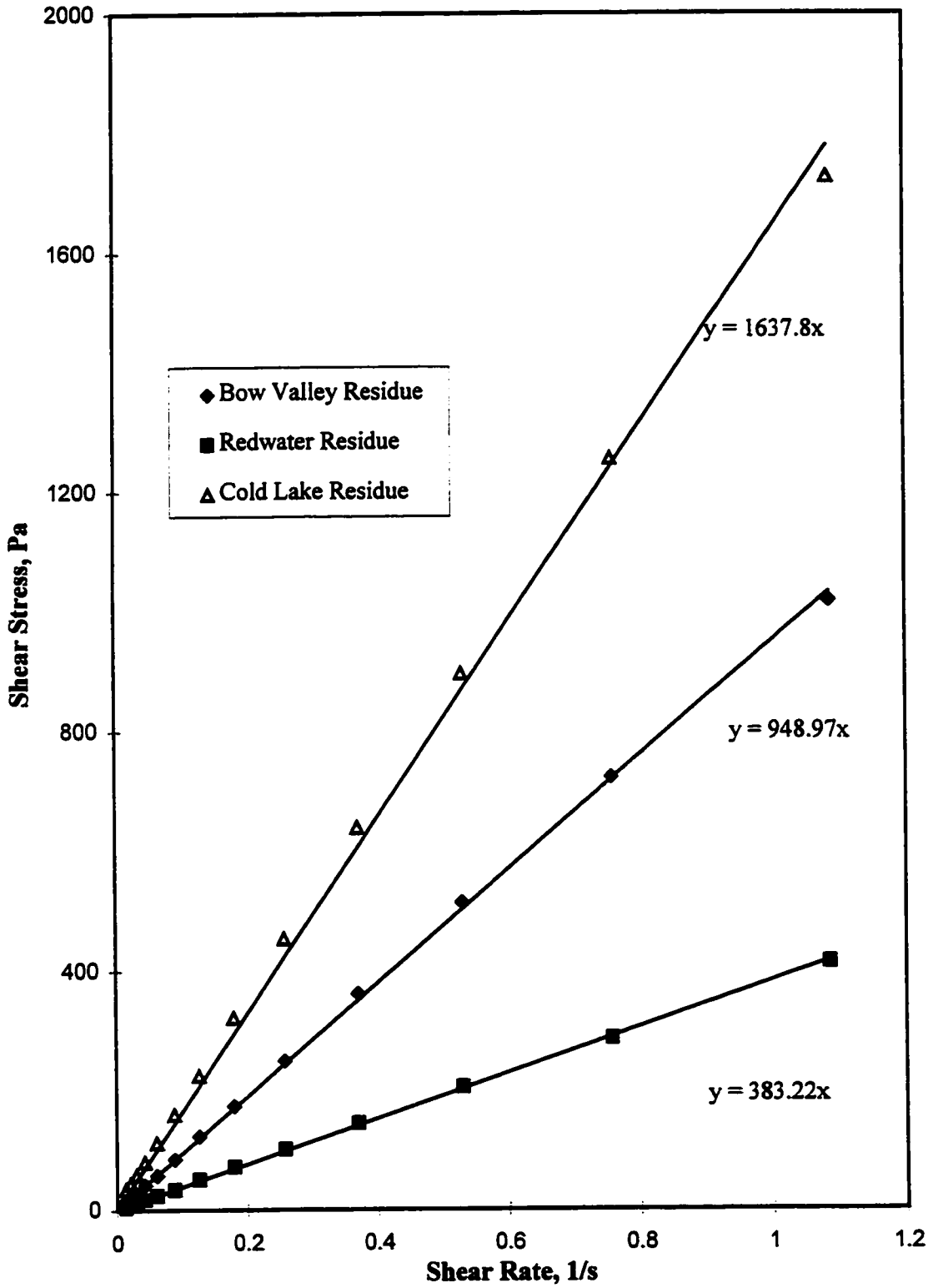

Figure 5.5 - Shear Stress vs. Shear Rate at 40°C

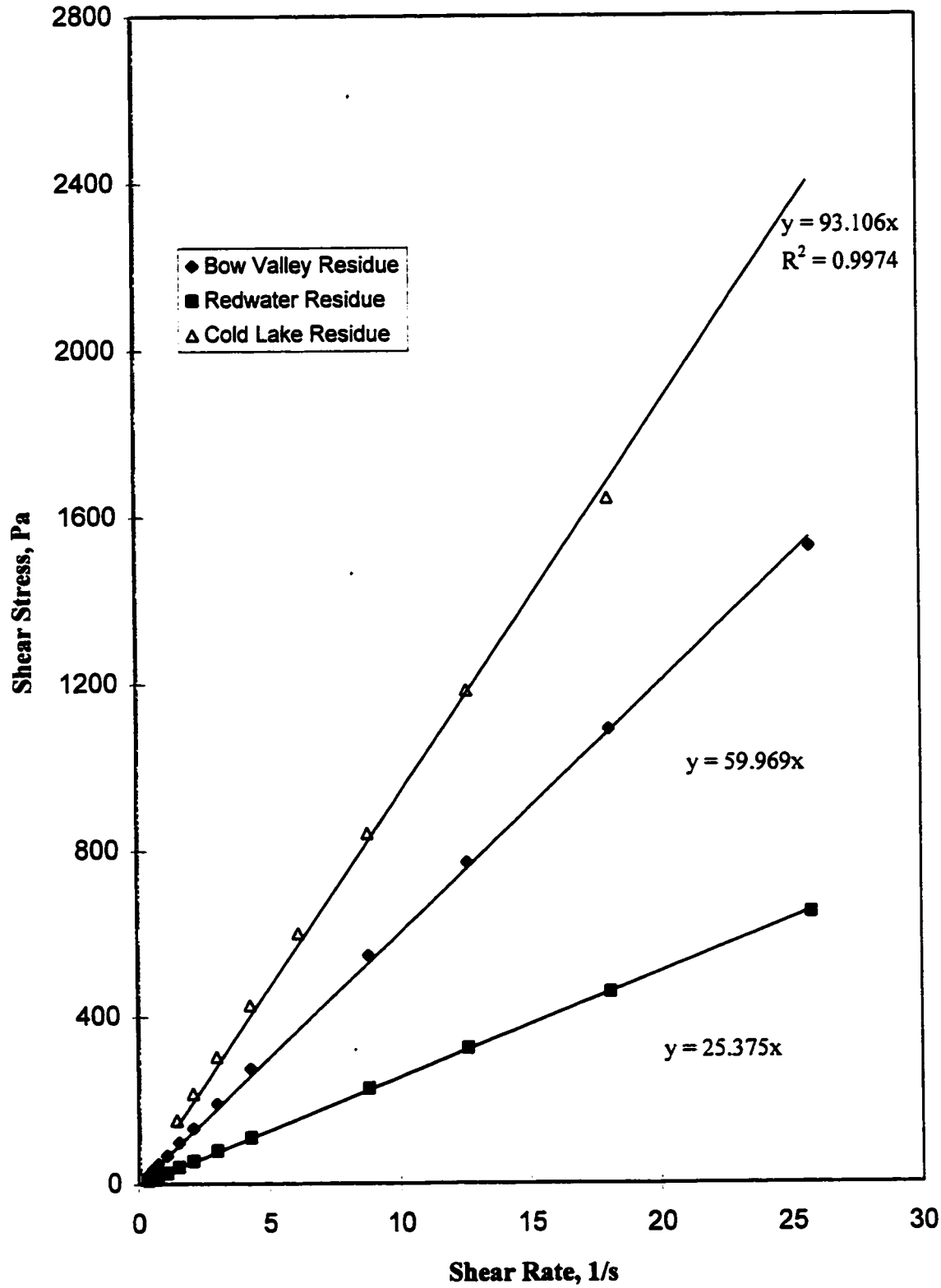

Figure 5.6 - Shear Stress vs. Shear Rate at 60°C

To further investigate dependence of viscosity of paving asphalt on temperature, measurements were made for CL4, BV4 and RW4 samples at various temperatures and the shear rate of 0.05 s^{-1}. The results are summarized in Table 5.4.

Table 5.4 : Viscosity Data at Various Temperatures

Temperature, °C	CL4	BV4	RW4
160	9.22×10^1	8.30×10^1	5.70×10^1
135	2.08×10^2	1.98×10^2	1.23×10^2
100	1.80×10^3	1.47×10^3	7.68×10^2
80	1.11×10^4	7.59×10^3	3.63×10^3
60	5.80×10^4	5.05×10^4	2.74×10^4
40	1.85×10^6	9.76×10^5	3.96×10^5

The vicosity-temperature data were correlated with the following equation (Mehrotra et. al. 1989):

$$\log\log(\eta + 0.7) = d_1 + d_2 \log(T) \qquad (5.5)$$

where η is in mPa.s and temperature in K.

Eastick (1989) has reported that several other researchers (Mehrotra and Svrcek 1984) have found this equation to be applicable for several bitumens. The values of d_1 and d_2 for each sample regressed from our data, are given in Table 5.5.

Table 5.5 : Viscosity - Temperature Correlation Parameters

Asphalt	d_1	d_2	r^2
CL4	9.96406	-3.6730	0.99
BV4	10.18924	-3.7711	0.99
RW4	10.10871	-3.7506	0.99

The viscosity-temperature data and the plots of Equation 5.5 for CL4, BV4 and RW4 samples are shown in Figure 5.7.

5.3 Flash Point Measurement for Original Samples

The flash point for different asphalt samples are reported in Table 5.6. Flash point - penetration at 25°C and flash point - viscosity at 60°C data are plotted in Figure 5.8 and Figure 5.9. CL asphalt has lower flash point compared to BV and RW asphalts. The flash point of BV and RW asphalt samples of same penetration or viscosity are nearly same. The flash point of an asphalt sample is dependent on its chemical composition. It can be seen from Figure 5.1 that Cold Lake crude requires lower distillation severety for the preparation of an asphalt sample of a certain penetration, compared to the other crude oils. Hence, Cold Lake asphalt sample has higher content of low boiling point fractions which attributes to its lower flash point.

5.4 TFO Aging and Testing of Aged Samples

The change in the mass of the asphalt samples was calculated after TFO aging. The results are reported in Table 5.7. CL asphalt samples show mass loss which is higher for the softer material. BV and RW asphalt samples gained weight after tht TFO aging. The weight gain by RW asphalt samples are nearly constant.

The penetration of TFO aged sample was measured at 25°C and the residual penetration was calculated as the ratio of penetration of TFO sample to that of the original sample. The results are reported in Table 5.8. The residual penetration is higher for the asphalt specimens with low $Pen_{25°C}$ for the original sample. This can be attributed to lower content of lighter fractions in the samples with low penetration. Redwater asphalt samples have lower residual penetration as compared to CL and BV asphalt samples.

Table 5.6 : Flash Point Data

Asphalt	$Pen_{25°C}$	$\eta_{60°C}$, Pa.s	Flash Point, °C
Cold Lake (CL1)	64	315	288
Cold Lake (CL2)	130	118	286
Cold Lake (CL3)	140	97	278
Cold Lake (CL4)	210	58	270
Cold Lake (CL5)	281	37	250
Bow Valley (BV 1)	38	489	361
Bow Valley (BV 2)	90	157	332
Bow Valley (BV 3)	145	83	321
Bow Valley (BV 4)	214	51	317
Bow Valley (BV 5)	228	42	307
Bow Valley (BV 6)	400	20	301
Redwater (RW 1)	100	94	338
Redwater (RW 2)	151	53	334
Redwater (RW 3)	195	41	322
Redwater (RW 4)	220	29	321
Redwater (RW 5)	295	28	318

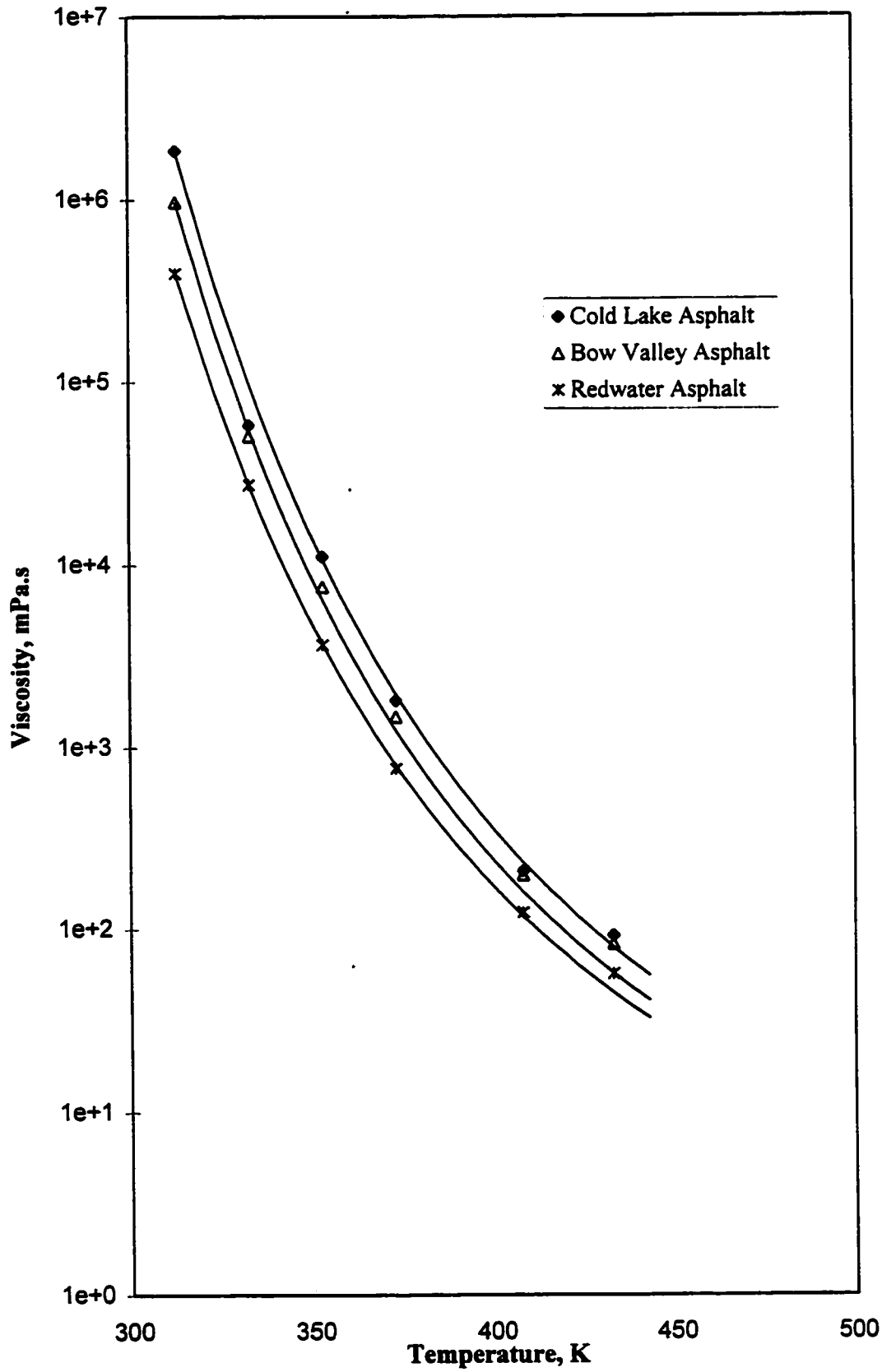

Figure 5.7 - Viscosity vs. Temperature

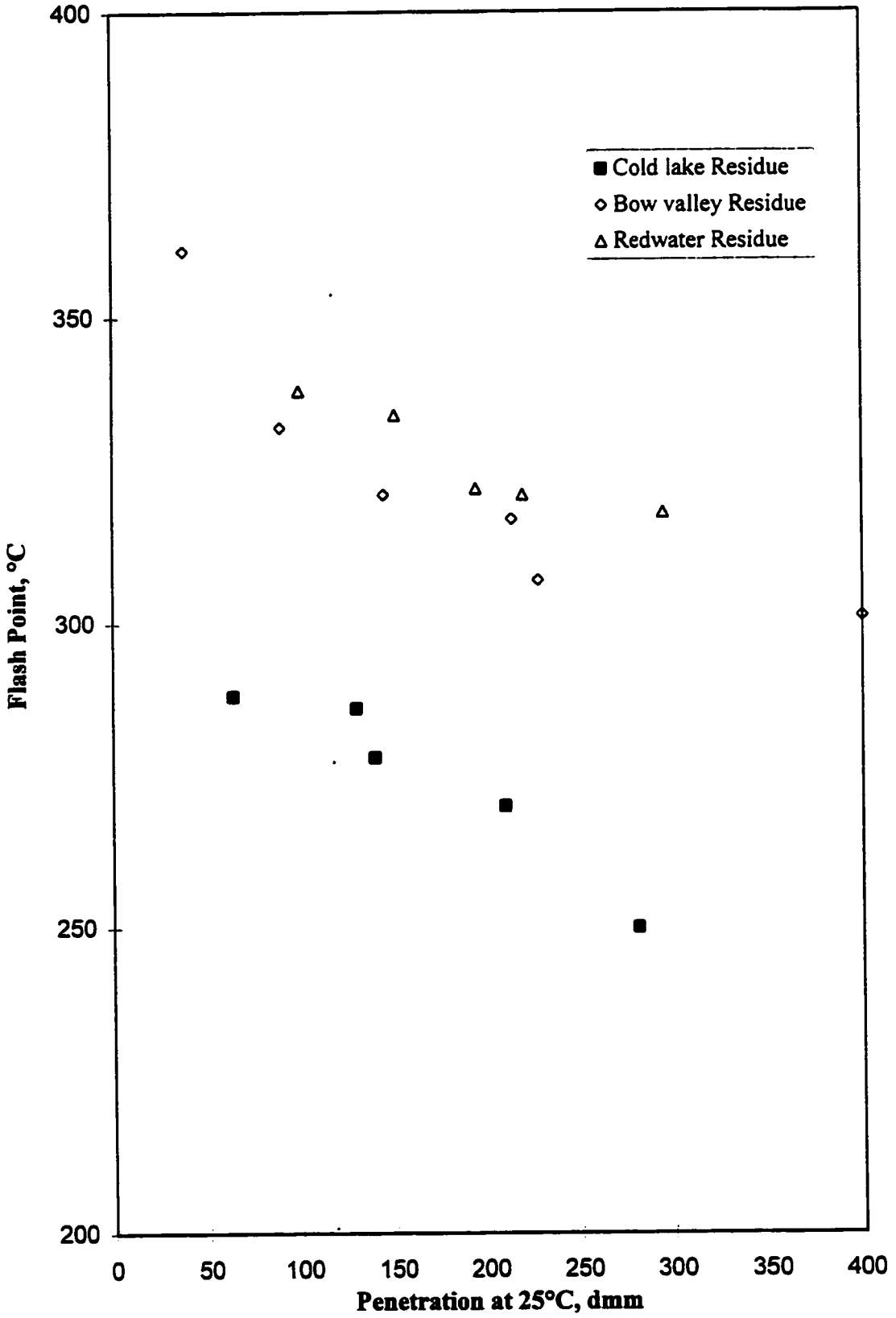

Figure 5.8 - Flash Point vs. Penetration at 25°C

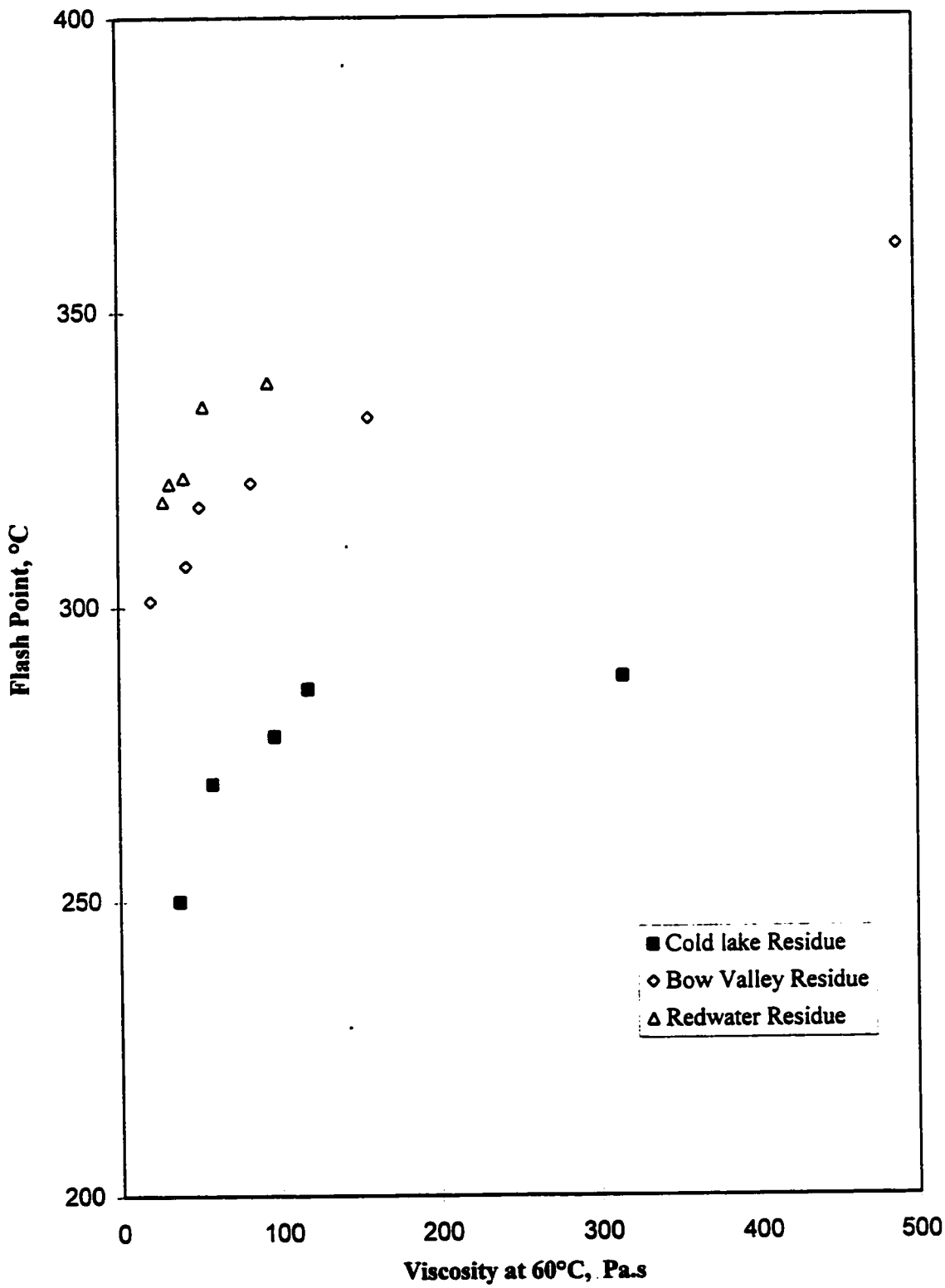

Figure 5.9 - Flash Point vs. Viscosity at 60°C

Table 5.7 : TFO Test Mass Loss Data

	% Mass Change		
Sample No.	Cold Lake	Bow Valley	Redwater
1	-0.01	+0.08	+0.12
2	-0.12	+0.09	+0.13
3	-0.18	+0.09	+0.14
4	-0.35	+0.08	+0.15
5	-0.72	+0.05	+0.12
6		+0.03	

The viscosity measurements were made at 60°C for the TFO aged samples and the aging indices were calculated as the ratio of the viscosity of the aged sample to the original sample. The results are reported in Table 5.9. There is no definite trend for the aging index with the viscosity of the original sample.

The ductility tests were carried out at 25°C for the samples with $Pen_{25°C}$ less than 200 and at 15.6°C for the other samples. The ductility of all the samples was more than 150 cm under the test condition.

5.5 RTFO Aging and Testing of Aged Sample

The mass change of the samples after RTFO aging has been reported in Table 5.10. Similar to the mass change after TFO aging, CL asphalt samples show mass loss whereas BV and RW samples show mass gain. The mass loss for CL sample with the higher penetration is lower compared to that for the CL sample of lower penetration. The mass gain is nearly same for all RW samples.

Table 5.8 : Residual Penetration after TFO Test

Asphalt	$Pen_{25°C}$ (Original)	$Pen_{25°C}$ (TFO Aged)	% Residual Penetration
Cold Lake (CL1)	64	52	74.0
Cold Lake (CL2)	130	93	64.5
Cold Lake (CL3)	140	103	64.0
Cold Lake (CL4)	210	130	56.0
Cold Lake (CL5)	281	181	55.6
Bow Valley (BV 1)	38	37	71.2
Bow Valley (BV 2)	90	69	65.1
Bow Valley (BV 3)	145	107	62.6
Bow Valley (BV 4)	214	139	58.4
Bow Valley (BV 5)	228	157	59.2
Bow Valley (BV 6)	400	314	63.3
Redwater (RW 1)	100	65	65.0
Redwater (RW 2)	151	91	60.2
Redwater (RW 3)	195	110	56.4
Redwater (RW 4)	220	125	56.8
Redwater (RW 5)	295	169	57.3

The RTFO-aged samples were further aged by PAV procedure. The DSR test results for the RTFO-aged samples and BBR tests results for the PAV-aged samples are discussed in the next section.

Table 5.9 : Aging Index after TFO Test

Asphalt	$\eta_{60°C}$, Pa.s (Original)	$\eta_{60°C}$, Pa.s (TFO Aged)	Aging Index
Cold Lake (CL1)	315	580	1.84
Cold Lake (CL2)	118	245	2.08
Cold Lake (CL3)	97	220	2.27
Cold Lake (CL4)	58	142	2.45
Cold Lake (CL5)	37	92	2.49
Bow Valley (BV 1)	489	1100	2.25
Bow Valley (BV 2)	157	325	2.07
Bow Valley (BV 3)	83	146	1.75
Bow Valley (BV 4)	51	92	1.83
Bow Valley (BV 5)	42	85	2.02
Bow Valley (BV 6)	20	34	1.73
Redwater (RW 1)	94	199	2.12
Redwater (RW 2)	53	96	1.81
Redwater (RW 3)	41	85	2.07
Redwater (RW 4)	29	50	1.70
Redwater (RW 5)	28	45	1.61

Table 5.10 : RTFO Test Mass Loss

	% Mass Change		
Sample No.	Cold Lake	Bow Valley	Redwater
1	-0.03	+0.07	+0.13
2	-0.21	+0.11	+0.13
3	-0.31	+0.09	+0.13
4	-0.56	+0.04	+0.14
5	-1.11	+0.01	+0.15
6		-0.03	

5.6 Highest and Lowest Service Temperatures

As per SHRP recommendation, DSR tests conducted on original and RTFO-aged samples give the highest temperature (T_{high}) up to which the asphalt can be used in pavement without causing escessive plastic deformation.

The bending beam rheometer (BBR) test is performed to evaluate binder properties at low pavement temperatures. The BBR test temperatures are also related to the lowest service temperature of a pavement. Based on the time-temperature superposition principle, SHRP study has concluded that 10°C lower than the BBR test temperature is the lowest service temperature (T_{low}) for a paving asphalt (Petersen and Anderson, 1994a).

In this study, DSR and BBR tests were carried out for asphalt specimens prepared from CL, BV and RW crude oils. The lower of the DSR test temperatures for original and aged asphalt is the highest allowable service temperature for that sample. The highest and the lowest temperatures obtained for these samples are reported in Table 5.11.

To investigate the possible relationship between empirical parameter such as penetration or rheological property such as viscosity with the highest service temperature, T_{high} has been plotted against $Pen_{25°C}$ and $\eta_{60°C}$ in Figure 5.10 and Figure 5.11 respectively. The plots show that T_{high} is higher for the stiffer material. It can be seen from the figures that the data points on T_{high} - $Pen_{25°C}$ plot are more scattered compared to that on T_{high}- $\eta_{60°C}$ plot. This can be attributed to the fact that DSR tests and viscosity measurement have been carried out over the same temperature range while penetration test is carried out at much lower temperature. Hence, the performance of paving asphalt at higher service temperature can be characterized by its viscosity measured at 60°C.

It is interesting to note that the relationship between T_{high} and $\eta_{60°C}$ for all specimens prepared from different crude oils can be described by a single correlation which is,

$$(T_{high})^2 = -656.98 + 890.15 \ln(\eta_{60°C}) \qquad (5.6)$$

The value of r^2 for the best fit of T_{high} vs $\eta_{60°C}$ described by Equation 5.6 is 0.9875 which is excellent. The proposed correlation has good predictive capability for the highest

service temperature for the specimens prepared in this study. The value of r^2 for the best fit of T_{high} vs $Pen_{25°C}$ is 0.94 which is lower compared to the value of r^2 for T_{high} vs $\eta_{60°C}$.

Table 5.11 : Highest and Lowest Service Temperatures

Asphalt	$Pen_{25°C}$	$\eta_{60°C}$, Pa.s	T_{high}, °C (Original)	T_{high}, °C (RTFO)	T_{high}, °C	T_{low}, °C
CL 1	64	315.0	68	64	64	-26
CL 2	130	118.0	59	62	59	-31
CL 3	140	97.0	58	58	58	-32
CL 4	210	58.0	55	55	55	-34
CL 5	281	37.0	51	51	51	-36
BV 1	38	489.0	73	70	70	-21
BV 2	90	157.0	63	63	63	-26
BV 3	145	83.3	58	57	57	-30
BV 4	214	50.5	54	52	52	-32
BV 5	228	42.1	54	51	51	-33
BV 6	400	19.8	46	45	45	-37
RW 1	100	94.0	60	59	59	-26
RW 2	151	53.0	54	54	54	-29
RW 3	195	41.0	52	52	52	-30
RW 4	220	29.4	51	51	51	-30
RW 5	295	28.0	49	49	49	-32

To test the applicability of the developed correlation, T_{high} for 18 Husky asphalts samples (Source: Bituminous Material Laboratory, The University of Calgary) were predicted. A comparison of the predicted and experimentally obtained data is reported in Table 5.12.

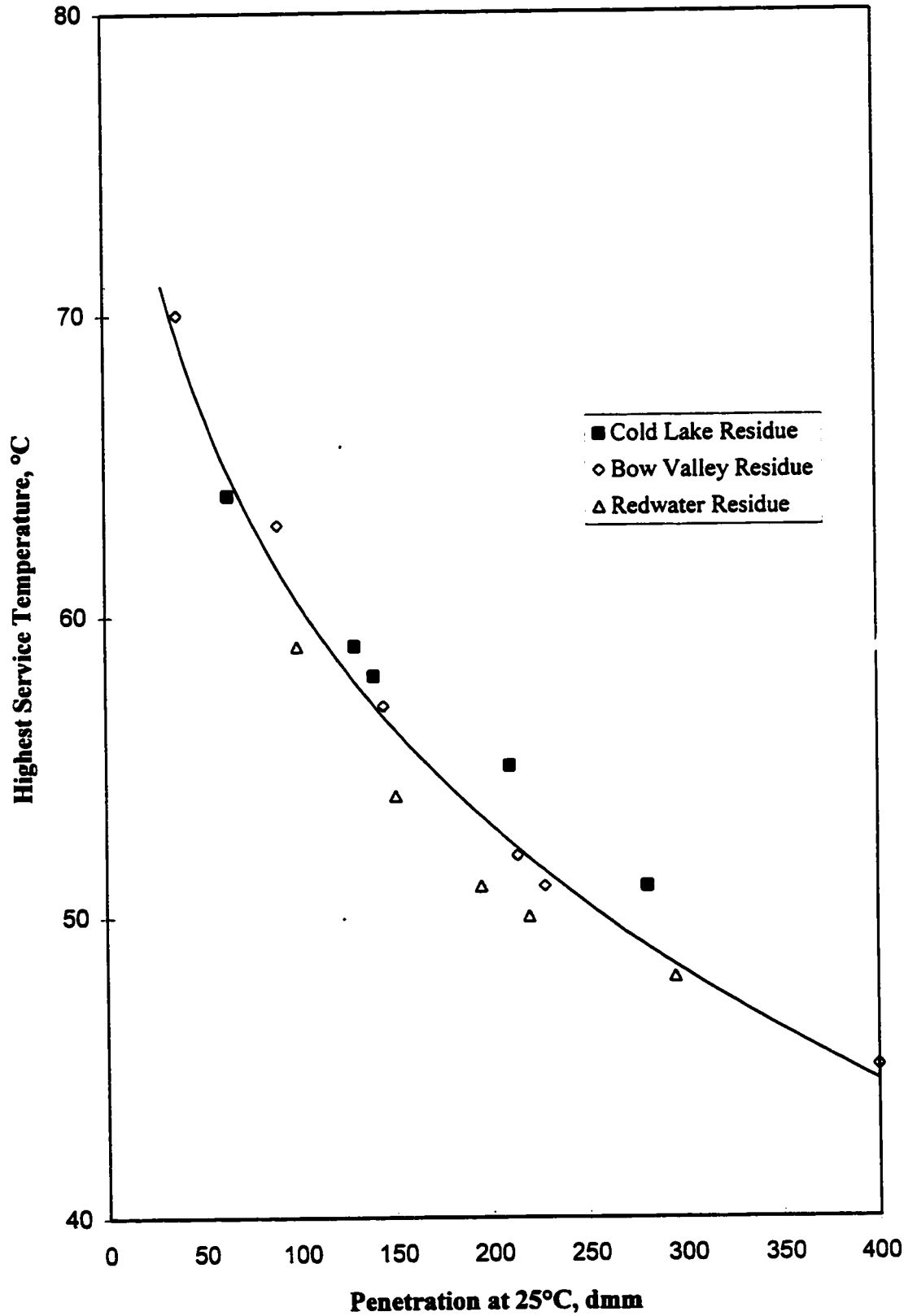

Figure 5.10 - Highest Service Temperature vs. Penetration at 25°C

Table 5.12 : Validity of Equation 5.6 for Other Samples

$\eta_{60°C}$, Pa.s	T_{high}, °C (DSR Test)	T_{high}, (Predicted)	°C Absolute Deviation	Percentage Deviation
210.0	65	64.05	0.95	1.46
220.0	66	64.37	1.63	2.46
117.0	58	59.85	1.85	3.19
100.0	60	58.67	1.33	2.21
90.0	57	57.87	0.87	1.52
40.5	53	51.36	1.64	3.10
47.2	54	52.67	1.33	2.47
46.0	52	52.45	0.45	0.87
46.4	53	52.52	0.48	0.90
45.2	52	52.30	0.30	0.58
46.3	53	52.51	0.49	0.93
34.0	52	49.82	2.18	4.19
35.9	51	50.30	0.70	1.37
32.0	49	49.28	0.28	0.56
28.5	48	48.22	0.22	0.45
26.0	51	47.36	3.64	7.13
19.5	47	44.58	2.42	5.16
17.9	46	43.71	2.29	4.97
Average Deviation			1.28	2.42

The deviations have been calculated as follows:

$$\text{Absolute Deviation} = \left| T_{high} - \hat{T}_{high} \right| \qquad (5.7)$$

$$\text{Percentage Deviation} = \frac{\left|T_{high} - \hat{T}_{high}\right|}{T_{high}} \qquad (5.8)$$

where T_{high} and $\hat{T}_{high}$ are data and predicted temperatures respectively.

The predicted T_{high} are within 8% of the experimentally estimated T_{high}. The low average absolute and percent deviations of predicted highest service temperature from data indicates that the correlation has excellent predictive capability for other regular asphalts also. Furthermore, it can be observed that for the predictions of highest temperature for 13 out of 18 asphalt samples are lower than the experimental data and hence, the estimate of T_{high} from the proposed correlation is conservative. The conservative estimate eliminates the hazard of over-predicting the performance of the paving asphalt.

The lowest service temperatures for CL, BV and RW asphalts have been plotted against their $Pen_{25°C}$ and $\eta_{60°C}$ in Figure 5.12 and Figure 5.13. Lower T_{low} can be achieved by the softer material. This behavior can be attributed to the lowering of the lighter fractions in the stiffer material which have lower stiffness compared to the heavier fractions. Comparison of CL, BV and RW asphalt of same $Pen_{25°C}$ or $\eta_{60°C}$ shows that CL asphalt will offer the best service at low temperature whereas RW asphalt will offer the worst among these three. The lowest expected service temperature for these asphalts of 100 Pa.s viscosity at 60°C are given in Table 5.13.

Table 5.13 : Comparison of Lowest Service Temperature

Asphalt	T_{low}, °C
Cold Lake	-32
Bow Valley	-29
Redwater	-26

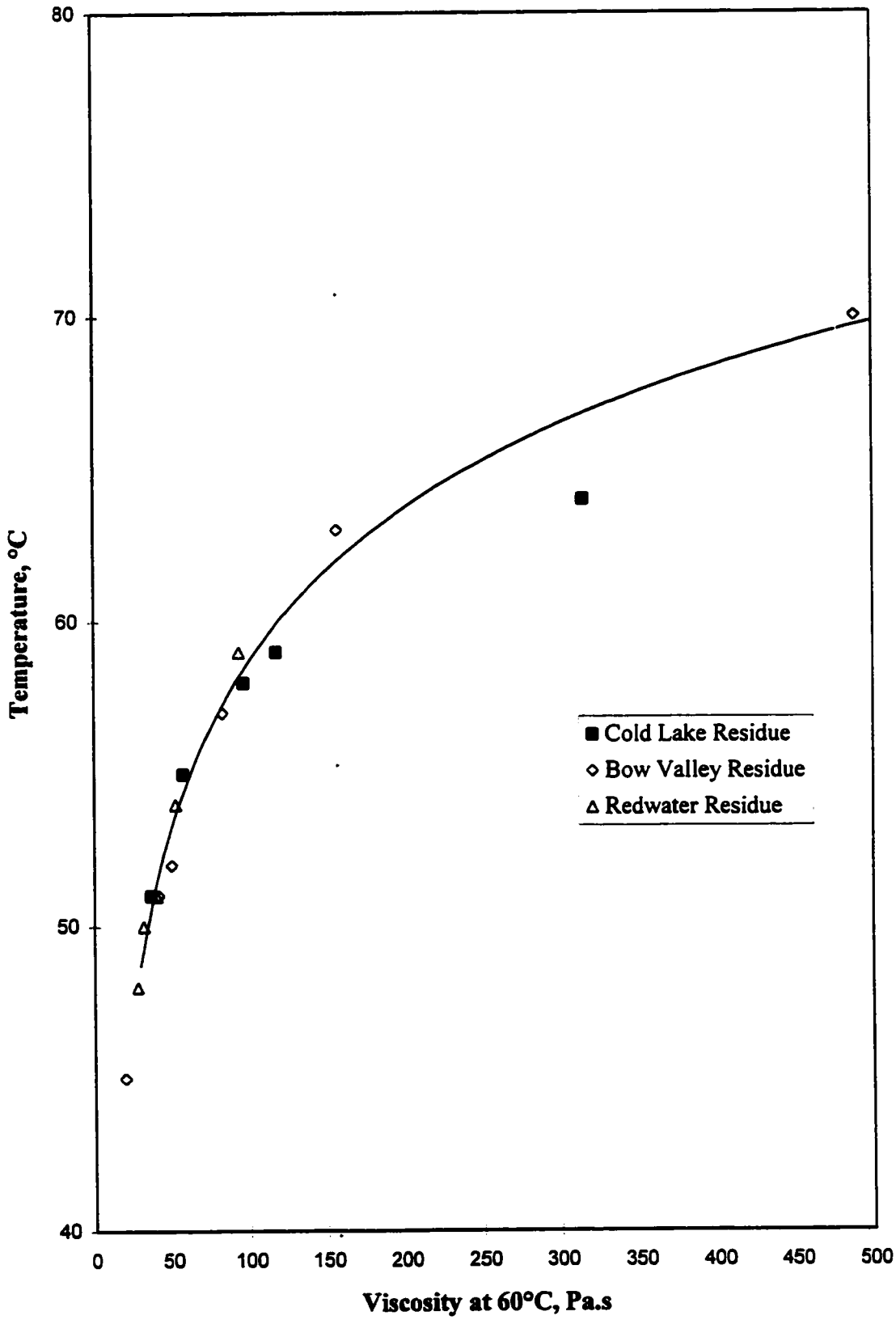

Figure 5.11 - Highest Service Temperature vs. Viscosity at 60°C

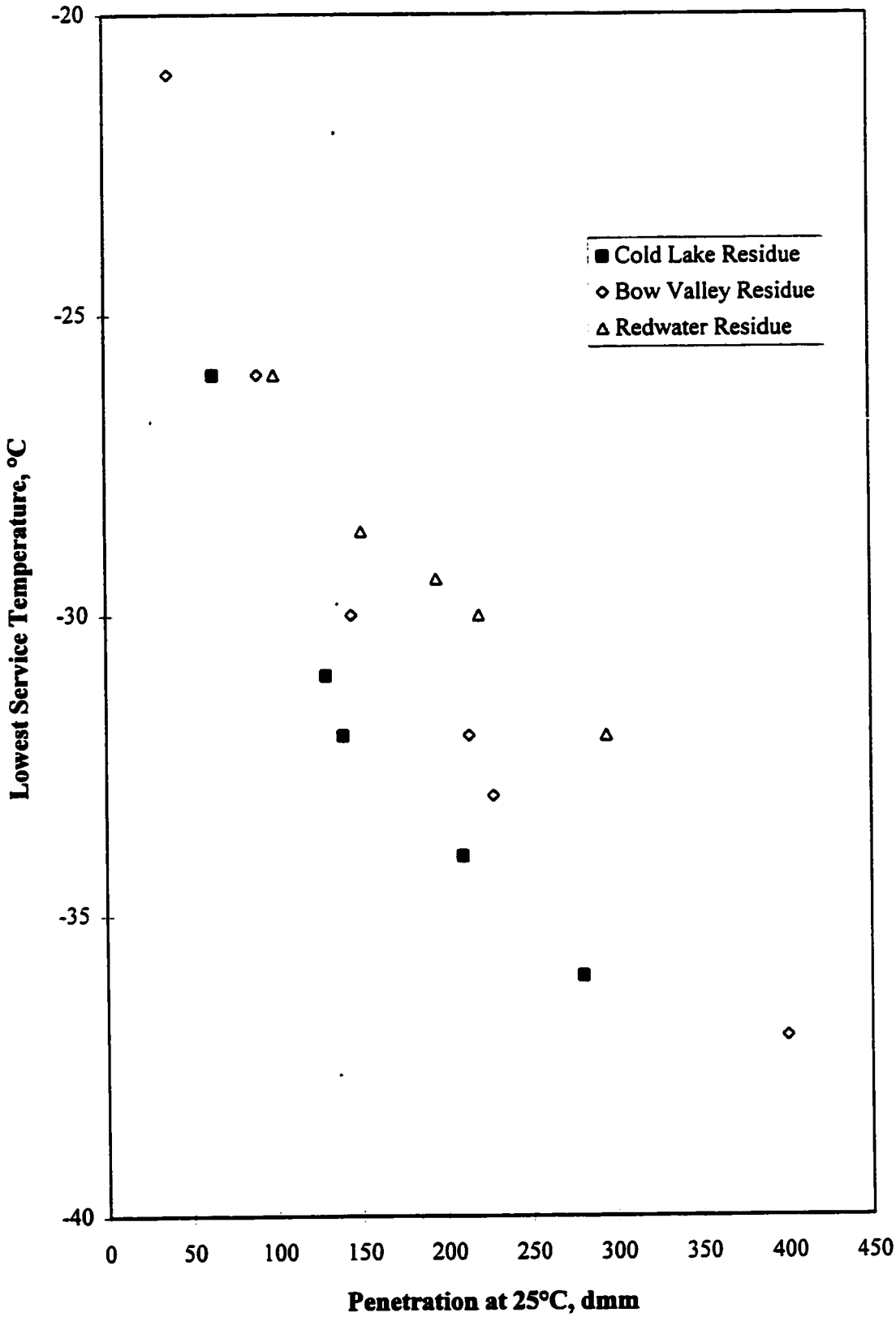

Figure 5.12 - Lowest Service Temperature vs. Penetration at 60°C

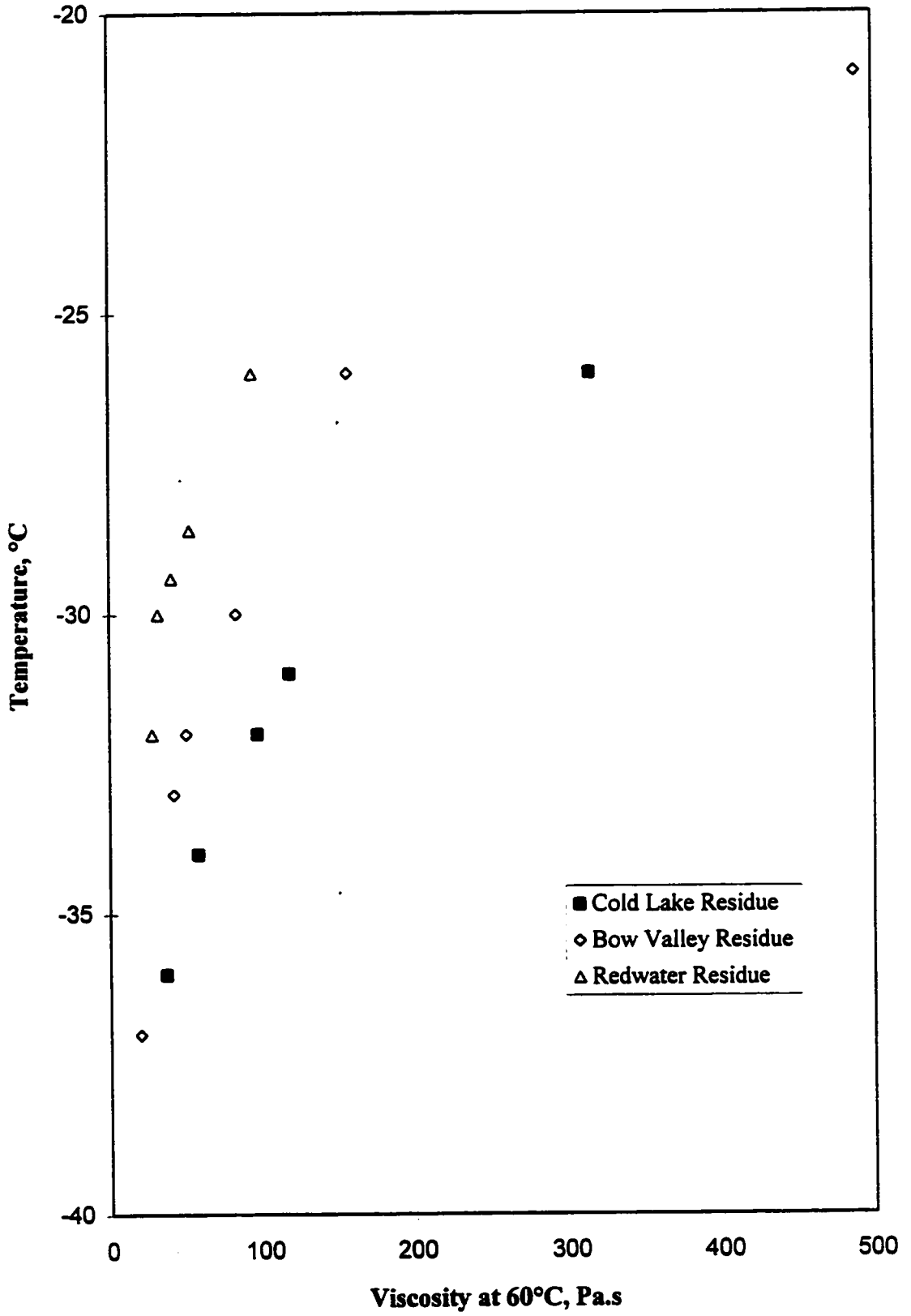

Figure 5.13 - Lowest Service Temperature vs. Viscosity at 60°C

There exists a relationship between the lowest service temperature and penetration or viscosity, but the relationship differs significantly for asphalt specimens prepared from different crude oils. An effort was made to develop a correlation for T_{low} based on penetration and viscosity measurements for paving asphalts which is independent of the crude source. The correlation obtained is as follows :

$$T_{low} = 17.600892 - 1.4379 (\ln X)^2 \qquad (5.9)$$

where $X = Pen_{25°C} * (\ln(\eta_{60°C}))^{1.4} / (\ln(Pen_{25°C}))^{0.8}$

The r^2 for this correlation is 0.9524 which is very good. This correlation is purely an empirical one and it is difficult to comment on the logic behind this relationship.

The applicability of the proposed correlation was further checked for 18 Husky asphalt samples and the results are reported in Table 5.14.

It can be observed that the average percentage deviation in the predicted T_{low} is less than 2%. and the average absolute deviation is 0.69°C. The low average absolute and percent deviations of predicted lowest service temperature from data indicates that the correlation is excellent for predicting low service temperatures of other regular asphalts also.

The maximum absolute deviation for the prediction of the highest and the lowest temperatures are 3.64°C and 1.57°C respectively, for 16 asphalt samples prepared in the study and 18 Husky asphalt samples. The temperature step between two SHRP grades are 6°C for the both high and low temperatures. Hence, the correlations developed in the study can be used as a reliable estimate for the samples which are in the middle of the temperature bracket. Only the samples on the boundaries of the temperature brackets are of real concern.

Table 5.14 : Validity of Equation 5.9

$\eta_{60°C}$, Pa.s	$Pen_{25°C}$	X	T_{low},°C (BBRTest)	T_{low},°C (Predicted)	Absolute Deviation	Percentage Deviation
210.0	91	285.10	-29	-28.35	0.65	2.25
220.0	91	288.58	-28	-28.54	0.54	1.94
117.0	147	361.18	-31	-32.27	1.27	4.10
100.0	157	364.23	-32	-32.41	0.41	1.30
90.0	168	373.33	-32	-32.83	0.83	2.61
40.5	274	430.60	-36	-35.29	0.71	1.96
47.2	281	465.71	-36	-36.67	0.67	1.86
46.0	288	471.21	-37	-36.88	0.12	0.33
46.4	276	455.75	-36	-36.29	0.29	0.80
45.2	262	431.70	-36	-35.34	0.66	1.84
46.3	279	459.63	-36	-36.44	0.44	1.22
34.0	357	505.30	-37	-38.12	1.12	3.03
35.9	329	481.11	-37	-37.25	0.25	0.67
32.0	378	518.17	-37	-38.57	1.57	4.25
28.5	427	549.13	-40	-39.62	0.38	0.95
26.0	453	556.00	-40	-39.85	0.15	0.38
19.5	512	543.44	-41	-39.43	1.57	3.83
17.9	571	573.74	-41	-40.42	0.58	1.42
Average Deviation					0.69	1.96

The determination of the highest and lowest service temperatures for paving asphalt from DSR and BBR tests is a time consuming process which requires sophisticated rheometers. The sample has to be first aged in RTFO for DSR test and then PAV aged for BBR test. The proposed correlations can predict these temperatures which require penetration

measurement at 25°C and viscosity measurement at 60°C for the original or unaged sample. These measurements can be made by simpler equipments in a shorter time. The proposed correlations can be used to estimate the service temperatures with fairly good accuracy, and hence, SHRP grade of the sample can be estimated with the information obtained from conventional tests.

The correlation for T_{low} can also be of help in selecting initial test temperature for BBR test. As a limited quantity of asphalt is available after PAV aging and a substantially large quantity of sample is required for this test, the proper initial guess for test temperature assumes a great importance.

5.7 Conventional and SHRP Grading of Samples Prepared and Comparison

The asphalt samples prepared for this study were graded as per ASTM penetration based, Alberta, CGSB and SHRP specifications. The grades are reported in Table 5.15. The asphalt specimens prepared from Cold Lake crude conform to CGSB A grades where as BV asphalts conform to both A and B grades. It is not possible to prepare A grade samples from Redwater crude. Redwater asphalt binders are either of B or C grades.

It can be observed from Table 5.15 that for the grades of different samples, there is no definite relationship between conventional and SHRP grades. The asphalt samples prepared from different crude oils which conform to the same CGSB grade, may be of different SHRP grades. For example, both CL4 and BV4 are graded as CGSB 200/300 A, but their SHRP grades are PG 52-34 and PG 52-28. Similarly, the samples which belong to the same SHRP grades, may not have the same CGSB grades. BW4 and RW4 confirm to the same SHRP grade, PG 52-28 but their CGSB grades are different. RW4 and RW5 samples are graded as CGSB 200/300 B and C respectively, but these samples cannot be graded as per SHRP specification. The low temperature service offered by these samples

do not meet the service required by the specification. Similarly, BV5 and BV6 cannot be classified as per SHRP specification as these samples fail either on high or low temperature service requirement.

Table 5.15 : Grades of Asphalt Samples

	Grades			
Sample	Pen	Alberta	CGSB	SHRP
CL1	-*	-	60/70 A	PG 64-22
CL2	120/150	-	120/150 A	PG 58-28
CL3	120/150	-	120/150 A	PG 58-28
CL4	200/300	200/300 A	200/300 A	PG 52-34
CL5	200/300	200/300 A	200/300 A	PG 52-34
BV1	-	-	-	PG 70-16
BV2	85/100	-	80/100 A	PG 58-22
BV3	120/150	-	120/150 A	PG 52-28
BV4	200/300	200/300 A	200/300 A	PG 52-28
BV5	200/300	200/300 B	200/300 B	-
BV6	-	200/300 A	300/400 B	-
RW1	85/100	-	80/100 B	PG 58-22
RW2	120/150	-	120/150 B	PG 52-28
RW3	-	-	150/200 B	PG 52-28
RW4	200/300	200/300 B	200/300 C	-
RW5	200/300	200/300 A	200/300 B	-

* Sample does not conform to any grade as per that specification

5.8 Transformation from CGSB to SHRP Grades for Canada

In this section, the impact of the transformation from present grade represented by CGSB grade to SHRP performance grade on the selection of paving asphalt is discussed. For this study, first the performance grades are predicted for the asphalt conforming to various CGSB grades (Section 5.8.1). Then the performance grade requirement for various locations in Canada are evaluated in Section 5.8.2. The transformation from CGSB to SHRP grade is discussed in Section 5.8.3

5.8.1 Expected SHRP Grade from CGSB Grades

From Figures 5.10 - 5.13, it can been seen that the high and the low service temperatures offered by CL, BV or RW asphalt samples are related to their viscosity or penetration. The T_{high} and T_{low} were estimated for the paving asphalt binders conforming to different CGSB grades from the intrapolation of their viscosity data. From the estimated service temperatures, these samples were graded as per SHRP specification into the performance grades. The expected service temperatures and PGs for these samples are reported in Table 5.16.

It can be observed from the results that the materials conforming to same CGSB grades can have different performance grades. For example, two different Cold Lake asphalt samples of $Pen_{25°C}$ values 80 and 100, belong to CGSB 80/100 A grade, but these samples are graded as PG 64-22 and PG 58-28. Similarly, CL and BV asphalts of $Pen_{25°C}$ value 80 which are graded as CGSB 80/100 A have different SHRP grades, PG 64-22 and PG 58-22 respectively.

5.8.2 SHRP Grades for Various Locations Across Canada

The selection of SHRP grades for the paving asphalt for a particular location is based on the high and low pavement service temperatures. For Canadian cities, these temperatures are calculated as per Canadian SHRP (C-SHRP) model. Federal Highway Administration has recommended a new model, Long Term Pavement Performance Seasonal AC Pavement Temperature (LTPP SAPT) model for estimation of these temperatures across US and Canada. These models are discussed in detail in Appendix C.

To compare the existing CGSB grades with the recommended SUPERPAVE™ performance grades for different parts of Canada, a few locations across the country were selected. The selections were based on the climatic conditions. These locations can be classified into three categories :

- Moderate Climate - Vancouver, Toronto and N.London, PEI
- Cold Climate - Calgary, Saskatoon, Regina and Winnipeg
- Extremely Cold Climate - Yellowknife and Whitehorse

The high and low pavement service temperatures and SHRP grades required for these Canadian cities are summarized in Table 5.17. These temperatures were calculated from both C-SHRP and LTPP-SAPT models (Appendix C). The estimations are made for both 50% and 98% ambient temperature reliabilities. As claimed by US Federal Highway Administration, the LTPP-SAPT model has a better prediction capabilities for the service temperatures compared to the C-SHRP model (Mohseni 1996, Mohseni 1998) the PGs based on the former model has been used to study the transformation from CGSB to SUPERPAVE™ specification.

Table 5.16 : Predicted PGs from CGSB Grades

Asphalt	CGSB Grade	Pen $_{25°C}$	$\eta_{60°C}$ Pa.s	Service Temperature, °C T_{high}	T_{low}	PG
Cold Lake	80/100 A	80	228.56	64.6	-27.5	64-22
		100	165.67	62.4	-29.1	58-28
Bow Valley	80/100 A	80	182.11	63.1	-24.8	58-22
		100	134.15	60.9	-26.7	58-22
Redwater	80/100 B	80	115.12	59.7	-25.5	58-22
		100	88.92	57.8	-26.2	52-22
Cold Lake	120/150 A	120	127.36	60.5	-30.5	58-28
		150	92.32	58.1	-32.2	58-28
Bow Valley	120/150 A	120	104.50	59.0	-28.3	58-28
		150	76.98	56.7	-30.2	52-28
Redwater	120/150 B	120	72.00	56.1	-27.0	52-22
		150	55.62	54.0	-28.2	52-28
Cold Lake	150/200 A	150	92.32	58.1	-32.2	58-28
		200	60.97	54.8	-34.1	52-34
Bow Valley	150/200 A	150	76.98	56.7	-30.2	52-28
		200	51.91	53.5	-32.5	52-28
Redwater	150/200 B	150	55.62	54.0	-28.2	52-28
		200	39.87	51.2	-29.7	-*
Cold Lake	200/300 A	200	60.97	54.8	-34.1	52-34
		300	33.97	49.8	-36.1	46-34
Bow Valley	200/300 B	200	51.91	53.5	-32.5	52-28
		300	29.79	48.6	-35.0	46-34
Redwater	200/300 C	200	39.87	51.2	-29.7	-
		300	24.94	47.0	-31.7	-
Cold Lake	300/400 A	300	33.97	49.8	-36.1	46-34
		400	22.44	46.0	-37.2	46-34
Bow Valley	300/400 B	300	29.79	48.6	-35.0	46-34
		400	20.09	44.9	-36.4	-
Redwater	300/400 C	300	24.94	47.0	-31.7	-
		400	17.87	43.7	-32.9	-

* The material cannot be graded as per performance grade.

Table 5.17 : PG Requirement for Various Canadian Cities

Location	C-SHRP (50%Rel)		C-SHRP (98%Rel)		LTPP (50% Rel)		LTPP (98% Rel)	
	1*	2**	1	2	1	2	1	2
Vancouver	41.8-7.6	46-NA	44.7-14.5	46-NA	45.8-8.9	46-NA	54.4-16.0	58-16
Toronto	49.3-21.3	52-22	54.8-26.3	58-28	51.7-18.3	52-22	62.4-24.3	64-28
N.London	45.6-23.0	46-28	47.8-28.2	52-34	48.8-20.8	52-22	56.7-26.8	58-28
Saskatoon	47.4-33.3	52-34	50.5-40.6	52-46	50.5-31.6	52-34	59.2-39.0	64-40
Regina	48.0-34.2	52-40	52.5-41.3	58-46	50.9-31.6	52-34	60.8-38.9	64-40
Calgary	44.9-29.0	46-34	48.3-35.9	52-40	48.4-27.6	52-28	57.3-34.8	58-40
Winnipeg	48.2-31.6	52-34	51.8-36.7	52-40	51.1-29.3	52-34	60.1-35.3	64-40
Whitehorse	38.9-38.5	NA-40	43.0-45.0	46-46	44.3-39.6	46-40	53.8-46.6	58-NA
Yellowknife	36.9-38.5	NA-40	40.6-42.9	46-46	42.9-40.6	46-46	52.1-46.4	58-NA

* Service temperatures requirement, mentioned as T_{high} - T_{low} ** Performance Grade

5.8.3 Transformation from CGSB to SHRP grade

5.8.3.1 Moderate Climate

The CGSB grade requirement for the cities with moderate climate is 80/100. 'A' grade paving asphalts are prescribed in Toronto and N. London whereas 'C' grade asphalt is allowed to be used for Vancouver.

Toronto and N. London, PEI At ambient temperature "reliability" of 50%, the required PG as per SAPT algorithm is PG 52-22. On comparing the required SHRP grades for these cities with the expected SHRP grades for the CL and BV asphalts confirming to the CGSB grade 80/100 A, it may be concluded that the performance desired for this temperature "reliability" can be achieved by these materials. Even 80/100 B grade material prepared from these crudes are capable of providing that service.

For 98% temperature "reliability", the PGs evaluated as per SAPT model for Toronto and N. London are PG 64-28 and PG 58-28 respectively. PG 64-28 grade cannot be prepared from the crude oils used in this study. Only softer Cold Lake asphalt (Pen ≈ 100) can provide service for N. London for this "reliability".

This observation seems to be very conservative when the actual pavement temperatures calculated as per SAPT algorithm and the expected services from the prescribed CGSB grades are compared. The low pavement temperature for Toronto based on 98% "reliability" of ambient temperature is -24.3°C. The harder BV asphalt (Pen ≈ 80), which provides worst low temperature performance among the above-mentioned asphalts, can be used for the low temperature service requirement down to -24.8°C. When this material is graded as per SHRP specification, it is considered to be fit for application till -22°C only and hence cannot be used for Toronto for desired "reliability" of 98%. The wide temperature difference of 6 degrees between two SHRP grades makes the requirement more stringent. Because of this, even the better quality asphalt can be graded as low "reliability" material.

For 98% temperature "reliability", the PGs evaluated as per C-SHRP model for Toronto and N. London are PG 58-28 and PG 52-34 respectively. Only softer Cold Lake asphalt (Pen ≈ 100) can provide service for Toronto for this "reliability". The CGSB grade 80/100 A will fail to provide service offered by PG 52-34 grade required for N. London. The CGSB 150/200 A grade Cold Lake Asphalt material can be used for this service.

Vancouver Asphalt samples of low quality, 80/100 C, are allowed to be used in the city of Vancouver. Since the residue obtained from the worst material used in this work, Redwater crude is of better quality, it is difficult to comment on the "reliability" of 80/100 C material. As per SAPT algorithm, PG 46-10 can provide service with 50%

"reliability" but there is no such grade in SHRP specification. For the SHRP grade confirming to high temperature of 46°C, the highest low pavement temperature is -34°C. It is advisable to introduce more grades with higher low pavement temperatures.

CGSB 80/100 A asphalt sample prepared from CL and BV crude oils can provide the service required for 98% temperature "reliability" whereas CGSB 80/100 B asphalt prepared from RW will fail to provide that service. Hence, it can be concluded that lower CGSB grade (80/100 C) cannot be used for the higher temperature "reliability".

5.8.3.2 Cold Climate

The CGSB grade requirement for the cities with cold climate is 150/200 A. The asphalts of this grade have been prepared from Cold Lake and Bow Valley crudes.

Winnipeg, Saskatoon and Regina As per SAPT model, the required PGs for the ambient temperature "reliability" of 50% and 98% are PG 52-34 and PG 64-40 respectively. The requirement for 50% reliability is same if estimated using C-SHRP model. Except for softer CL asphalts (Pen ≈ 200), no other specimens which conform to 150/200 A, can provide the service even for 50% ambient temperature "reliability". The asphalt will fail to provide the low temperature service.The comparison of actual low temperature requirement and expected service from these asphalts shows that all material barring BV asphalts of Pen ≈ 150 can provide the service with 50% "reliability". The PGs requirement for 98% "reliability" estimated by C-SHRP model cannot be met by this grade material.

Calgary The City of Calgary recommends use of 150/200 A grade paving asphalt. Any asphalt sample prepared from CL and BV crudes in this penetration range, is expected to provide the service with 50% temperature "reliability" for both SAPT and C-SHRP

model. The low temperature service desired for 98% temperature "reliability" cannot be provided by the asphalts prepared from the oils used in this study.

5.8.3.3 Extremely Cold Climate

Softer material confirming to CGSB grade 200/300 A is used for places like Whitehorse and Yellowknife. The required SHRP grade estimated by SAPT model for Yellowknife is PG 46-46 for 50% "reliability". PG 46-40 will be required for Whitehorse for this "reliability". The expected low service temperature for these places for 98% reliabity is lower than -46°C which is the lowest limit for any performance grade. Hence, it is not possible to classify the required material under statutory performance grade. The high temperature service is s achievable from the currently used CGSB grade but no material prepared from the crude oils used in this work is capable of providing the required low temperature service.

Similar to SAPT model, the PGs required as per C-SHRP model for Yellowknife and Whitehorse for either 50% or 98% "reliability" cannot be provided by the curently used asphalts.

(Note : Experimental results for the empirical and performance-based characterization of the prepared asphalt samples are compiled in Appendix E)

CHAPTER 6
Rheological Characterization

In this chapter, rheological characterization of the selected asphalt samples has been done based on elaborate rheological measurements. Two asphalt samples, which are predicted to provide different performance as per SUPERPAVE™ specification in the previous part of study, were selected to investigate the differences in their rheological behavior.

Asphalt, according to the majority of authors and experimental evidence, is a multidisperse micellar system (Yen, 1982, Speight and Long, 1982). The study of its internal structure is difficult because of its high viscosity and the complexity of its components. The most of studies are done in a solvent, which depending on its type, inadvertently changes the asphalt structure. The results of tests conducted on such diluted materials contribute considerably to our knowledge of the material which are however not sufficient enough. Thus, if one can find a less invasive method, which does not rely on dissolution of a sample, one can obtain additional information about the real internal structure of asphalt. In this part of the study, an attempt has been made to use the rheological characterization of asphalts for a study of their molecular weight distribution.

6.1 Linear Viscoelasticity

6.1.1 Viscoelastic Behavior

To understand mechanical property of any material it is necessary to know its stress-strain or rate of strain behavior which tells how a material will deform when load is applied on it. In characterizing the stress-strain behavior in the laboratory, the simple test methods are shear and extension/flexure tests. The creep, stress relaxation and dynamic loading are

three different modes of loading. Such tests may be conducted under a constant stress, constant strain, gradually increasing stress or gradually increasing strain.

Materials for which the stress-strain relationship is linear and the response is immediate, are known as elastic solids. After removal of stress, the deformation is recovered and the material regains its original shape. On the other hand, Newtonian fluids exhibit a linear relationship between stress and the rate of change of strain. In these materials, the deformation cannot be recovered even after removal of load. Materials such as asphalts, which exhibit both elastic and viscous behavior are called viscoelastic. In these materials only a part of deformation is recovered on removal of load.

6.1.2 Linear Viscoelastic Behavior

The elastic, viscous and viscoelastic behavior discussed above relate to linear behavior. In a simplified picture of the linear behavior, the deformation at any time and temperature is directly proportional to the applied force. Non-linear viscoelastic response is extremely difficult to characterize in the laboratory and to apply to engineering problem (Christensen 1992). The constitutive equations for the non-linear viscoelastic behavior are very complicated and difficult to solve (Rudraiah and Kaloni 1986).

For these reasons, in this work, characterization of the asphalt has been considered only for linear viscoelastic region.

6.2 Rheological Properties/ Viscoelastic Functions

From the three common loading modes (creep, stress relaxation, dynamic testing) and the two general geometries (shear and extension/flexure), there are six commonly used linear viscoelastic functions (Ferry 1980, Petersen et. al. 1994b) :

1. Creep compliance in shear, J(t)
2. Creep compliance in extension or flexure, D(t)
3. Relaxation modulus in shear, G(t)
4. Relaxation modulus in extension or flexure, E(t)
5. Dynamic complex modulus in shear, G*(ω)
6. Dynamic complex modulus in extension or flexure, E*(ω)

Various other viscoelastic functions like dynamic viscosity, dynamic complex compliance etc. can be defined through the dynamic complex modulus.

6.2.1 Dynamic Mechanical Analysis

In the most common method of dynamic mechanical analysis, a sinusoidal strain is applied to a specimen, and the resulting stress is monitored as a function of frequency. The material function in such an experiment is the complex modulus G*(ω) or the complex viscosity $\eta^* = G^*(\omega)/i\omega$. In a strain controlled testing, the complex modulus is computed using the following equation:

$$G^*(\omega) = \tau^*(\omega)/\gamma^*(\omega) \qquad (6.1)$$

where $\tau^*(\omega)$ is the complex shear stress response, Pa, and
$\gamma^*(\omega)$ is the complex shear strain, m/m

In reporting the results of dynamic mechanical analysis, three other functions are used : the storage modulus G'(ω), the loss modulus G''(ω) and the phase angle δ(ω). These functions are related to the complex modulus and can be computed by following equations,

$$G'(\omega) = |G^*(\omega)| \cos\delta(\omega) \tag{6.2}$$

$$G''(\omega) = |G^*(\omega)| \sin\delta(\omega) \tag{6.3}$$

The storage modulus represents the in-phase component of the complex modulus while the loss modulus represents the out-of-phase component of the complex modulus. They are named so as the storage modulus characterizes the elastic or recoverable part of the complex modulus whereas the loss modulus represents the viscous or non-recoverable part.

In strain controlled dynamic testing, the phase angle $\delta(\omega)$ indicates the lag in the stress response compared to the applied strain. For stress controlled experiment, $\delta(\omega)$ represents the lag in the strain response compared to the applied stress. For purely elastic materials, the phase angle will be zero, whereas for purely viscous materials, the phase angle will be 90°. Thus, the phase angle is an important parameter for describing the viscoelastic properties of materials such as asphalt. The phase angle is calculated as follows,

$$\tan\delta(\omega) = \frac{G''(\omega)}{G'(\omega)} \tag{6.4}$$

The complex modulus can be expressed in the following two form of any complex function:

$$G^*(\omega) = |G^*(\omega)| \exp[i\delta(\omega)], \tag{6.5}$$

or

$$G^*(\omega) = G'(\omega) + iG''(\omega) \tag{6.6}$$

6.2.2 Linear Viscoelastic Models

It is often desirable to describe the material function, G* in our case, in the form of a model which can describe the rheological properties of the material. Since the mechanical response of asphalt, like other viscoelastic materials, is a function of time and temperature, an infinite number of loading conditions and responses constitute its overall behavior. In some situations, it is necessary to know the response of an asphalt sample at loading frequency and temperatures different from those on which directly measured data are available. Mathematical models allow such calculations to be made directly and quickly in a repeatable fashion. Furthermore, the mathematical model can be used for approximate conversions from one viscoelastic function to another.

Maxwell model is the perhaps the most common model for complex modulus. The model is extensively used for the polymers and other viscoelastic materials. The model is,

$$G^*(\omega) = \sum_{k=1}^{n} \frac{g_k i\omega\lambda_k}{1 + i\omega\lambda_k} \tag{6.7}$$

where λ_k are the relaxation times and g_k are the weighing factors.

Stastna et. al. (1996) and Zanzotto et. al. (1996) have used following fractional model in rheological characterization of asphalts,

$$G^*(\omega) = i\omega\eta_0 \left[\frac{\prod_{1}^{m}(1 + i\omega\mu_k)}{\prod_{1}^{n}(1 + i\omega\lambda_k)} \right]^{\frac{1}{n-m}} \tag{6.8}$$

where η_0 is the zero shear rate viscosity,

λ_k, μ_k are the relaxation times and $m < n$

In this study both of these models have been used for the characterization of asphalt.

6.2.3 Time-Temperature Superposition

One of the primary analytical techniques used in analyzing the dynamic mechanical data for the viscoelastic materials involves construction of master curves for the complex modulus and phase angle. In constructing such master curves, the time-temperature superposition principle is used (Ferry 1980). In oscillatory experiments, the dynamic data are first collected over a range of temperatures and frequencies. A reference temperature is selected. The data at all other temperatures are then shifted with respect to time until the curves merge into a single smooth function. The advantage of this exercise is that we can have a master curve for the material at a certain temperature over a wide range of deformation or frequencies which is otherwise not possible to determine experimentally.

The amount of shifting required at each temperature to form the master curve is of special importance, and is called the shift factor, a(T). A plot of logarithmic of a(T) versus temperature is generally prepared in conjuction with the master curve. This type of plot gives an indication of how the properties of a viscoelastic material changes with temperature. The master curve at a reference temperature can be shifted to get master curve at any other temperature from the relationship between a(T) and temperature. The shifted frequency, frequency multiplied by a(T) is termed as the reduced frequency.

For asphalts, the relationship between a(T) and T is generally expressed by Williams-Landel-Ferry (WLF) equation (Williams et. al. 1955) or by Arrhenius type relationship (Christensen 1992).

WLF Equation

$$\log a(T) = \frac{-C_1(T - T_d)}{C_2 + (T - T_d)} \tag{6.9}$$

where C_1 ans C_2 are empirically determined coefficients and T_d is the reference temperature.

Arrhenius Type Relationship

$$\log a(T) = \frac{E_a}{R}\left(\frac{1}{T} - \frac{1}{T_d}\right) \tag{6.10}$$

Where E_a is the activation energy for the flow and R is the ideal gas constant.

6.3 Molecular Weight Distribution from Rheological Measurements

It is known that the rheological properties of viscoelastic materials such as polymers are strongly dependent on molecular weight (Ferry 1980). Generally it is possible to invert such a relationship and obtain the molecular weight distribution (MWD) from the measured material functions. Considerable efforts have been made developing procedures for determination of MWD for polymeric materials based on rheological measurements (Peticolas 1963, Wu 1984, Tuminello 1986, Tuminello 1987, Wu 1988, Paula and Dealy 1996, Lavallee and Berker 1997). Even though there are well established techniques for determining molecular weight distribution i.e. size exclusion chromatography (SEC), researchers have strived to develop alternate methods. This is because SEC requires a dilute solution and making such solutions is not always practical. Notable examples are

poly-tetrafluoroethylene and other copolymers of this family. A few solvents have been found for these polymers, but the extreme temperatures required make their use impractical. In the case of asphalt, its internal structure can be changed by the dilution and the molecular weight distribution obtained from such experiment may not reflect the state of material in individual form.

Many of the techniques used for the rheological characterization of asphalt were originally developed for polymers. The polymers are the well studied materials for which rheological properties match to some extent with asphalts. But, care should be taken in drawing direct parallels between polymers and asphalts. There are numerous differences between properties of asphalts and polymers. The molecular weights of commercial polymers typically lie in the range 10,000-100,000 whereas the number average molecular of typical paving grade asphalts is between 500 and 2,000 (Christensen 1992, Zanzotto et al. 1996). Another difference is in the homogeneity of polymers whereas asphalts are highly heterogenous materials and are composed of infinite variety of molecular types. There are however some important concepts in polymer chemistry which can be effectively applied to asphalts. For example, it is evident that as for polymers, the molecular weight of asphalts plays an important role in determining its physical properties, although the mechanism is probably much different from that which is effective in much higher molecular weight polymers (Christensen 1992).

Recently Zanzotto et al.(1996) have characterize asphalts by their complex moduli and phase angles, and determined molecular weight distribution using the following relationship:

$$\delta(\omega) = \int_0^\infty W(M')\, c(M', \omega)\, dM' \qquad (6.11)$$

where c(M,ω) represents the monodisperse phase angle and W(M) is the weight distribution function. Considering the following step form of c(M, ω) :

$$c(M, \omega) = [\, 1 - H(M' - M) \,] \tag{6.12}$$

where H represents the Heaviside function and the frequency region (ω) is related to the mass region (M) by a simple power law :

$$M = k\omega^{-\alpha} \tag{6.13}$$

where k and α are constants.

For the normalized W, it follows from Equations 6.11, 6.12, and 6.13 that

$$\delta(\omega) = 1 - \int_{M=k10^{-\alpha x}}^{\infty} W(M')dM' \tag{6.14}$$

Denoting, x = log ω and differentiating the last equation yields

$$W(M) = -\frac{10^{\alpha x}}{\alpha k \ln 10}\frac{d\delta}{dx} \tag{6.15}$$

Thus, in principle, it is possible to obtain additional information about the structure of asphalt from the study of the phase angle. The following forms of |G*| and δ are generated by equation 6.10

$$|G^*(\omega)| = \eta_o \omega \left[\frac{\prod_{1}^{m}(1+(\omega\mu_k)^2)}{\prod_{1}^{n}(1+(\omega\lambda_k)^2)} \right]^{1/2(n-m)} \tag{6.16}$$

$$\delta(\omega)=\frac{\pi}{2}-\frac{1}{(n-m)}\left[\sum_{1}^{n}a\tan(\omega\lambda_k)-\sum_{1}^{m}a\tan(\omega\mu_k)\right] \qquad (6.17)$$

Calculating the limit of equation 6.16 at infinity, one obtains

$$\lim_{\omega\to\infty}|G^*(\omega)| \equiv G_N=\eta_o\left[\frac{\mu_1\mu_2....\mu_m}{\lambda_1\lambda_2....\lambda_n}\right]^{1/(n-m)} \qquad (6.18)$$

If, in asphalts as in polymers, the zero shear rate viscosity is proportional to a power of M, then from Equation 6.18 it follows that,

$$G_N = AM^b\left[\frac{\mu_1\mu_2....\mu_m}{\lambda_1\lambda_2....\lambda_n}\right]^{1/(n-m)} = AM^b\bar{\lambda}^{1/(n-m)} \qquad (6.19)$$

where A and b are constants. Introducing a characteristic frequency $\bar{\omega}=2\pi/\bar{\lambda}$, we can write

$$M=\left[\frac{2\pi G_N}{A}\right]^{1/b}\omega^{-1/b}\equiv k\left(\bar{\omega}\right)^{-\alpha} \qquad (6.20)$$

Thus, the molecular weight domain (M) is related to the frequency domain via a transformation given in Equation 6.20. This form of equation ($M \sim \omega^{-\alpha}$) has frequently been used (Ferry 1980, Tuminello 1986). A very good correlation of M with frequency for narrow-distribution polystyrenes was shown by Tuminello (1986). It can be noted that Equation 6.20 leads to the known relationship $\eta_o \sim M^b$, which is applicable to

polydisperse systems (Ferry 1980, Tuminello 1986, Bird et. al. 1987). The correlation of M and $\bar{\omega}$ given in Equation 6.20 can be written as

$$\log M = \log k - \alpha \log \bar{\omega} \tag{6.21}$$

Zanzotto et. al.(1996) have reported $\alpha = 0.1231$ and $\log k = 2.976$ after studying 12 regular asphalts samples from vapor pressure osmometry measurements. Thus using Equation 6.15, one can calculate W from the derivative of the phase angle, and using the transformation Equation 6.21, the molecular weight distribution can be obtained.

The procedure used for $\delta(\omega)$ can also be repeated for the magnitude of the complex modulus, $|G^*|$. Assuming, in accordance with Tuminello (1986) , that

$$\left[\frac{|G^*(x)|}{G_N}\right]^{1/2} = 1 - \int_0^M W(M')\, dM' \tag{6.22}$$

one can again simply calculate the molecular weight distribution function as follows:

$$W(M) = \frac{10^{\alpha x}}{\alpha k \ln 10} \frac{d}{dx}\left[\left(\frac{|G^*|}{G_N}\right)^{1/2}\right] \tag{6.23}$$

Wu (1984) used G' in place of magnitude of complex modulus in Equation 6.23 for determination of MWD of polystyrene. The weight distribution function thus obtained is

$$W(M) = \frac{10^{\alpha x}}{\alpha k \ln 10} \frac{d}{dx}\left[\left(\frac{G'}{G_N}\right)^{1/2}\right] \tag{6.24}$$

6.4 Measurement of Complex Modulus : Experimental Work

6.4.1 Material

For the rheological characterization, samples of asphalt from Cold Lake crude oil (CL 4) and Redwater crude oil (RW 4) were selected. Both of these samples are of Pen 200/300 grade.

6.4.2 Equipment and Experimental Procedure

Bohlin VOR Rheometer was used in this study for carrying out rheological experiments on the selected asphalt samples. The principle of operation is that a controlled shear strain or shear rate is applied to the sample and the resulting shear stress s monitored. Figure 6.1 shows the principal parts of the rheometer.

Small amplitude, position controlled, angular deflection is used in the oscillation mode. This motion is obtained through the position servo actuator with the clutch engaged. The frequency of a digitally generated sine wave is set from the software by a programmable divider. For the existing configuration, the frequency range used is 10^{-3} Hz to 20 Hz. The temperature is measured by the sensor in the cryogenic oven. The normal temperature range used is -30°C to +60°C. The temperature is controlled by liquid nitrogen and the hot air. The torque measurement involves both the torque bar and LVDT. The choice of torque bar determines the sensitivity, while the small angular deflections measured by the LVDT gives the desired torque signal to the software

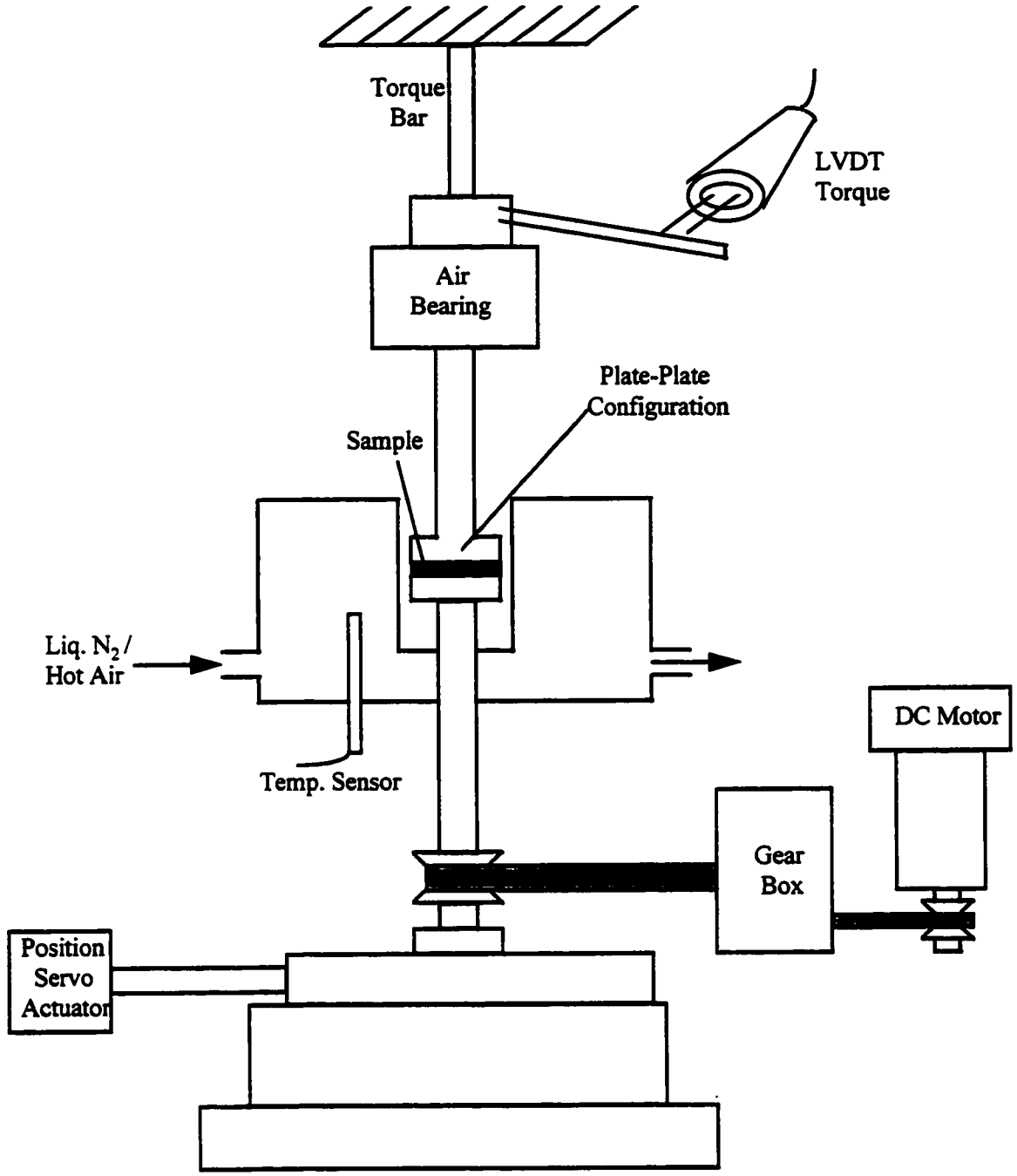

Figure 4.1 - Bohlin VOR Rheometer

The test conditions (temperature and frequency) are summarized in Table 6.1 . Parallel plate configuration was used to apply the oscillatory shear. The diameters of the plates selected at different temperatures are mentioned in Table 6.2.

Table 6.1 : Test Conditions

Sample	Temperature, °C	Frequency Range, Hz
Cold Lake	-30, -20, -10, 0, 20, 40, 50, 60	0.01 - 20
Redwater	-30, -20, -10, 0, 20, 40, 50	0.01 - 20

Table 6.2 : Diameter of Plate-Plate Configuration

Temperature, °C	Plate Diameter, mm	Gap Between Plates, mm
-30	6	1.5-2
-20	6	1.5-2
-10	6	1.5
0	10	1.5
20	25	1-1.5
40	25	1-1.5
50	30	1
60	30	1

6.5 Complex Modulus and Phase Angle Measurement : Results and Discussion

The measurements of complex moduli and phase angles were made for the selected samples at various temperatures. The results are reported in Appendix D. The G' and G" for Cold Lake asphalt at various temperatures are plotted in Figure 6.2 and 6.3 respectively. The same plots for Redwater asphalt are given in Figure 6.4 and 6.5.

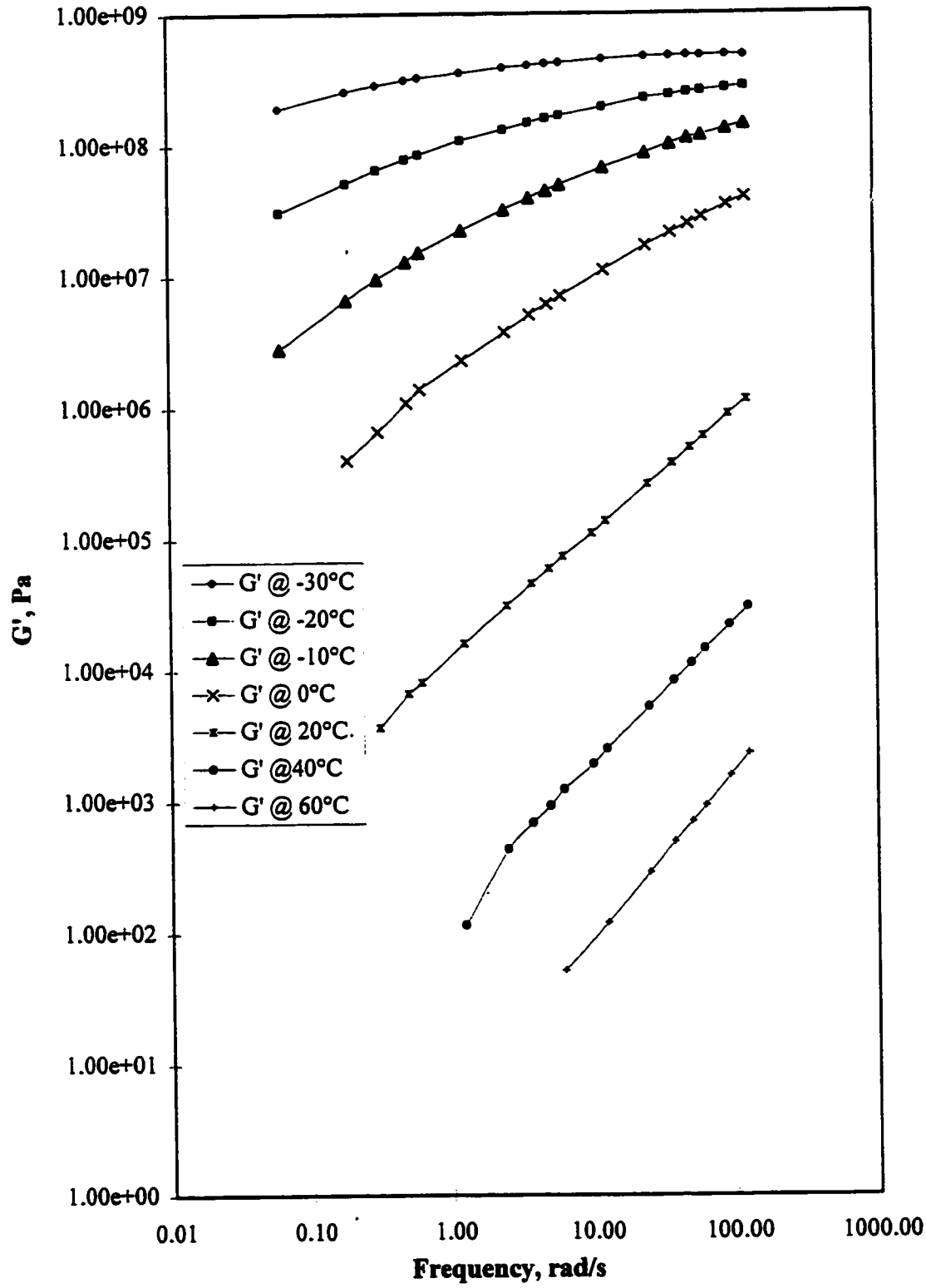

Figure 6.2 - Cold Lake Asphalt : Storage Modulus

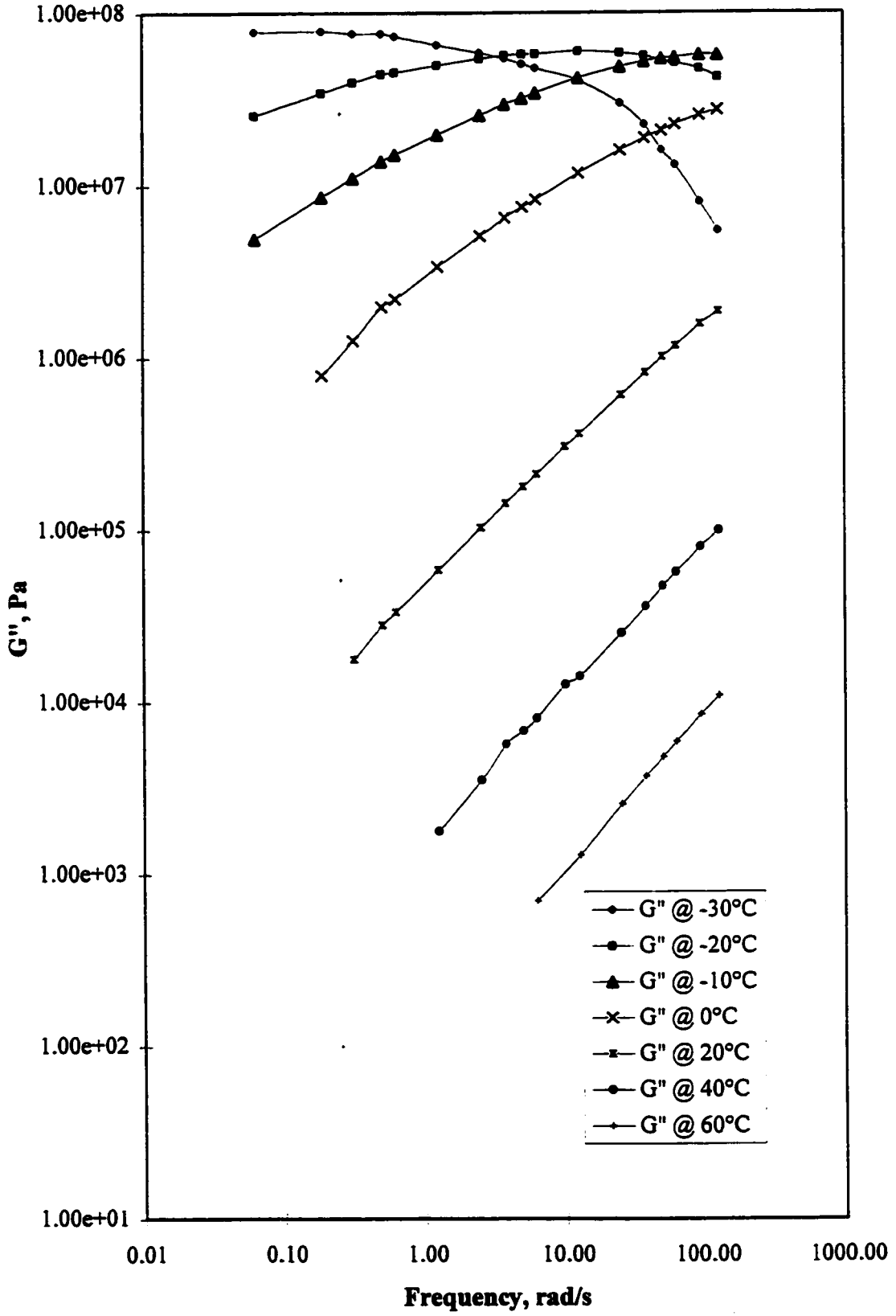

Figure 6.3 - Cold Lake Asphalt : Loss Modulus

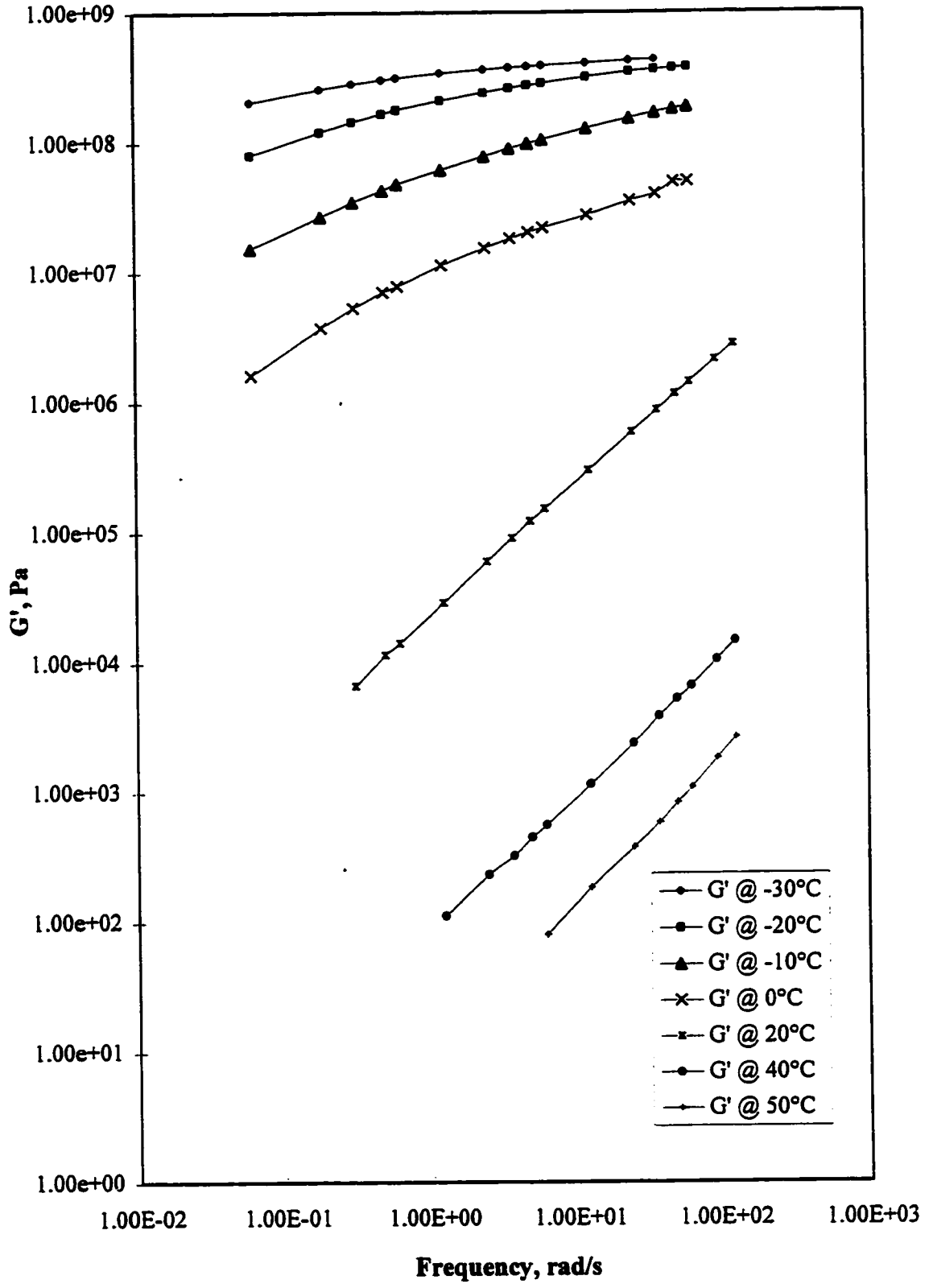

Figure 6.4 - Redwater Asphalt : Storage Modulus

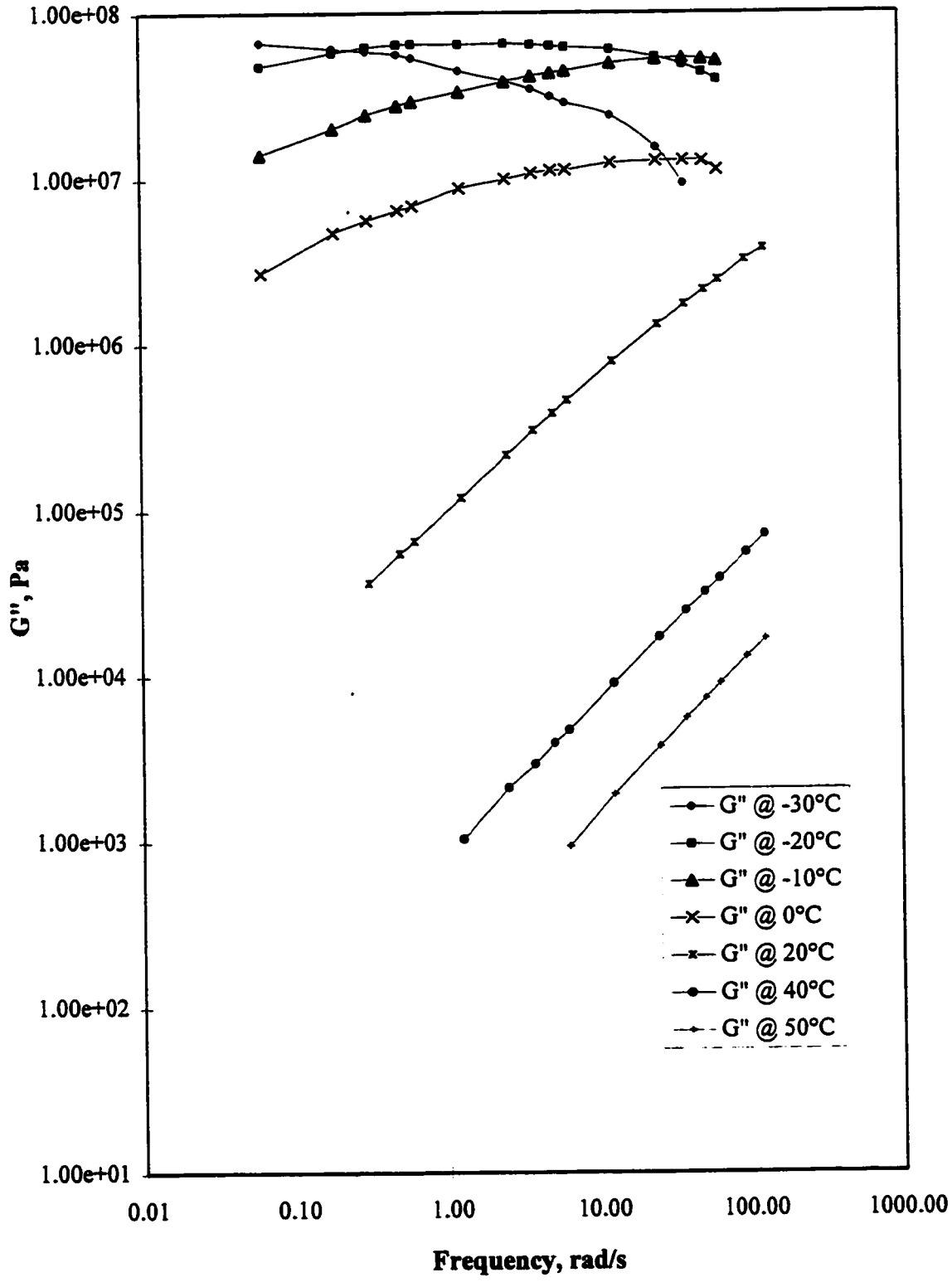

Figure 6.5 - Redwater Asphalt : Loss Modulus

6.5.1 Time-Temperature Shift

The time-temperature superposition principle explained in Section 6.4 was used to create the master curves for the components of complex modulus and the loss tangent. This was achieved by using a rheological software, IRIS developed by Baumgaertel, Soskey and Winter (1987). The values of G' and G'' measured by Bohlin VOR Rheometer at various temperatures over a range of frequency are fed to this software as the input data. The data are then shifted manually or automatically to construct the master curve. The software calculates the shift factors and express them with WLF and Arrhenius parameters. The reference temperature was selected as 20°C. The shift factors for CL 4 and RW 4 are reported in Table 6.3 and 6.4 respectively and plotted in Figure 6.6.

Table 6.3 : Shift Factors for Cold Lake Asphalt Sample

No.	Temperature ,K	log a (T)
1	243	7.21
2	253	5.35
3	263	3.92
4	273	2.65
5	293	0.00
6	313	-1.75
7	333	-2.86

The parameters of WLF equation, C_1 and C_2 for logarithmic of shift factor, log a(T) of Cold Lake asphalt sample are 12.79 and 130.59 K, respectively. The parameters for Redwater asphalt are 46.21 and 394.94 K, respectively. The Arrhenius equation parameter, E_a/R for Cold Lake and Redwater asphalt samples are 21181 K and 21546 K, respectively. The WLF equations has lower standard deviations compared to Arrhenius equations for both samples and hence appears to be more suitable in characterizing time-

temperature superposition for these samples. The shifted frequency which is a product of actual frequency and a (T) is also termed as reduced frequency.

Table 6.4 : Shift Factors for Redwater Asphalt Sample

No.	Temperature, K	log a (T)
1	243	6.21
2	253	5.00
3	263	3.73
4	273	3.03
5	293	0.00
6	313	-2.29
7	323	-3.03

On comparison of log a(T) vs. temperature curves (see Figure 6.6) for both samples, it can be seen that the values of log a(T) for both samples are close in the range of -20°C (253 K) to 30°C (303 K). But a difference in the values can be seen for higher as well as lower temperatures where the values of shift parameter are higher for CL4 compared to that of RW4.

6.5.2 Master Curves of CL4 and RW4

The master curves for the loss modulus of CL4 and RW4 samples are made at 20°C and plotted in Figure 6.7. The curves for both samples attain a maximum value and then the value of G" is decreasing. The maxima are positioned on the higher frequency side of the plot which demonstrates the behavior at lower temperatures. The peak in the master curve for G" characterizes the glass transition stage. It can be seen from the curves that Redwater asphalt sample approaches glass transition at lower frequency compared to Cold Lake asphalt sample. As per SHRP testing performed in previous chapter, the

lowest service temperature down to which RW4 sample can be used is -30°C whereas CW4 can provide service down to -34°C. The positioning of the maxima of G" may be attributed as a probable reason for this behavior, but it is difficult to quantify its effect.

The master curve for the storage modulus of CL4 and RW4 samples are also made at 20°C and plotted in Figure 6.8. The curves for both samples attain a maximum value at higher frequency and G' remains approximately constant after that. The maximum value of storage modulus is 3.5×10^8 Pa for CL4 and 1×10^8 Pa for RW4.

The master curve for the phase angle of CL4 and RW4 samples are made at 20°C and plotted in Figure 6.9. It can be seen from the curves that the values of δ are similar for both samples at the lower frequencies. The values of δ are lower for Redwater sample at the reduced frequencies higher than 1×10^2 rad/s. From the extrapolation of master curves, we can see that RW4 will approach to zero phase angle at approximately 1×10^8 rad/s. CL4 will have zero phase angle at approximately 2×10^8 rad/s. The zero phase angle signifies the elastic behavior of a material and hence it can be inferred that Cold Lake asphalt sample will attain fully elastic behavior at higher frequency or lower temperature compared to Redwater asphalt sample.

In SUPERPAVE™ specification, the dynamic mechanical testing is carried out at 10 rad/s. From the master curves of G', G" and G*/ sin δ, it can be observed that the selected asphalt samples exhibit a stable behavior at this deformation rate. There is no appreciable change in there behavior in the neighborhood of 10 rad/s. The nature of curves are different at the higher frequency region which is the region of rapid loading Hence, the prediction of performance for 10 rad/s may not be applicable for the rapid loading scenario. This advocates against the testing at a single point as prescribed by SHRP program.

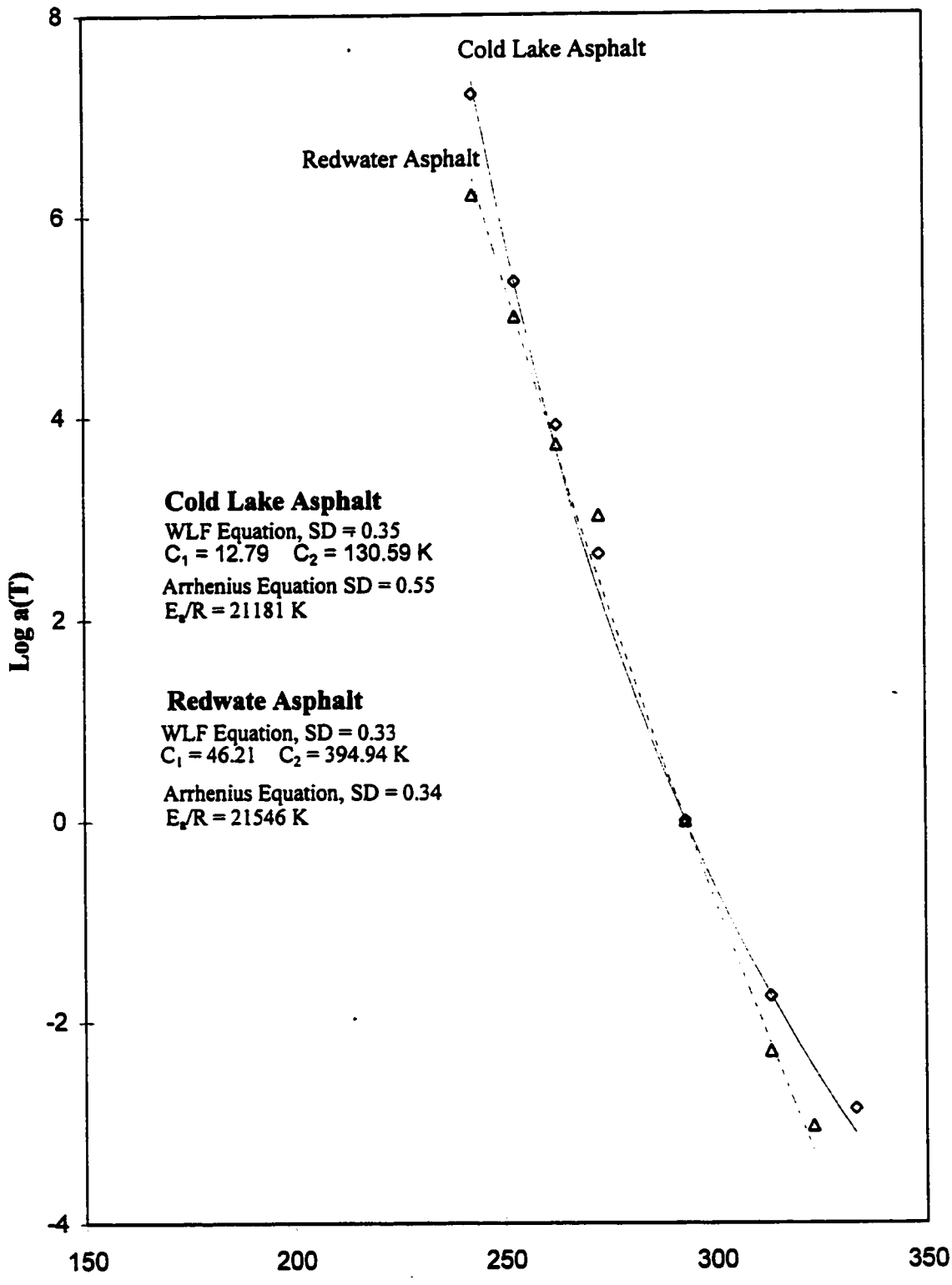

Figure 6.6 - Shift Factors vs. Temperature

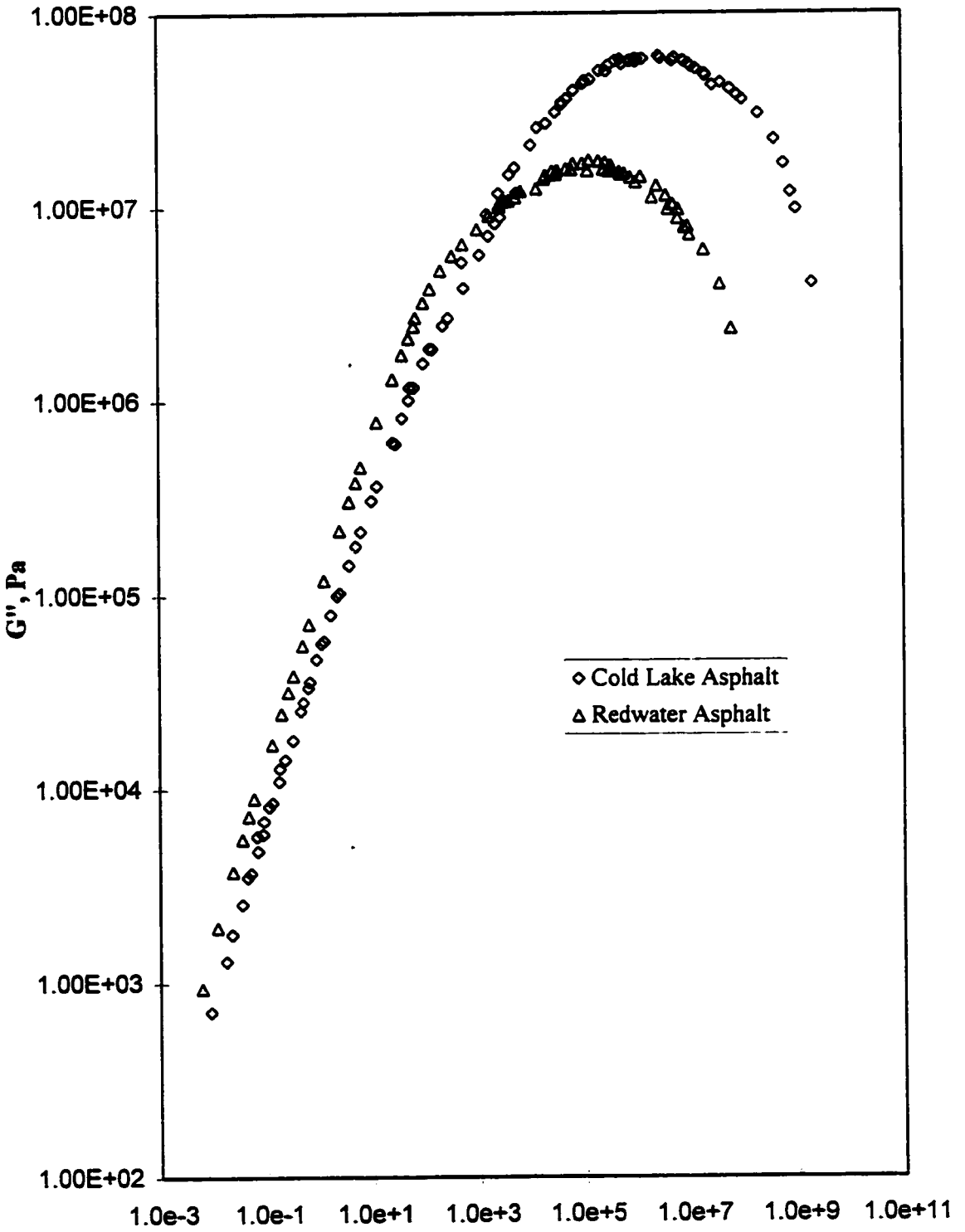

Figure 6.7 - Master Curve for Loss Modulus at 20°C

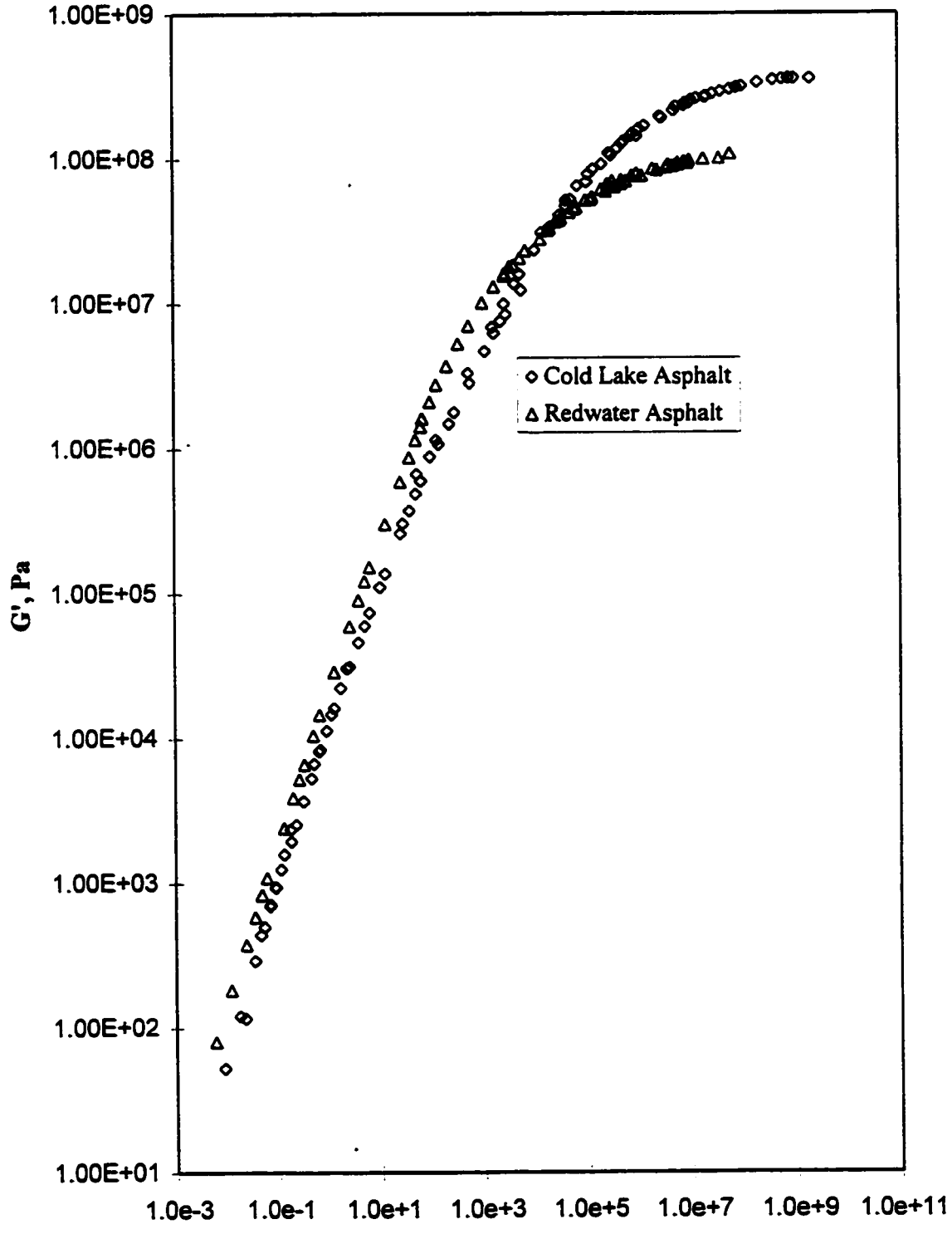

Figure 6.8 - Master Curve for Storage Modulus at 20°C

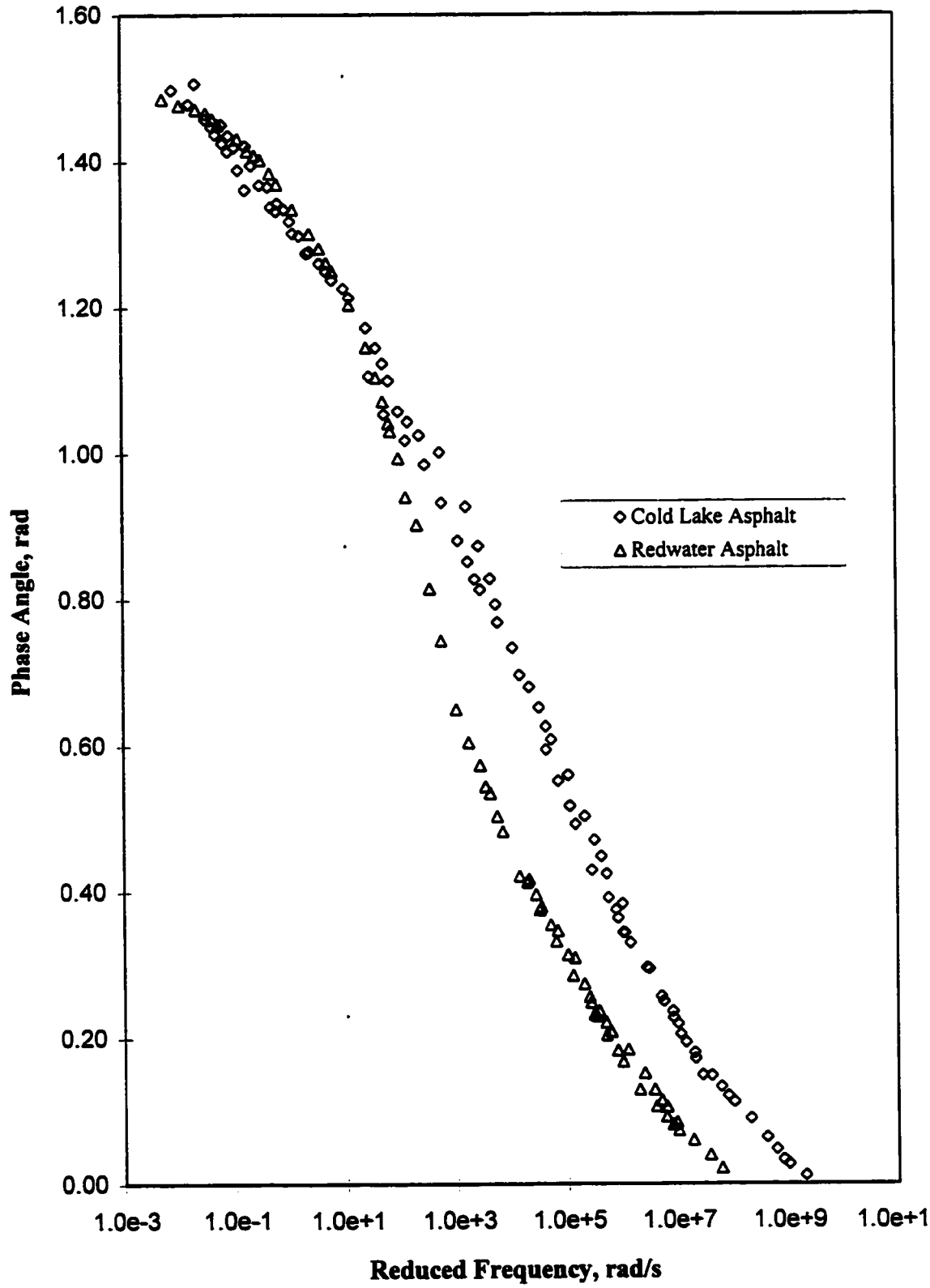

Figure 6.9 - Master Curve for Phase Angle at 20°C

6.5.3 Comparison of DSR and VOR Results

SHRP specification prescribes the limiting value of G*/sin δ at the test temperature as greater than 1 kPa while carrying out the dynamic shear testing at 10 rad/s. In previous part of our study, this parameter was measured by DSR and the test temperature obtained for CL4 and RW4 were 55°C and 51°C, respectively. To compare the results of DSR and VOR, the master curve for G*/ sin δ was developed at 20°C from the |G*| and phase angle measured by VOR. The master curve gives relationship of G*/ sin δ with reduced frequency. From WLF equations for our samples, the estimated shifting parameter, log a(T) for CL4 at 55°C is -2.70. The same shifting parameter for RW4 at 51°C is -3.36. Hence, actual test frequency of 10 rad/s will be reflected on reduced frequency scale as 1.98×10^{-2} rad/s for CL4 and 4.37×10^{-3} rad/s for RW4. The value of G*/ sin δ for CL4 and RW4 samples at these reduced frequencies are 1.2 kPa and 1.0 kPa respectively (Figure 6.10). These results show that there is a good agreement between VOR and DSR results. It also brings froth the adequacy of time-temperature superposition principle in describing the rheological behaviour of material at different conditions.

6.6 Modeling of Complex Modulus and Phase Angle

The master curves for Cold Lake and Redwater asphalt samples which were developed in the previous section, were modeled by Maxwell's model (Equation 6.9) and fractional model (Equation 6.10). The parameters of the Maxwell's equation were determined by IRIS program and are reported in Table 6.3. Cold Lake asphalt sample requires 29 parameters compared to 27 parameters required by Redwater sample. The plot of G' and G" from Maxwell's equation is shown in Figure 6.11 for CL asphalt and in Figure 6.12 for RW asphalt. Excellent fits for both G' and G" with the value of r^2 more than 0.99 were obtained. The parameters of Equation 6.10 were determined with the help of software -Table Curve and are reported in Table 6.3. In this case |G*| and phase angle

were simultaneously fitted . For the simultaneous fitting of |G*| and phase angle, first the phase angles vs. frequency data were shifted by 10^{10} on the x-axis by multiplying frequency by 10^{10} . Then both |G*| and phase angle were plotted on the same graph on Table-curve and the parameters of the best fit equation were determined.

The selected asphalt samples can be modeled with value of m equal to zero and hence, the number of parameters are low. The number of parameters required is 10 for both Cold Lake and Redwater asphalt sample. The plots of |G*| and δ were made for both Cold Lake and Redwater sample (Figure 6.13-6.14)

Thus we can conclude that our samples can be modeled and characterized by both Maxwell and fractional models.

Table 6.5 : Parameters of Maxwell Model

	Cold Lake (CL 4) Asphalt		Redwater (RW 4) Asphalt	
i	g_i	λ_i	g_i	λ_i
1	5.403×10^{7}	1.093×10^{-8}	7.161×10^{6}	6.813×10^{-8}
2	3.220×10^{7}	5.306×10^{-8}	1.724×10^{7}	4.725×10^{-7}
3	7.568×10^{7}	2.576×10^{-7}	1.919×10^{7}	3.357×10^{-6}
4	5.317×10^{7}	1.250×10^{-6}	1.833×10^{7}	1.584×10^{-5}
5	5.106×10^{7}	6.069×10^{-6}	1.500×10^{7}	8.313×10^{-5}
6	2.951×10^{7}	2.946×10^{-5}	9.850×10^{6}	4.262×10^{-4}
7	1.611×10^{7}	1.430×10^{-4}	6.325×10^{6}	1.933×10^{-3}
8	7.543×10^{6}	6.942×10^{-4}	2.885×10^{6}	9.380×10^{-3}
9	1.837×10^{6}	3.370×10^{-3}	5.010×10^{5}	4.906×10^{-2}
10	6.475×10^{5}	1.636×10^{-2}	1.036×10^{5}	2.656×10^{-1}
11	1.024×10^{5}	7.940×10^{-2}	1.787×10^{4}	1.572
12	4.505×10^{4}	3.854×10^{-1}	2.058×10^{3}	1.256×10^{1}
13	3.578×10^{3}	1.871	1.980×10^{2}	1.226×10^{2}
14	2.466×10^{3}	9.082		
G_N, Pa	3.5×10^{8}		1×10^{8}	

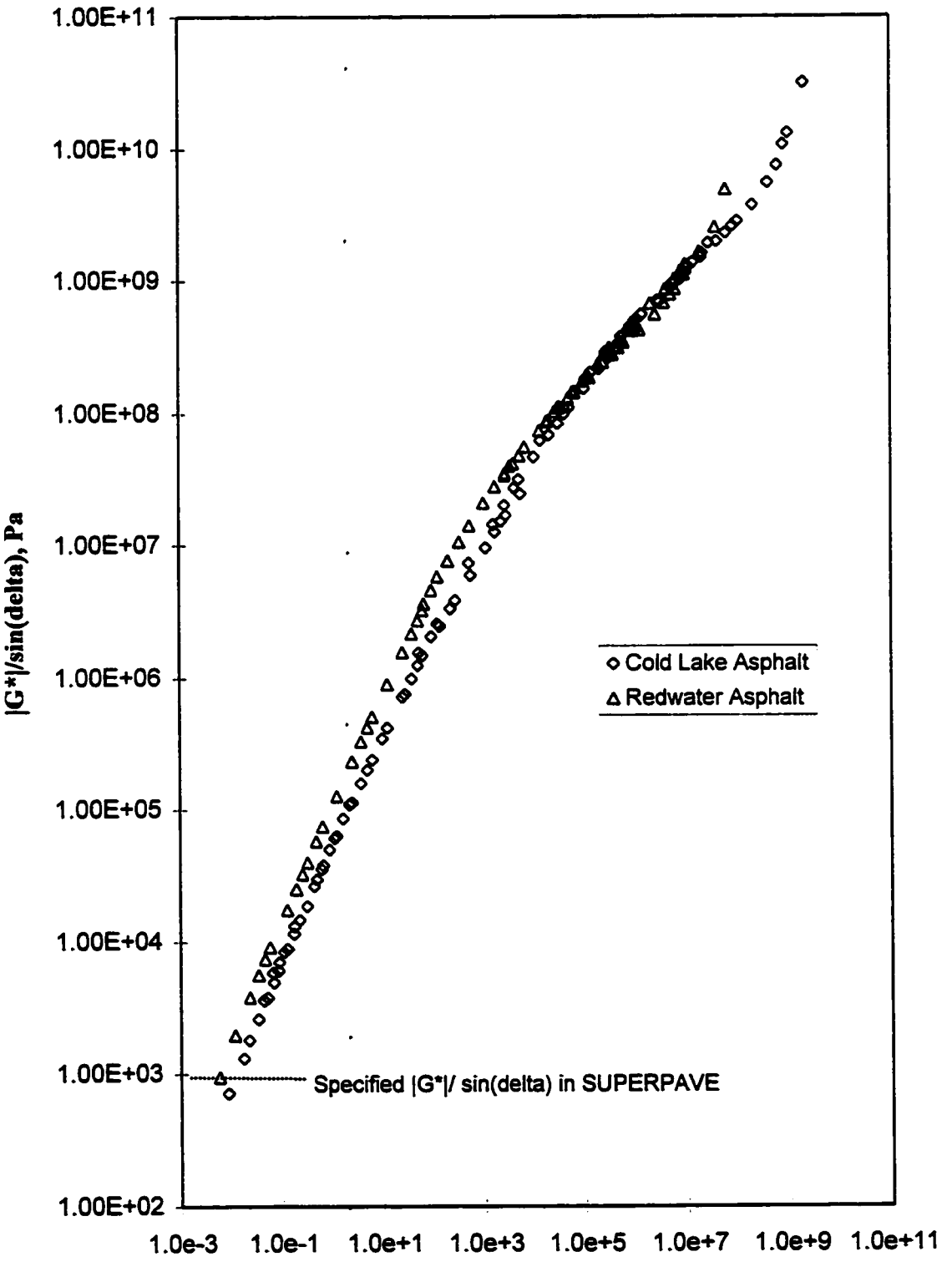

Figure 6.10 - Master Curve of |G*|/sin (delta) at 20°C

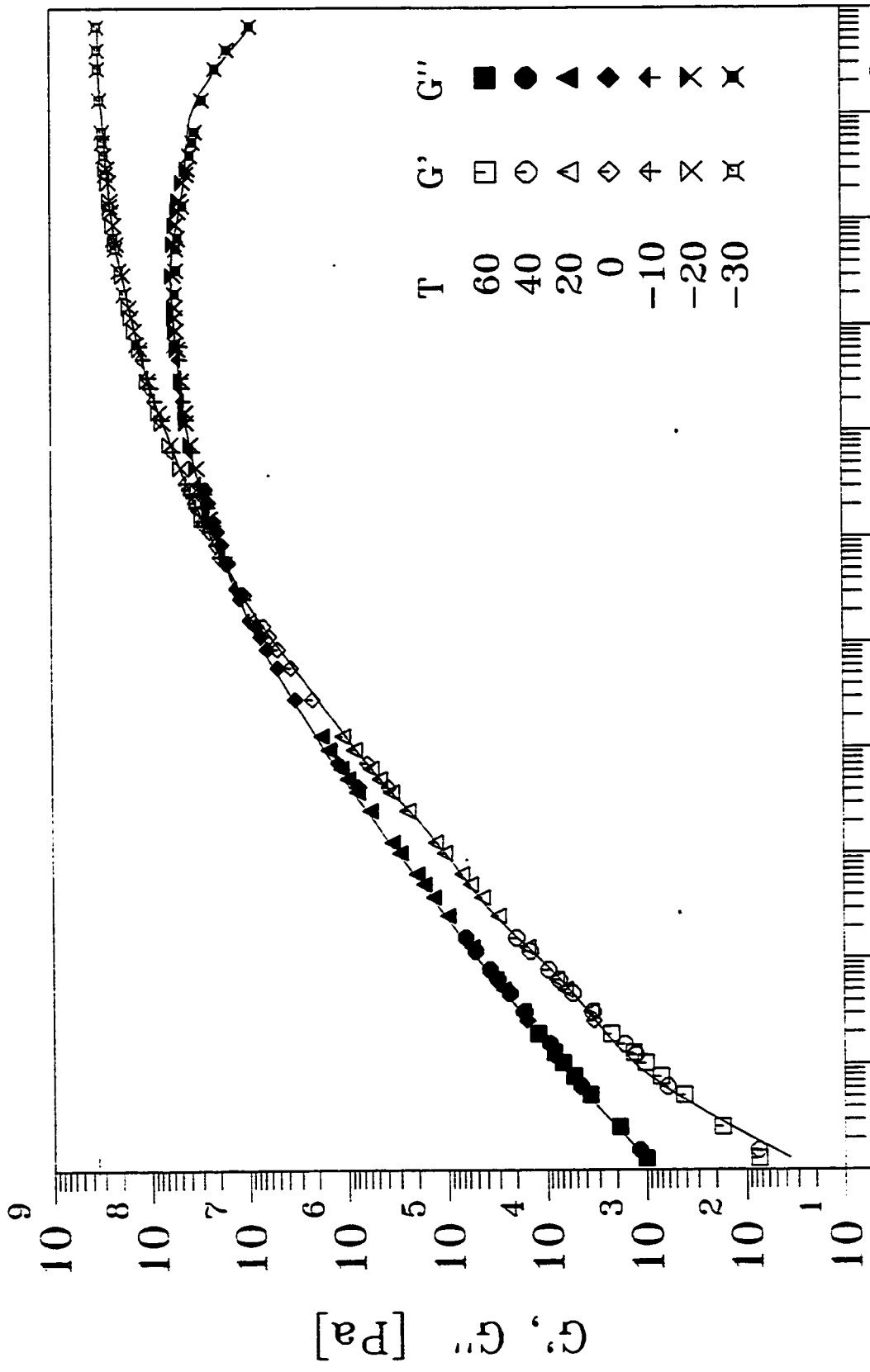

Figure 6.11: Cold Lake Asphalt – Maxwell Model for G' and G"

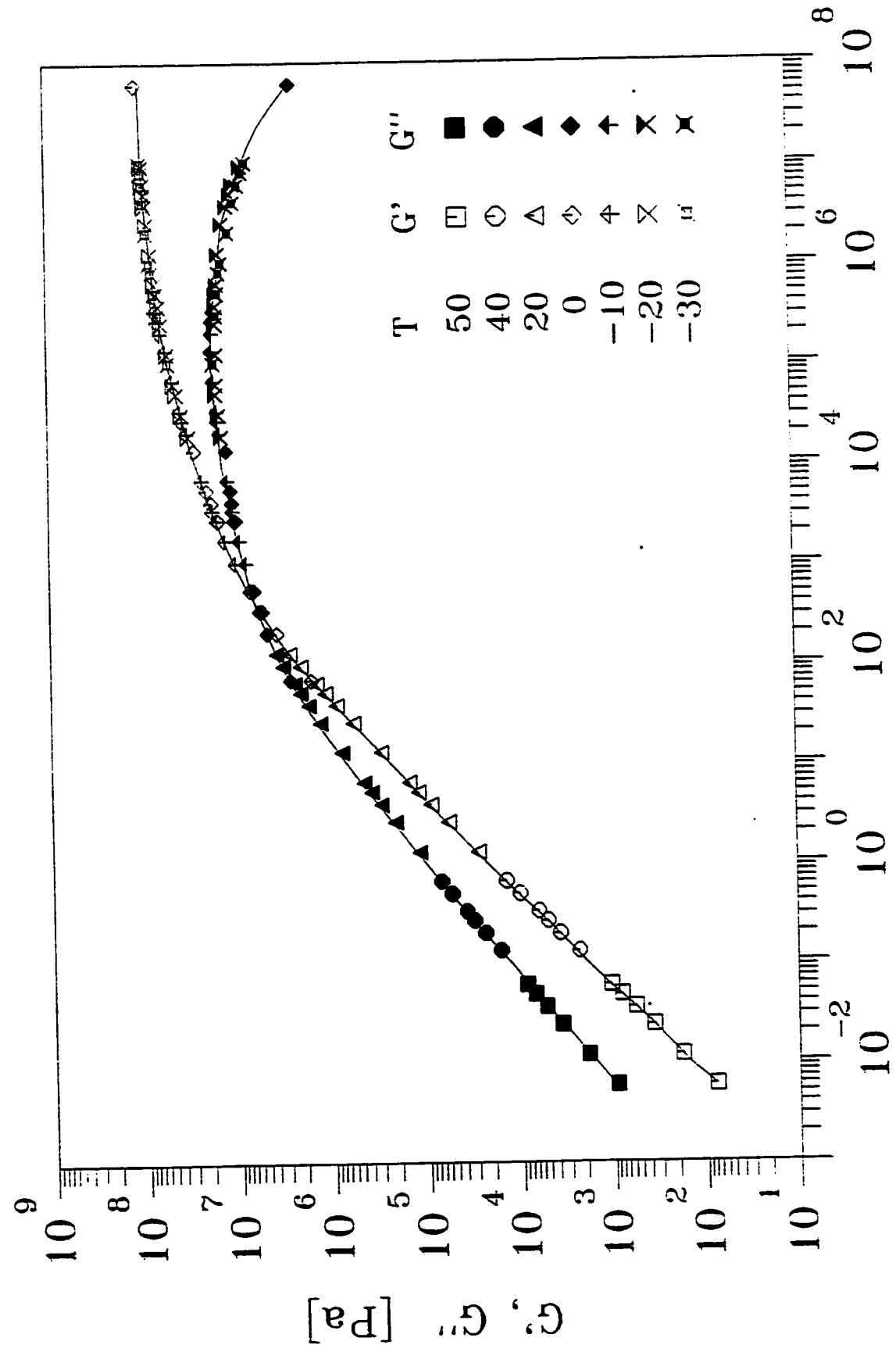

Figure 6.12: Redwater Asphalt – Maxwell Model for G' and G"

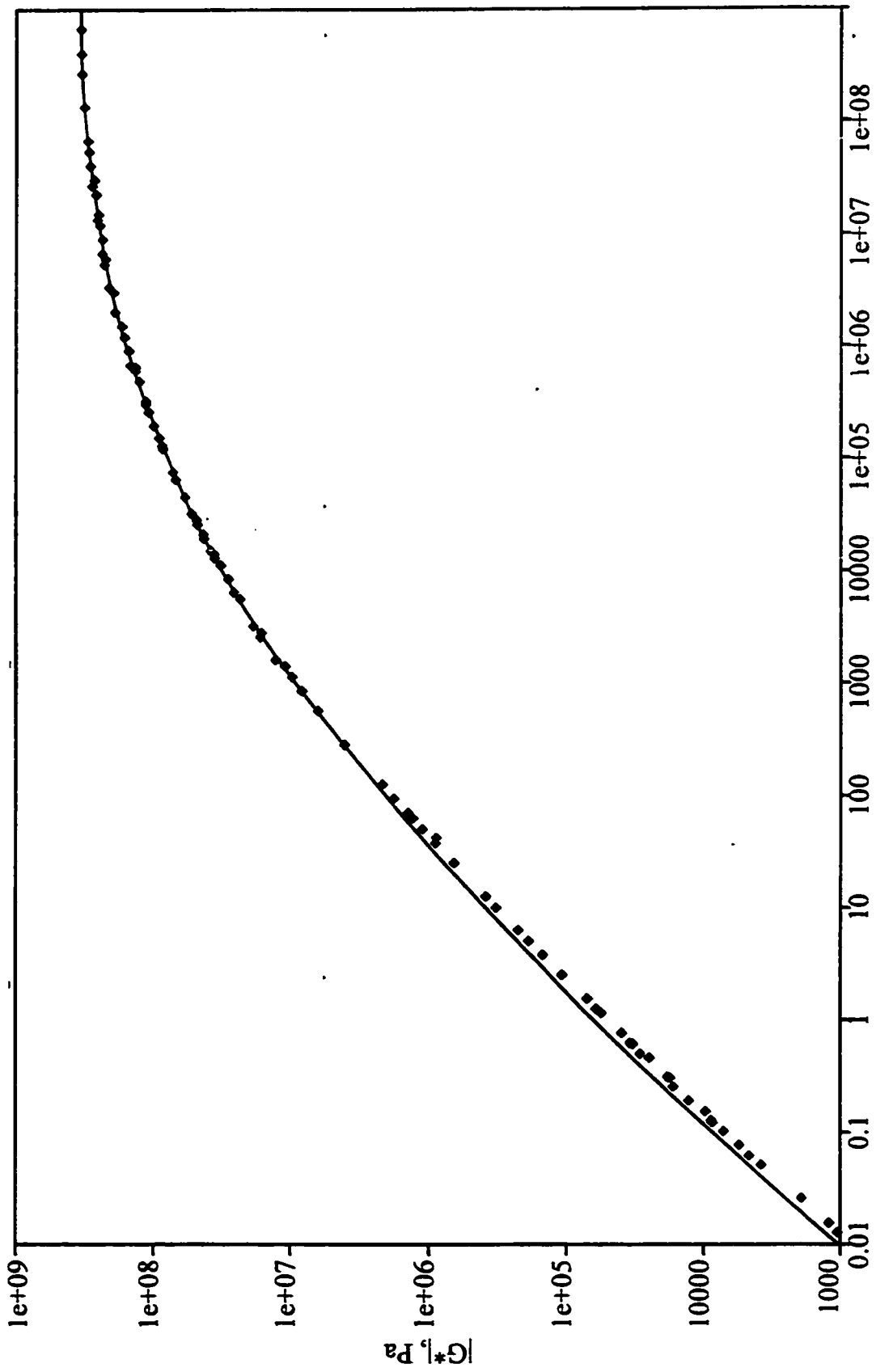

Figure 6.13: Cold Lake Asphalt – Fractional Model for |G*|

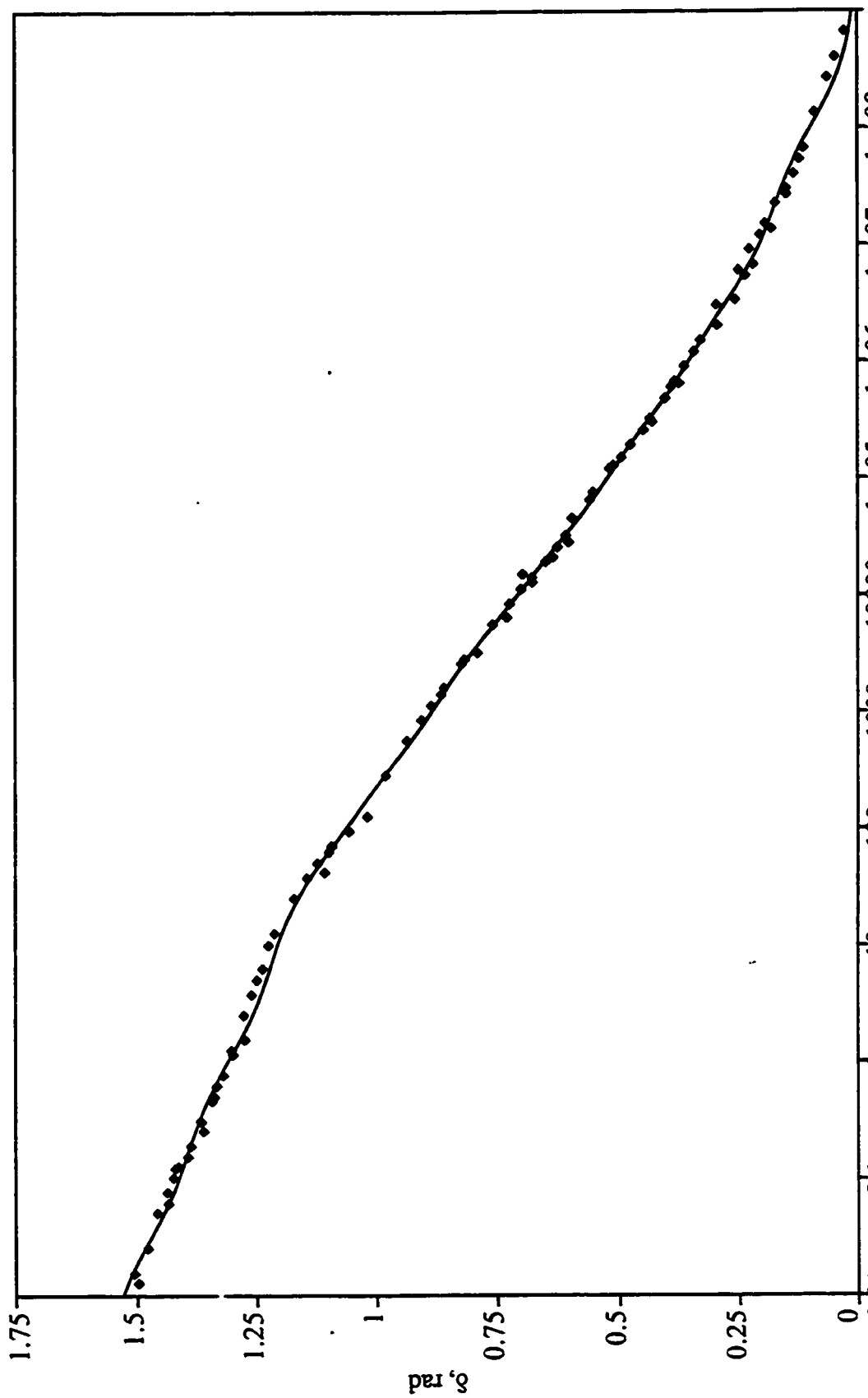

Figure 6.14: Cold Lake Asphalt – Fractional Model for δ

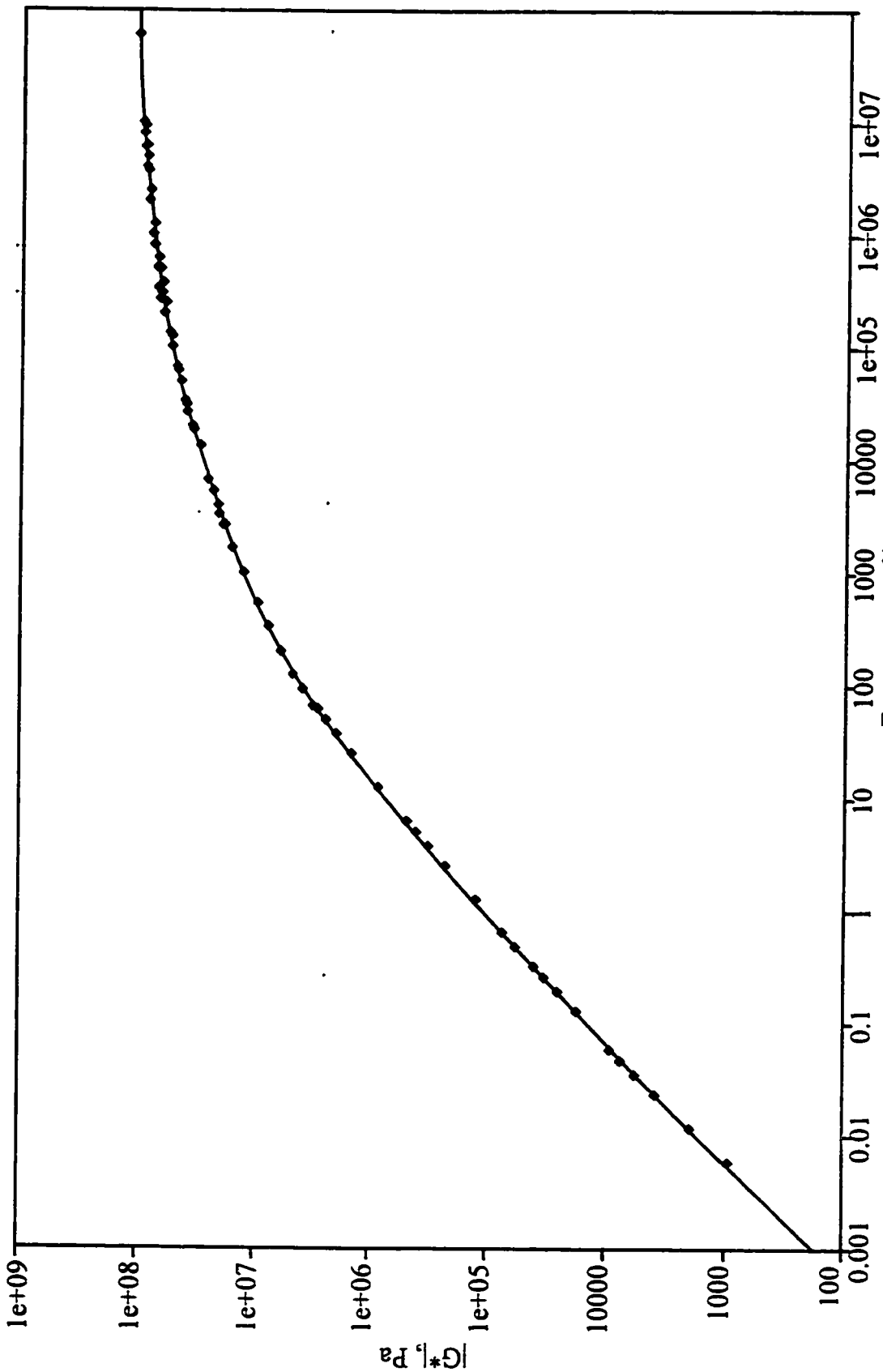

Figure 6.15: Redwater Asphalt – Fractional Model for |G*|

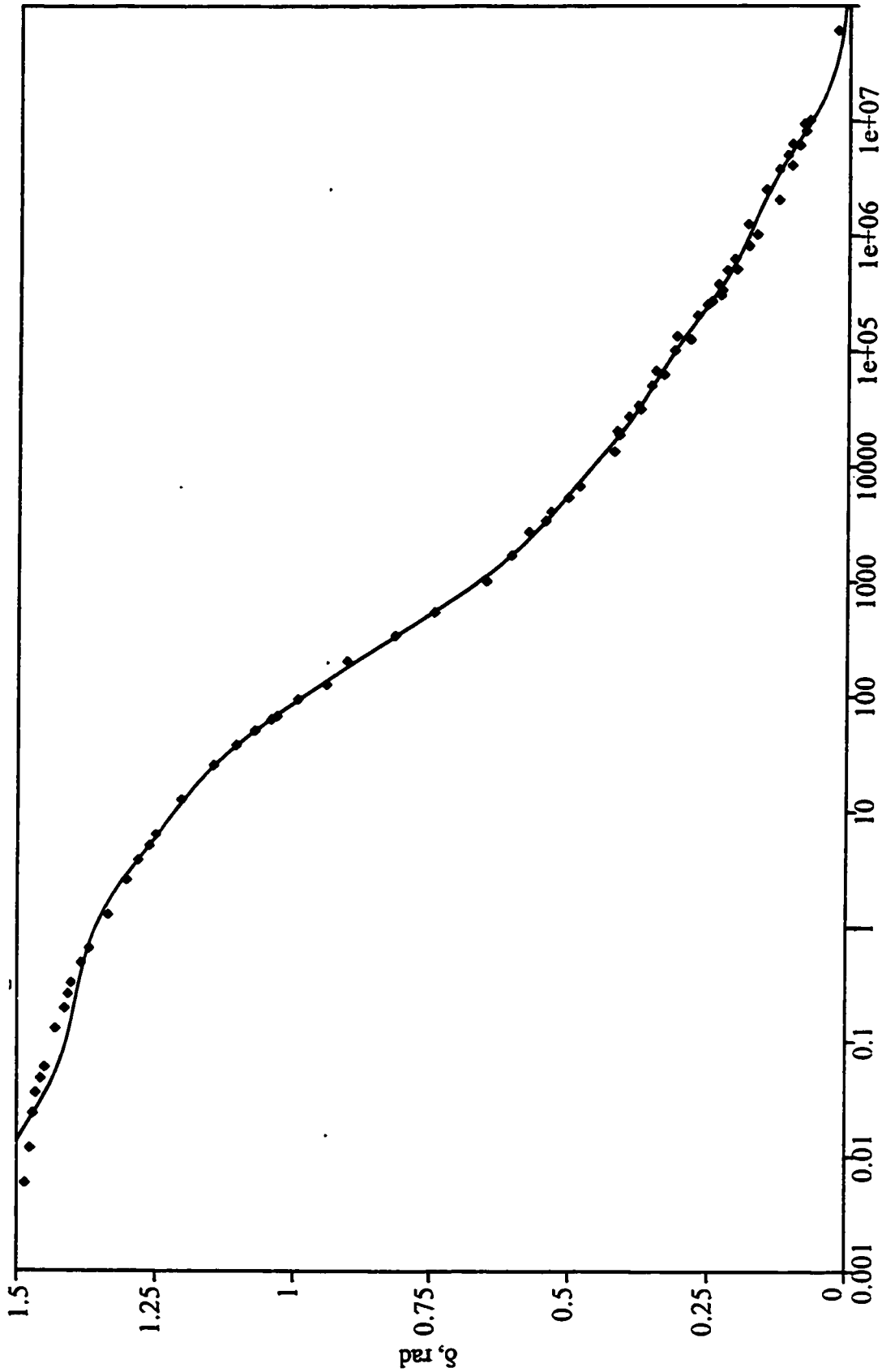

Figure 6.16: Redwater Asphalt – Fractional Model for δ

Table 6.6 : Parameters of Fractional Model

	Cold Lake (CL4) Asphalt	Redwater (RW4) Asphalt
i	λ_i	λ_i
1	1.486×10^{-7}	2.824×10^{-6}
2	2.558×10^{-6}	4.676×10^{-5}
3	1.110×10^{-8}	1.097×10^{-7}
4	8.520×10^{-4}	7.470×10^{-3}
5	2.279×10^{-4}	3.655×10^{-3}
6	2.342×10^{-5}	5.466×10^{-4}
7	1.014×10^{-2}	1.622×10^{-2}
8	5.553×10^{-1}	3.536×10^{-1}
9	5.081×10^{1}	7.856×10^{1}
η_o, Pa.s	8.277×10^{4}	1.760×10^{5}

6.7 Molecular Weight Distribution (MWD) : Results and Discussion

The possibility of calculating molecular weight distributions of regular asphalts from dynamic rheological data is investigated in this study. The distributions determined for Cold Lake and Redwater asphalt samples using rheological methods are compared with the size exclusion chromatography (SEC) results. The SEC results were obtained from Dr. Susanna Ho, Bituminous Material Laboratory, The University of Calgary. The results for Cold Lake asphalt are plotted in Figure 6.17 and that for Redwater asphalt are shown in Figure 6.18.

It is evident from the results that there is almost no agreement between the MWDs obtained from the rheological measurements and the SEC results. When the figures with the MWDs of the two asphalt samples are inspected and compared with the MWD from

SEC, two distinct features are apparent. First, when the width of the molecular weight distributions from rheological method is compared with the molecular weight distribution from SEC, one can see a difference. The widths given by rheological methods are significantly lower than the width obtained by SEC. In the region of high molecular weight, as per SEC, approximately 5% to 10% of the material has molecular weight higher than 4000. The distributions obtained from rheological measurements do not show any significant presence of material of molecular weight higher than 3000. Unlike SEC, rheological methods do not give a longer tail in the high molecular weight region. In the region of low molecular weight, the distributions obtained by rheological measurements appear to be shifted towards the lower end compared to SEC data.

The second difference can be seen in the position and number of peaks in the molecular weight distributions obtained by different methods. SEC results show that the distributions for both samples are basically unimodal. The position of peak is at around 700-900 molecular weight. A plateau can be seen in the high molecular weight region. The distributions obtained by phase angle using fractional model and G' using Maxwell model are multimodal. The distribution for Redwater asphalt obtained by $|G^*|$ is of unimodal nature whereas the same for Cold Lake asphalt has two modes in close vicinity. The position of highest peak for $|G^*|$ and δ are nearly the same, but the position appears to be shifted compared to the location of peak for SEC data.

To position the distribution curves obtained from different rheological properties, the calibration parameters of Zanzotto et. al.(1996) were used. An attempt was made to match the distribution obtained by $|G^*|$ measurement with SEC data by changing these parameters. The results are shown in Figure 6.19 for Cold Lake asphalt and in Figure 6.20 for Redwater asphalt. It can be seen from the figures that it is possible to match the position of the peak and peak height up to a great extent, but it is not possible to obtain the broad width as in SEC data.

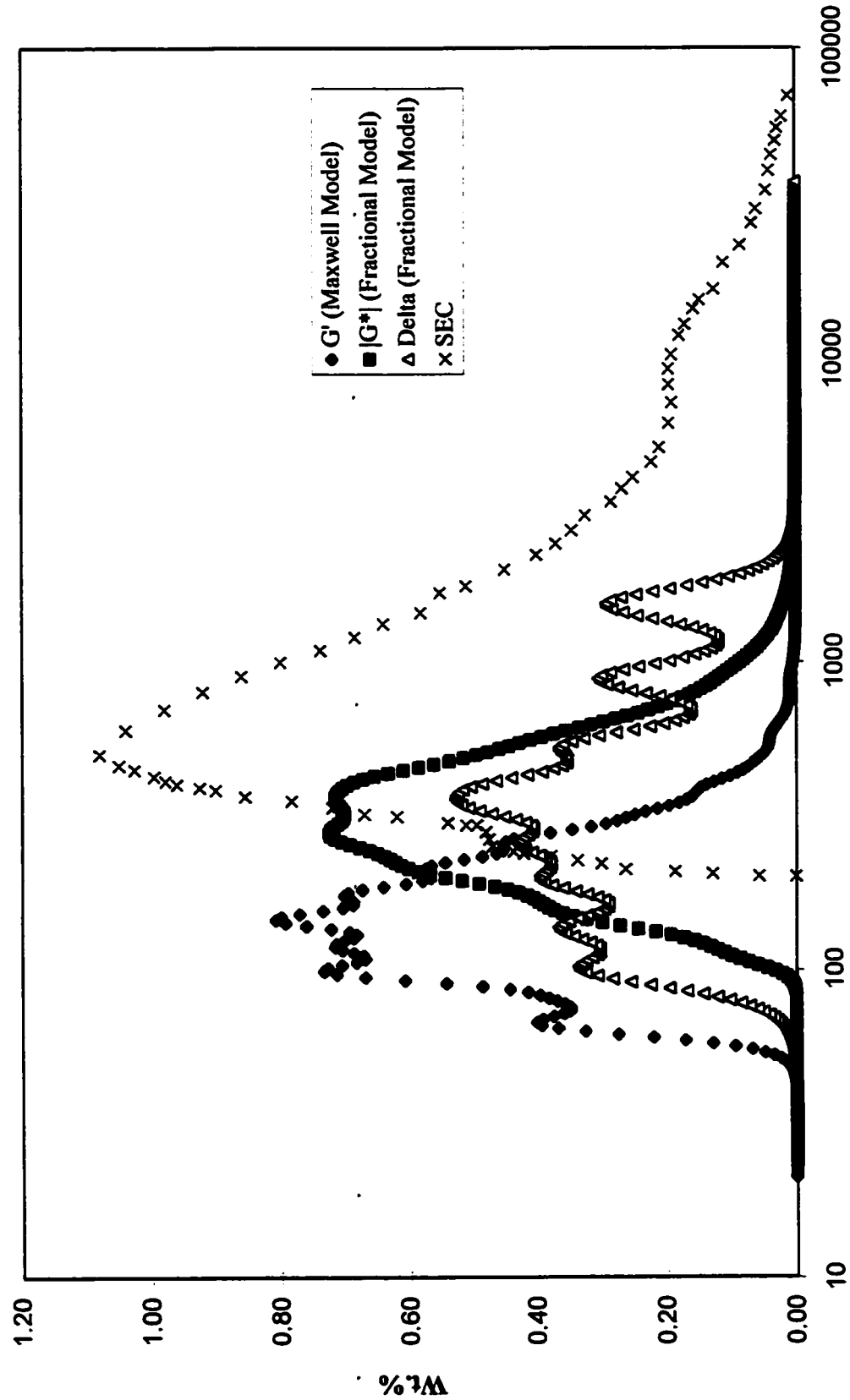

Figure 6.17 - Cold Lake Asphalt : Molecular Weight Distribution

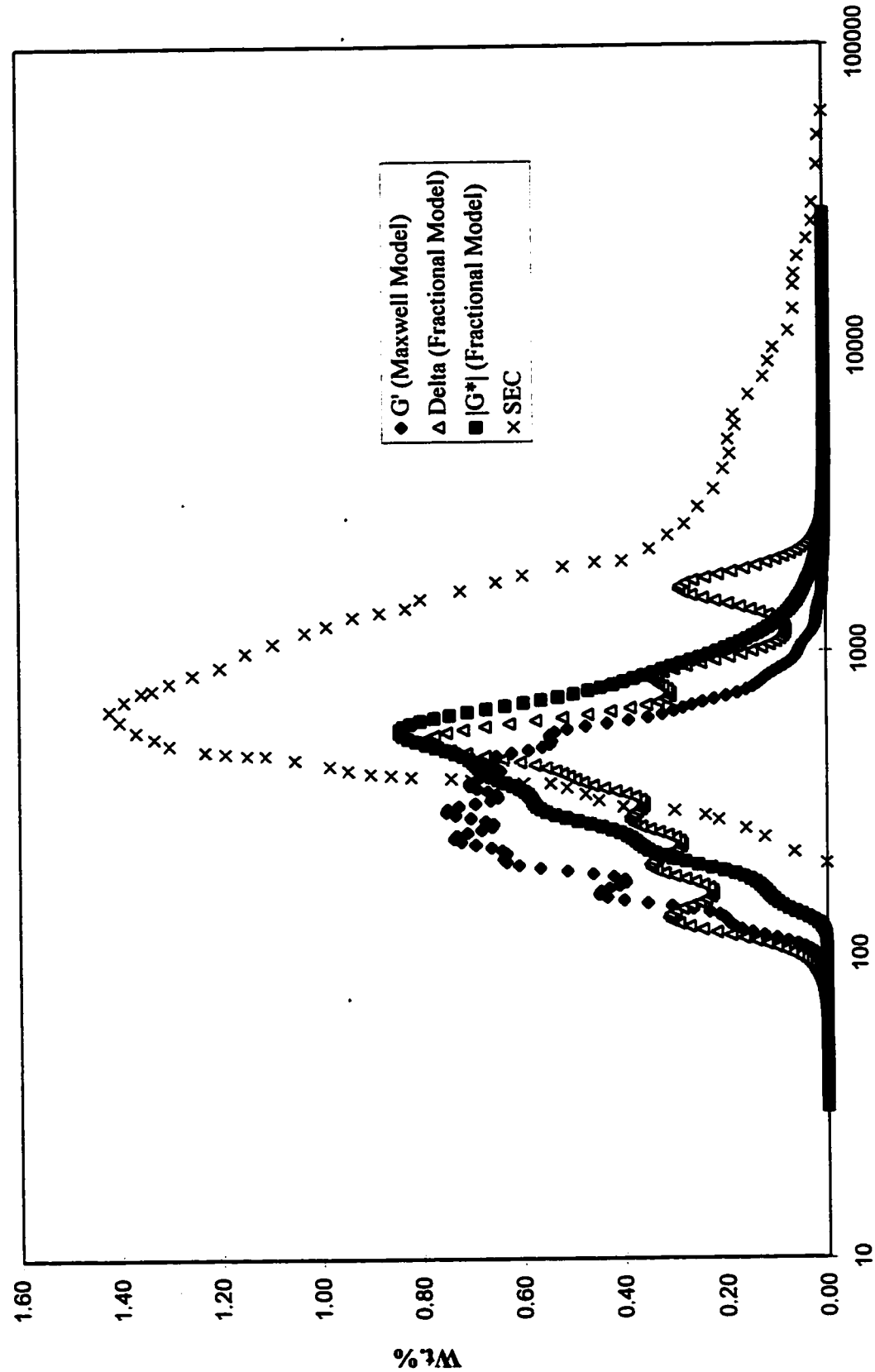

Figure 6.18 - Redwater Asphalt : Molecular Weight Distribution

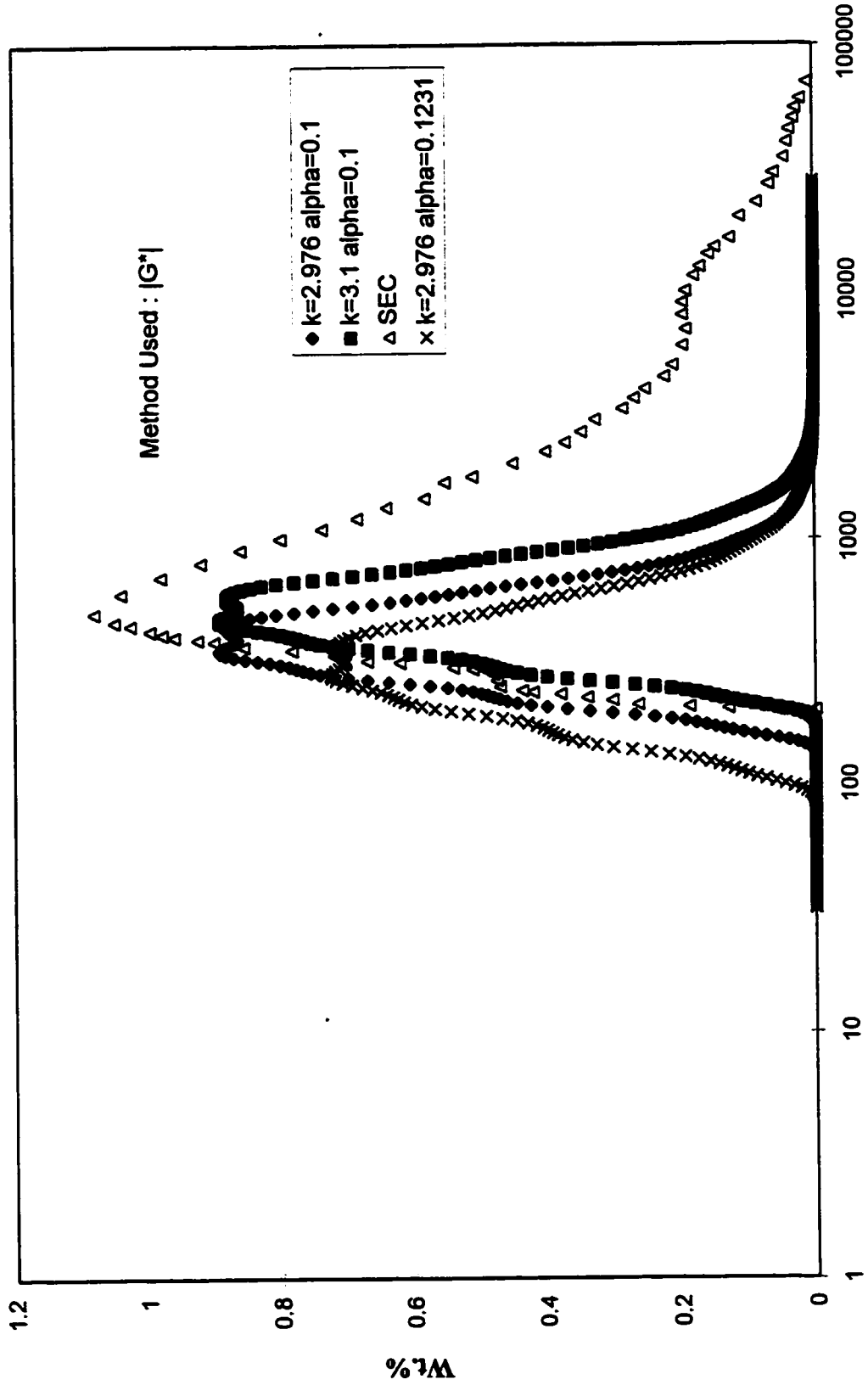

Figure 6.19 - Cold Lake Asphalt : Effect of Calibration Parameter on MWD

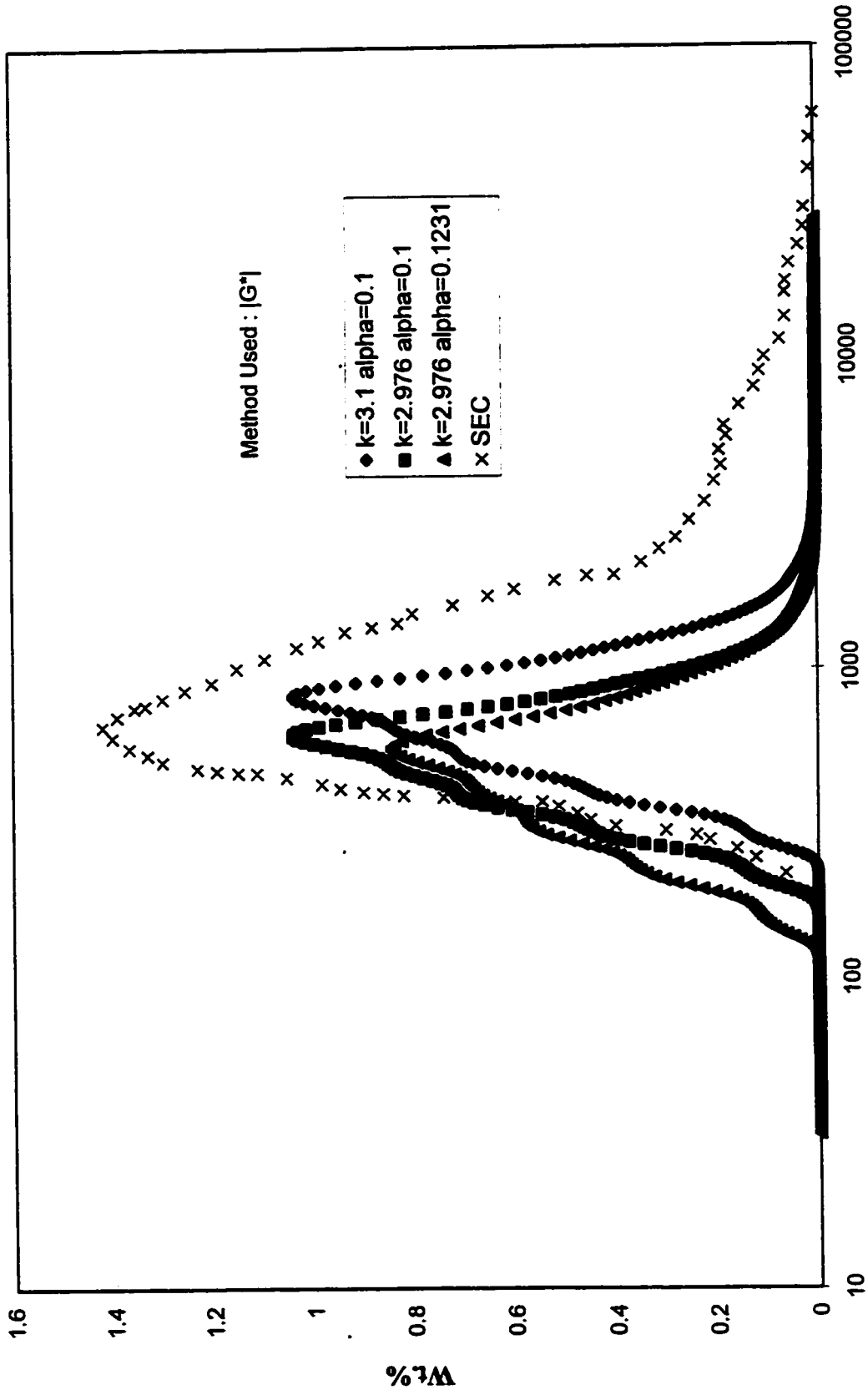

Figure 6.20 - Redwater Asphalt : Effect of Calibration Parameters on MWD

On comparison of molecular weight distributions obtained by G', |G*| and phase angle, it can be observed that these distributions have similar widths. Zanzotto et. al. (1996) have found that for asphalt, the phase angle is more sensitive to molecular weight compared to other rheological properties used in the study. It is difficult to explain the presence of multimodes in the curve obtained from phase angle - whether it is artifact of the mathematical model used or it is a better representation of the internal structure of asphalt.

In molecular weight distribution obtained from rheological properties, the region of high molecular weight is obtained by the measurements at higher temperatures. The lower tail in high molecular weight region in the distribution curve can be attributed to various factors - inadequacy of the plate-plate configuration used in our rheometer for measurements at higher temperature, the inability of the model used to describe the properties in that region or dissociation of the loosely held high molecular weight associates by oscillatory deformations.

These observations raise more questions than providing the answers. Most studies of the composition and structure of asphalts are done using solvents, which changes the structure of the potential associates created either by the highest molecular weight components or the most polar components of these materials. Thus, molecular weight distribution obtained from SEC do not necessarily represent the structural conditions of the undiluted asphalt.

Researchers like Wu (1988), Tuminello (1986), Paula et. al. (1996) have obtained the molecular weight distributions for different polymers from the rheological properties. These distributions show a fair agreement with chromatography data. Our study is based on the fact that asphalt exhibits a similar rheological behavior as polymers. But asphalt has completely different internal structure compared to polymers. Unlike polymers,

asphalt has a large number of dissimilar constituents held together with different kind of chemical and physical bonds. The stark difference in the internal structure of asphalt and polymers may be attributed to the failure of rheological measurements to give molecular weight distribution similar to that obtained by SEC. It may also demonstrate that the internal structure of asphalt, which impacts on its rheological behavior is very different than is shown by molecular weight distribution of highly diluted materials. The molecular structure may be dissolved, or created by the impact of solvent.

Conclusions and Recommendations

Conclusions

The main objective of the study was to evaluate the impact of the transition from the present empirical asphalt specifications to new SUPERPAVE™ performance testing on Canadian asphalt industry.

In the following, the findings are summarized on some aspects of the transition and rheological testing of asphalt :

- When comparing asphalt materials prepared in this study with other bituminous fractions, it can be concluded that at higher temperatures (40°C and above) their behavior is similar. A double log correlation used by other researchers to describe the dependence of bitumen fractions on temperature applies also to asphalt.

- The following are the findings of an attempt to correlate the parameters in the present specification (CGSB) and SUPERPAVE™ specification :

    - The highest allowable service temperature to which asphalt binder can be exposed during its service life as measured by the SUPERPAVE™ parameter $G^*/\sin\delta$ correlates with the viscosity at 60°C used in the present specification. A single correlation is applicable for asphalt binders prepared from different crude sources. However, grades based on viscosity at 60°C in present specifications do not correlates with the grades in SUPERPAVE™ specification, based on the high service temperature parameter.

- The correlation between the penetration at 25°C from the present specification and the parameter for the lowest allowable service temperature to which asphalt binder can be exposed during the service life as measured by the SUPERPAVE™ parameter 'S' (stiffness parameter) is considerably poorer and the correlation depends on the crude oil source.

- A crude-source independent correlation was developed to predict the lowest allowable service temperature temperature based on a function which includes both viscosity measurement at 60°C and penetration measurement at 25°C. It can be used to find where to start with the stiffness measurements for asphalt (penetration test is less labor intensive than stiffness measurement).

From the above, it is clear that there is no direct relationship between the existing conventional specifications and the SUPERPAVE™ specification. Thus, materials conforming to the same CGSB grade can be graded differently by SUPERPAVE™ specification.

- Capability of conventional (regular) asphalts to meet SUPERPAVE™ requirements in Canadian climate :

  - The determination of highest and lowest service temperatures across Canada was performed using LTPP-SAPT and C-SHRP models, for both 50% and 98% "reliability" as described by SUPERPAVE™. It appears, that for 98% reliability the LTPP-SAPT model has more stringent requirements. The SUPERPAVE™ low service temperature requirements for some areas in

Canada, as expected, leads to grades, which are extreme and presently, in the most severe cases, probably non-existent.

- Conventional asphalts prepared by straight distillation of Canadian crude oils can not meet the requirements of SUPERPAVE™ specification in places where the low pavement design temperature is below -37°C. That applies even for the conventional asphalts with best low temperature behavior.

- The requirements of the currently used CGSB grades for most of the selected Canadian locations are more stringent at high temperatures than grades required by SUPERPAVE™. The impact of these lower requirements of SUPERPAVE™ specification on rutting will have to be found from service trials.

- Overall, the presently used CGSB grades of asphalt provides the service to meet the SUPERPAVE™ requirements at 98% "reliability" calculated according to LTPP-SAPT and C-SHRP models in cities with moderate climate like Toronto and N. London and in eastern and western coastal areas of Canada. The high quality conventional asphalt are capable of meeting the SUPERPAVE™ specification requirements at 50% reliability in the area representing the belt along with the US border. No conventional asphalt meets the low temperature requirements in northern part of Canada

- From comparison of the SUPERPAVE™ specification requirements with Canadian climatic conditions the following can be concluded

- In some areas the climatic requirements are such that adequate SUPERPAVE™ grades do not exist. Such areas are that of extremely mild climate i.e. Vancouver where according to C-SHRP at 98% "reliability" a grade 46-16 would be required, and in areas of extremely cold climate (Whitehorn), where according to C-SHRP 50% "reliability" requirement grade 40-40 and according to LTPP-SAPT 98% "reliability" requirement grade 58-52 would be needed. These grades are not defined in SUPERPAVE™.

- The temperature difference of 6°C for grading is very wide. This makes the service requirements very conservative and even material of adequate properties can be rejected. The local requirements, before these are transformed into official grades, have to be taken into account.

- The characterization based on SHRP testing shows that the paving asphalts derived from Cold Lake crude oil will provide better performance compared to asphalts derived from Redwater oil. The detailed rheological characterization from dynamic mechanical analysis for the selected Cold Lake and Redwater asphalts reveals that Cold Lake asphalt has higher maximum storage modulus compared to Redwater asphalt. Cold Lake asphalt will attain glassy modulus at a lower temperature as compared to Redwater asphalt. The shift factors for time-temperature superposition for the selected Cold Lake asphalt is higher than that of Redwater asphalt for temperatures lower than -20°C and higher than 30°C.

- The measurement of $G^*/ \sin \delta$ parameter at a single point loading in SUPERPAVE™ specification may not be adequate to completely describe the rheological behavior of asphalts.

- The molecular weight distributions for selected Cold Lake and Redwater asphalt samples determined from the rheological measurements do not show an agreement with SEC results. As both of these methods have there own limitations for determining the molecular weight distribution for the complex multidisperse micellar system like asphalt, it is difficult to comment on the supremacy of any of these method over other.

Recommendations

The conventional paving asphalts cannot provide the service required with higher reliability in the region along the US border and service even with lower reliability in the Northern part of Canada. For the selection of paving asphalt grades, each region should calculate exact required grade and compare it with available asphalts. Also, experience of field engineers have to be used to find reasonable compromises.

The temperature range of 6°C in a PG grade is very wide and it should be reduced. More higher low temperature grades should be introduced for the SUPERPAVE™ grade conforming to high temperature of 46°C.

A number of questions are still left unanswered, and only further work in this area will put them to rest. First, the results of characterization based on empirical and performance tests can only be applied to the asphalts prepared from Cold Lake, Bow Valley and Redwater crude oils. More work is required on other crude oils to validate and generalize the findings of our study.

A second area may be the rheological characterization of paving asphalts at different loading and temperatures. A detailed work will help in understanding the behavior of paving asphalts and reasons for the pavement failures.

Another area which requires further investigation is the determination of molecular weight distribution from rheological measurements. More rheological and chromatographic measurements are required before this method is established as an important tool for the study of internal structure of asphalts.

REFERENCES

Anderson D.A., and. Dukatz E.L; "Asphalt Properties and Composition : 1950-80," Proceedings of the Assn of Asphalt Pav. Tech., 49, 21-22 (1980)

Anderson, D.A., Luhr D.R., Antle C.E, Siddiqui Z., Fernando E.G., Chizewick T., and Tarris J.P.; "Performance-Related Specification for Hot-Mix Asphaltic Concrete," Final Report, Project No. HR-10-26A, Pennsylvania Trans. Inst., Univ. Park, PA, PTI 8805 (1990)

Anderson D.A., Christensen D.W., and Bahia H.B.; "Physical Properties of Asphalt Cements and Development of Performance Based Specifications," Proceedings of Technical Sessions, J. Assn. Asphalt Pav. Tech., 60, 291-324 (1991)

Baumgartel M., Soskey P.R. and Winter H.H., Innovative Rheological Interface Software, IRIS Development, Amherst, USA (1987)

Bird R.B., Curtiss C.F., Armstrong R.A. and Hassager O.; "Dynamics of Polymer Liquids," Wiley, New York, Vol.1 (1987)

Christensen, D.W. Jr ; "Mathematical Modeling of the Linear Viscoelastic Behavior of Asphalt Cement", PhD Thesis, The Pennsylvania State University (1992)

Corbett L.W., and Schweyer H.E.; "Viscosity characterization of asphalt cement," Viscosity Testing of Asphalt and Experience with Viscosity Graded pecifications, ASTM STP 532, American Society for Testing and Materials, 40-49(1973)

De Kee D., Stastna J., and Powley C., "Investigation of a New Complex Viscosity Model," J of Non-Newtonian Fluid Mechanics, 26, 149-160 (1987)

Dormier,E.J., Tong P., and Lagasse R.R.; "Characterization of Linear Polyethylene by GPC and Rheological Techniques," SPE Technical Papers: 1984 ANTEC Vol XXX 421(1984)

Eastick, R.R; "Properties of CO_2- Saturated Bitumen Fractions", M.Sc. Thesis, The University of Calgary (1989)

Ferry, J.D.; Viscoelastic Properties of Polymers, 3rd ed., Wiley, New York (1980)

Griffen, R.L., Miles T.K., Penther C.J., and Simpson W.C.; "Sliding Plate Microviscometer for Rapid Measurement of Asphalt Viscosity in Absolute Units," ASTM, Special Technical Publication, 212, 36-45 (1956)

Haas, R.C.G., and Topper T.H.; "Thermal Fracture Phenomena in Bituminous Surfaces," Highway Research Board Special Report, Natural Res. Coun., Washington, D.C., 101, 136-153 (1969)

Heukelom W., and Klomp J.G.; "Road Design and Dynamic Loading," Proceedings of the Assn. Asphalt Pav.Tech., 33, 92-125 (1964)

Kim, O.K., Bell C.A., Wilson J.E., and Boyle G.; "Development of Laboratory Oxidative Aging Procedures for Asphalt Cements and Asphalt Mixtures," Transport Res. Rec., 1987, 1115, 101-112 (1987)

Lavallee C. and Berker,A; "More on the Prediction of MWD of Linear Polymers from Their Rheology," J.Rheology, 41(4), 851-871 (1997)

Lee, D.Y.; "Development of a Laboratory Durability Test for Asphalts," Highway Research Board Records, 231, 34-49 (1968)

Letton A and Tuminello, W.H.,"A Method for Calculating the Molecular Weight Distribution from the storage Modulus Curve," SPE Technical Papers: 1987 ANTEC Vol. XXXIII 997(1987)

LTPP Data Analysis : Improved Low Pavement Temperature Prediction, Publication No. FHWA-RD-97-103, Federal Highway Administration, McLean, VA (1997)

McCleod N.W.; " A 4-years Survey of Low Temperature Transverse Pavement Cracking on the Three Ontario Roads," Proceedings of the Assn. Asphalt Pav.Tech., 41, 424-493 (1972)

Mehrotra, A.K. and Svrcek W.Y.; "Measurement and Correlation of Viscosity, Density and Gas Solubiliy for Marguerite Lake Bitumen Saturated with Carbon Dioxide", AOSTRA J. Res., 1, 1, 51-62 (1984)

Mehrotra, A.K., Eastick R.P., and Svrcek W.Y.; "Viscosity of Cold Lake Bitumen and its Fractions", Can. J. Chem. Engg., 67, 6, 1004-1009 (1989)

Menefee, E., and Peticolas, W.L.,"Molecular Weight Distribution from the Normal Coordinate Theory of Viscoelasticity," J. Chem.Phys., 35, 946 (1961)

Moavenzadeh, J., and Stander R.R. Jr.; "Effect of Aging on Flow Properties of Asphalt," Highway Research Board Records, 178, 1-29 (1965)

Mohseni, A.; "LTPP Seasonal AC Pavement Temperature Models", Pavement Performance Division, HNR-30, Federal Highway Administration, McLean, VA (1996)

Moheseni, A., and Symons M.; "Effect of Improved LTPPAC Pavement Temperature Models on SUPERPAVE Performance Grades", 77th Annual Meeting, Transportation Research Board, Washington D.C. (1998)

Monismith, C.L., Secor G.A., and Secor K.E.; "Temperature Induced Streses and Deformations in Asphalt Concrete," Proceedings of Technical Sessions, J. Assn. Asphalt Pav. Tech., 34, 227-232 (1965)

Paula M. W. and Dealy, J.M.; "Use of Rheological Measurements to Estimate the Molecular Weight Distribution of Linear Polyethylene," J. Rheology, 40(5), 761-778 (1996)

Petersen J.C., and Anderson D.W.; "Binder Characterization and Evaluation," Vol. 1, Strategic Highway Research Program, National Research Council, Washington D.C. (1994a)

Petersen J.C., and Anderson D.W.; "Binder Characterization and Evaluation," Strategic Highway Research Program, Vol. 3, National Research Council, Washington D.C. (1994b)

Peticolas, W.L.," Molecular Weight Distribution of Linear Polymers from Stress Relaxation in Polymer Melts," J. Chem.Phys., 39, 3392 (1963)

Pfeiffer J.P., and Van Doormaal P.M.; "The Rheological Properties of Asphaltic Bitumen", J. Instt. Pet. Tech., 22, 414-418 (1936)

Puzinauskas, V.P.; "Properties of Asphalt Cements," Proceedings of Technical Sessions, J. Assn. Asphalt Pav. Tech., 48, 646-710 (1979)

Romberg J.W., and Traxler R.N.; "Rheology of Asphalt," Colloid Science, 2, 33-47 (1947)

Rudraiah N. and Kaloni P.N.; Encyclopedia of Fluid Mechanics. Vol.1; Gulf Publication Company, 1-61 (1986)

Solc A; "Classification of Bitumen - Viscocity vs. Penetration," RAPP Symp. Susceptibility Theo., 1979, 195-198 (1979)

Special Report 202, "America's Highways: Accelarating the search for innovation", Transportation Research Board, Washington, D.C. (1984)

Speight J.G. and Long R.B.; "Spectroscopy and Asphaltene Structure", Atomic and Nuclear Methods in Fossil Energy Research, Plenum Press, New York, 2895-321 (1982)

Stastna J., Zanzotto L. and Kennepohl G.; "Dynamic Material Functions and the Structure of Asphalts," Transportation Research Record 1535, 3-9 (1996)

Strategic Highway Research Plans, Final Report, Transportation Research Board, Washigton D.C. (1986)

Superpave, Performance graded asphalt binder specification and testing, Superpave Series No. 1 (SP-1), Published by Asphalt Instt., Lexington (1995)

Tuminello,W.H., Encyclopedia of fluid Mechanics,Vol. 9, N.P. Cheremisinoff, Editor, Gulf Publishing Company, 209-242 (1986)

Tuminello, W.H.,; "Determination of Molecular Weight Distribution by Melt Rheology: A Review," SPE Technical Papers, 1987 ANTEC Vol XXXIII 926(1987)

Tuminello,W.H., "Molecular Weight Distribution of TFE-HFP Copolymers," Polym. Eng. Sci., 29,645 (1989)

Vallerga, B.A.; "Pavement Deficiencies Related to Asphalt Durability," Proceedings of Technical Sessions, J. Assn. Asphalt Pav. Tech., 50, 221-236 (1980)

Van der Poel, C.; "A General System Describing the Viscoelastic Properties of Bitumen and Its Relation to Routine Test Data," Applied Chemistry, 4, 221-236 (1954)

William, M.L., Landel, R.F., and Ferry, J.D.; "The Temperature Dependence of Relaxation Mechanism in Amorphous Polymers and Other Glass-formong Liquids," Journal of the American Chemical Society, Vol. 77, 3701-3706 (1955)

Wu,S.,"Characterization of Polymer Molecular Weight Distribution by Dynamic Melt Rheology,"Polym. Mater.Sci. Eng.,50,43 (1984)

Wu,S.,"Characterization of Polymer Molecular Weight Distribution by Transient Viscoelasticity," Polym. Eng. Sci., 28, 538 (1988)

Yen, T.F.; Characterization of Heavy Oil, 2nd Conference on Heavy Crude and Tar Sands, Proc., Caracas, Venezuela (1982)

Zaman, J.; Personal Communication, The University of Calgary (1996)

Zanzotto, L.; Study Material on Bituminous Materials, The University of Calgary (1996)

Zanzotto L., Stastna J. and Ho K.; "Characterization of Regular and Modified Bitumens via Their Complex Modulus," Journal of Applied Polymer Science, Vol. 59, 1897-1905 (1996)

APPENDIX - A

Paving Asphalt Specification Systems

A.1 Penetration-Based ASTM Specification

The standard specification for penetration-graded asphalt for use in a pavement construction is described in ASTM D946. The requirements for various penetration grades of asphalts are mentioned in Table A.1.

A.2 Canadian General Standards Board (CGSB) Specification

Paving asphalts are classified in the following penetration grades and groups in CGSB specification :

Penetration Grade

60-70	80-100	120-150
150-200	200-300	300-400

Temperature Susceptibility Group

Group A - Includes asphalts which have a high viscosity at 60°C and at 135°C (for a given penetration at 25°C)

Group B - Includes asphalts which have a medium viscosity at 60°C and at 135°C (for a given penetration at 25°C)

Group C - Includes asphalts which have a low viscosity at 60°C and at 135°C (for a given penetration at 25°C)

The asphalt sample shall comply with the requirements prescribed in Table A.2, according to penetration grade.

Table A.1 : Penetration-Based ASTM Specification

	Penetration Grade									
	40-50		60-70		85-100		120-150		200-300	
	Min	Max	Min	Max	Min	Max	Min	Max	Min	Max
Penetration @25°C, 100 g, 5 s, dmm	40	50	60	70	85	100	120	150	200	300
Flash Point (Cleveland Open Cup), °C	450	-	450	-	450	-	450	-	350	-
Solubility in trichloro-ethylene, % mass	99.0	-	99.0	-	99.0	-	99.0	-	99.0	-
Ductility @25°C, 5cm/min, cm	100	-	100	-	100	-	100	-	100*	-
Residue Penetration after TFOT, %	55+	-	52+	-	47+	-	42+	-	37+	-
Ductility @25°C after TFOT, 5cm/min, cm	-	-	50	-	75	-	100	-	100*	

* If ductility at 25°C is less than 100 cm, material will be accepted if ductility at 15.5°C is 100 cm minimum at the pulling rate of 5 cm/min.

Table A.2 : Canadian General Standards Board (CGSB) Specification

Grades	60-70		80-100		120-150		150-200		200-300		300-400	
Requirement	Min	Max	Min	Max	Min	Max	Min	Max	Min	Max	Min	Max
Penetration at 25°C, 100g, 5s, dmm	60	70	80	100	120	150	150	200	200	300	300	400
Viscosity at 60°C, Pa-s* Viscosity at 135°C,mm^2/s*												
Group A* Group B* Group C*	User must specify either Figure A.1 or Figure A.2 for all asphalt grades. Both figures shall not be used simultaneously.											
Flash Point (Cleveland Open Cup), °C	230	-	230	-	220	-	220	-	175	-	175	-
Thin Film Oven Test, % loss in mass	-	0.8	-	0.85	-	1.3	-	1.3	-	1.5	-	1.5
Residual Penetration after TFOT, %	52	-	47	-	42	-	40	-	37	-	35	-
Solubility. in trichloro-ehtylene, % mass	99	-	99	-	99	-	99	-	99	-	99	-

* All requirements, except for viscosity at 60°C or 135°C, are same for Group A, B, and C. Minimum viscosity is by the bottom line of each group as shown in Figure A.1 or A.2.

APPENDIX - B

Atmospheric Equivalent Temperature

The following correlation (Zaman 1996) is used for the conversion of temperature at vacuum to atmospheric equivalent temperature (AET) for vacuum distillation of crude oils :

$$A = \frac{7.6723 - \log_{10} P}{3410.77} \tag{B.1}$$

$$AET = \frac{5}{9}\left[\frac{748.1\,A}{1/(1.8\,T + 491.6) + 0.2145\,A - 0.0002867} - 491.6\right] \tag{B.2}$$

where,

P Pressure, mmHg

T Temperature, °C

AET Atmospheric Equivalent Temperature, °C

APPENDIX - C

Models for Estimation of Low and High Pavement Temperature

SHRP binder selection procedure used in SUPERPAVE™ is based on asphalt Performance Grades (PG). The selection of PG for a particular site is based on low and high pavement temperature. The models for the estimations of low and high pavement temperature are SHRP, Canadian SHRP (C-SHRP) and Long Term Pavement Performance Seasonal AC Pavement Temperature (LTPP-SAPT or simply SAPT) model. Each model utilizes two different equations to estimate low and high pavement temperature.

C.1 SHRP Model

SHRP model considers the low air temperature as the design low pavement temperature. An equation was developed by SHRP for the change in temperature with depth (d) which is,

$$T_d(low) = (T_{air} - n\,\sigma_{air}) + 0.051\,d - 0.000063\,d^2 \qquad (C.1)$$

where $T_d(low)$ = Low pavement temperature at depth, °C

T_{air} = Air Temperature, °C

d = Depth, mm

n = No. of standard deviation lower than temperature

σ_{air} = Standard deviation of the air temperature

The low temperature is calculated based on the lowest air temperature during the year. On the pavement surface, the design temperature is same as air temperature. The term 'n times σ_{air}' accounts for the reliability of the selected ambient temperature.

High pavement temperature in SHRP binder selection procedure is calculated from the highest seven day average air temperature during the year and geographical location. The model was

developed from theoretical heat transfer models. Several sites throughout the US were considered and a regression model was developed from the data. The model is shown in Equation C.2.

$$T_d(high) = [(T_{air} + n\,\sigma_{air}) - 0.00618\,Lat^2 + 0.2289\,Lat + 24.4]\,[1 - 0.063\,d + 0.007\,d^2 - 0.0004\,d^3] \quad (C.2)$$

where $T_d(high)$ is high pavement temperature at depth, °C , depth 'd' is measured in inches and the other symbols are same as for Equation C.1.

C.2 C-SHRP Model

The SHRP model was developed from the data collected over several locations in US. Because of largely colder climate in Canada, the low temperature SHRP model was found to be inadequate. A new model, C-SHRP was developed from the Canadian data. The model is as follows :

$$T_d(low) = 0.859\,(T_{air} - n\,\sigma_{air}) + [0.002 - 0.0007\,(T_{air} - n\,\sigma_{air})]d + 0.17 \quad (C.3)$$

The symbols are same as in Equation C.1.

C-SHRP uses the same equations as in SHRP model for the estimation of high pavement temperature.

C.3 LTPP-SAPT Model

A new model for estimation of low and high pavement temperature has been developed by US Federal Highway Administration using data available from Long Term Pavement Seasonal Monitoring Program (LTPP-SMP) after evaluation of both SHRP and C-SHRP models. In this program, two years of field data for different stations throughout US and Canada was used to

verify the existing models and improved models for SUPERPAVE™ binder selection were developed. The equations developed for low and high pavement temperature are -

$$T_d \text{ (low)} = -1.56 + 0.72\, T_{air} - 0.004\, Lat^2 + 6.264\, \log(d+25) - n\,(4.4 + 0.52\,(\sigma_{air})^2)^{0.5} \qquad \text{(C.4)}$$

$$T_d \text{ (high)} = 54.32 + 0.77585\,(T_{air} + n\,\sigma_{air}) - 0.002468\, Lat^2 - [\,15.137 \log(d+25)\,] + n\,\sigma_{pav} \qquad \text{(C.5)}$$

where σ_{pav} is the standard deviation of the calculated pavement temperature which same as RMSE of the model. The value of σ_{pav} is 3.0 for the high pavement temperature model.
The other symbols used in these equations are same as in Equation C.1 and C.2. Depth is measured in mm.

In this study, the service temperatures for different locations are calculated at the pavement surface using C-SHRP and LTPP SAPT models.

APPENDIX D

Complex Modulus Data

Table D.1 : Complex Modulus for Cold Lake Asphalt Sample @ -30°C

No.	Frequency, Hz	G`, Pa	G", Pa
1	0.01	1.93e+08	7.80e+07
2	0.03	2.59e+08	7.88e+07
3	0.05	2.90e+08	7.64e+07
4	0.08	3.16e+08	7.63e+07
5	0.10	3.29e+08	7.35e+07
6	0.20	3.59e+08	6.54e+07
7	0.40	3.93e+08	5.89e+07
8	0.60	4.08e+08	5.46e+07
9	0.80	4.19e+08	5.08e+07
10	1.00	4.26e+08	4.81e+07
11	2.00	4.53e+08	4.07e+07
12	4.00	4.73e+08	3.00e+07
13	6.00	4.78e+08	2.25e+07
14	8.00	4.83e+08	1.60e+07
15	10.00	4.83e+08	1.31e+07
16	15.00	4.86e+08	3.62e+06
17	20.00	4.83e+08	5.45e+06

Table D. 2 : Complex Modulus for Cold Lake Asphalt Sample @ -20°C

No.	Frequency, Hz	G`, Pa	G", Pa
1	0.01	3.06e+07	2.56e+07
2	0.03	5.11e+07	3.46e+07
3	0.05	6.47e+07	3.99e+07
4	0.08	7.80e+07	4.45e+07
5	0.10	8.44e+07	4.54e+07
6	0.20	1.09e+08	5.00e+07
7	0.40	1.32e+08	5.46e+07
8	0.60	1.49e+08	5.68e+07
9	0.80	1.61e+08	5.77e+07
10	1.00	1.69e+08	5.80e+07
11	2.00	1.96e+08	6.00e+07
12	4.00	2.29e+08	5.87e+07
13	6.00	2.42e+08	5.62e+07
14	8.00	2.54e+08	5.30e+07
15	10.00	2.61e+08	5.15e+07
16	15.00	2.72e+08	4.74e+07
17	20.00	2.82e+08	4.24e+07

Table D.3 : Complex Modulus for Cold Lake Asphalt Sample @ -10°C

No.	Frequency, Hz	G', Pa	G", Pa
1	0.01	2.83e+06	4.91e+06
2	0.03	6.64e+06	8.65e+06
3	0.05	9.57e+06	1.11e+07
4	0.08	1.29e+07	1.39e+07
5	0.10	1.51e+07	1.52e+07
6	0.20	2.22e+07	1.98e+07
7	0.40	3.20e+07	2.57e+07
8	0.60	3.92e+07	2.97e+07
9	0.80	4.45e+07	3.21e+07
10	1.00	4.96e+07	3.45e+07
11	2.00	6.72e+07	4.21e+07
12	4.00	8.72e+07	4.88e+07
13	6.00	1.02e+08	5.24e+07
14	8.00	1.13e+08	5.43e+07
15	10.00	1.19e+08	5.52e+07
16	15.00	1.34e+08	5.73e+07
17	20.00	1.45e+08	5.71e+07

Table D.4 : Complex Modulus for Cold Lake Asphalt Sample @ 0°C

No.	Frequency, Hz	G', Pa	G", Pa
1	0.03	3.96e+05	7.94e+05
2	0.05	6.51e+05	1.26e+06
3	0.08	1.08e+06	1.97e+06
4	0.10	1.37e+06	2.19e+06
5	0.20	2.27e+06	3.38e+06
6	0.40	3.75e+06	5.09e+06
7	0.60	5.09e+06	6.49e+06
8	0.80	6.14e+06	7.51e+06
9	1.00	7.07e+06	8.30e+06
10	2.00	1.11e+07	1.18e+07
11	4.00	1.69e+07	1.60e+07
12	6.00	2.13e+07	1.88e+07
13	8.00	2.47e+07	2.08e+07
14	10.00	2.81e+07	2.26e+07
15	15.00	3.48e+07	2.56e+07
16	20.00	3.99e+07	2.74e+07

Table D.5 : Complex Modulus for Cold Lake Asphalt Sample @ 20°C

No.	Frequency, Hz	G', Pa	G", Pa
1	0.05	3.67e+03	1.79e+04
2	0.08	6.67e+03	2.82e+04
3	0.10	8.12e+03	3.35e+04
4	0.20	1.61e+04	5.85e+04
5	0.40	3.12e+04	1.03e+05
6	0.60	4.58e+04	1.43e+05
7	0.80	5.96e+04	1.79e+05
8	1.00	7.33e+04	2.12e+05
9	1.60	1.10e+05	3.06e+05
10	2.00	1.36e+05	3.64e+05
11	4.00	2.57e+05	6.10e+05
12	6.00	3.71e+05	8.18e+05
13	8.00	4.85e+05	1.01e+06
14	10.00	5.96e+05	1.17e+06
15	15.00	8.78e+05	1.56e+06
16	20.00	1.14e+06	1.85e+06

Table D.6 : Complex Modulus for Cold Lake Asphalt Sample @ 40°C

No.	Frequency, Hz	G', Pa	G", Pa
1	0.20	1.16e+02	1.79e+03
2	0.40	4.40e+02	3.54e+03
3	0.60	6.93e+02	5.73e+03
4	0.80	9.35e+02	6.86e+03
5	1.00	1.24e+03	8.15e+03
6	1.60	1.93e+03	1.28e+04
7	2.00	2.52e+03	1.42e+04
8	4.00	5.27e+03	2.54e+04
9	6.00	8.31e+03	3.59e+04
10	8.00	1.13e+04	4.71e+04
11	10.00	1.46e+04	5.68e+04
12	15.00	2.22e+04	7.96e+04
13	20.00	3.04e+04	9.96e+04

Table D.7 : Complex Modulus for Cold Lake Asphalt Sample @ 60°C

No.	Frequency, Hz	G', Pa	G", Pa
1	1.00	5.21e+01	7.09e+02
2	2.00	1.21e+02	1.30e+03
3	4.00	2.91e+02	2.56e+03
4	6.00	4.99e+02	3.71e+03
5	8.00	7.08e+02	4.82e+03
6	10.00	9.32e+02	5.90e+03
7	15.00	1.57e+03	8.53e+03
8	20.00	2.33e+03	1.10e+04

Table D.8 : Shifted G' and G" for Cold Lake Asphalt Sample (Reference Temp. 20°C)

Red. Freq., Hz	G', Pa	G", Pa	Red. Freq., Hz	G', Pa	G", Pa	Red. Freq., Hz	G', Pa	G", Pa
0.001	5.21e+1	7.09e+2	15.00	8.78e+5	1.56e+6	8.32e+4	1.27e+8	5.76e+7
0.003	1.21e+2	1.30e+3	20.00	1.14e+6	1.85e+6	8.95e+4	1.32e+8	5.46e+7
0.004	1.16e+2	1.79e+3	22.34	1.07e+6	1.84e+6	1.25e+5	1.44e+8	5.67e+7
0.006	2.91e+2	2.56e+3	35.70	1.48e+6	2.44e+6	1.34e+5	1.49e+8	5.68e+7
0.007	4.40e+2	3.54e+3	44.67	1.77e+6	2.67e+6	1.62e+5	1.43e+8	5.78e+7
0.008	4.99e+2	3.71e+3	83.17	3.31e+6	5.18e+6	1.67e+5	1.57e+8	5.63e+7
0.011	6.93e+2	5.73e+3	89.62	2.83e+6	3.82e+6	1.79e+5	1.61e+8	5.77e+7
0.011	7.08e+2	4.82e+3	178.50	4.67e+6	5.66e+6	2.24e+5	1.69e+8	5.80e+7
0.014	9.32e+2	5.90e+3	249.04	6.85e+6	9.15e+6	4.49e+5	1.96e+8	6.00e+7
0.014	9.35e+2	6.86e+3	268.15	6.20e+6	7.09e+6	4.86e+5	1.92e+8	5.84e+7
0.018	1.24e+3	8.15e+3	357.01	7.52e+6	8.19e+6	8.11e+5	2.15e+8	5.66e+7
0.021	1.57e+3	8.53e+3	415.92	9.84e+6	1.18e+7	8.95e+5	2.29e+8	5.87e+7
0.028	1.93e+3	1.28e+4	664.81	1.35e+7	1.47e+7	1.34e+6	2.42e+8	5.62e+7
0.036	2.52e+3	1.42e+4	831.69	1.57e+7	1.59e+7	1.62e+6	2.44e+8	5.45e+7
0.05	3.67e+3	1.79e+4	896.18	1.22e+7	1.18e+7	1.79e+6	2.54e+8	5.30e+7
0.07	5.27e+3	2.54e+4	1668.79	2.32e+7	2.09e+7	2.24e+6	2.61e+8	5.15e+7
0.08	6.67e+3	2.82e+4	1785.03	1.75e+7	1.54e+7	3.25e+6	2.66e+8	4.85e+7
0.10	8.12e+3	3.35e+4	2238.85	3.06e+7	2.56e+7	3.36e+6	2.72e+8	4.74e+7
0.11	8.31e+3	3.59e+4	2681.53	2.15e+7	1.76e+7	4.49e+6	2.82e+8	4.24e+7
0.14	1.13e+4	4.71e+4	3324.84	3.34e+7	2.70e+7	6.48e+6	2.91e+8	4.37e+7
0.20	1.61e+4	5.85e+4	4466.56	2.75e+7	2.04e+7	1.30e+7	3.11e+8	3.77e+7
0.27	2.22e+4	7.96e+4	4993.63	4.02e+7	3.08e+7	1.62e+7	3.16e+8	3.57e+7
0.36	3.04e+4	9.96e+4	6648.09	4.68e+7	3.39e+7	3.25e+7	3.36e+8	3.02e+7
0.40	3.12e+4	1.03e+5	6700.64	3.38e+7	2.31e+7	6.48e+7	3.51e+8	2.22e+7
0.60	4.58e+4	1.43e+5	6702.23	5.11e+7	3.46e+7	9.74e+7	3.54e+8	1.67e+7
0.80	5.96e+4	1.79e+5	8316.88	5.18e+7	3.61e+7	1.30e+8	3.58e+8	1.19e+7
1.00	7.33e+4	2.12e+5	8961.78	3.80e+7	2.40e+7	1.62e+8	3.58e+8	9.71e+6
1.60	1.10e+5	3.06e+5	11194.27	6.47e+7	3.99e+7	2.43e+8	3.60e+8	2.68e+6
2.00	1.36e+5	3.64e+5	16687.90	6.88e+7	4.32e+7	3.25e+8	3.58e+8	4.04e+6
4.00	2.57e+5	6.10e+5	17898.09	7.80e+7	4.45e+7			
6.00	3.71e+5	8.18e+5	33248.41	9.15e+7	5.04e+7			
8.00	4.85e+5	1.01e+6	44920.38	1.09e+8	5.00e+7			
8.39	6.65e+5	1.17e+6	49936.31	1.05e+8	5.37e+7			
10.00	5.96e+5	1.17e+6	66480.89	1.18e+8	5.67e+7			

Table D.9 : Complex Modulus for Redwater Asphalt Sample @ -30°C

No.	Frequency, Hz	G', Pa	G", Pa
1	0.01	2.05e+08	6.66e+07
2	0.03	2.58e+08	6.12e+07
3	0.05	2.83e+08	5.88e+07
4	0.08	3.04e+08	5.64e+07
5	0.10	3.14e+08	5.33e+07
6	0.20	3.41e+08	4.45e+07
7	0.40	3.62e+08	3.87e+07
8	0.60	3.74e+08	3.46e+07
9	0.80	3.82e+08	3.11e+07
10	1.00	3.88e+08	2.86e+07
11	2.00	4.05e+08	2.40e+07
12	4.00	4.23e+08	1.54e+07
13	6.00	4.29e+08	9.34e+06

Table D.10 : Complex Modulus for Redwater Asphalt Sample @ -20°C

No.	Frequency, Hz	G', Pa	G", Pa
1	0.01	8.03e+07	4.80e+07
2	0.03	1.21e+08	5.79e+07
3	0.05	1.45e+08	6.24e+07
4	0.08	1.67e+08	6.46e+07
5	0.10	1.79e+08	6.50e+07
6	0.20	2.11e+08	6.48e+07
7	0.40	2.42e+08	6.53e+07
8	0.60	2.61e+08	6.44e+07
9	0.80	2.75e+08	6.32e+07
10	1.00	2.85e+08	6.21e+07
11	2.00	3.16e+08	6.00e+07
12	4.00	3.48e+08	5.40e+07
13	6.00	3.61e+08	4.89e+07
14	8.00	3.70e+08	4.37e+07
15	10.00	3.75e+08	3.95e+07

Table D.11 : Complex Modulus for Redwater Asphalt Sample @ -10°C

No.	Frequency, Hz	G', Pa	G", Pa
1	0.01	1.54e+07	1.41e+07
2	0.03	2.71e+07	2.02e+07
3	0.05	3.52e+07	2.44e+07
4	0.08	4.32e+07	2.77e+07
5	0.10	4.83e+07	2.93e+07
6	0.20	6.20e+07	3.34e+07
7	0.40	7.85e+07	3.84e+07
8	0.60	9.00e+07	4.16e+07
9	0.80	9.81e+07	4.33e+07
10	1.00	1.05e+08	4.46e+07
11	2.00	1.28e+08	4.95e+07
12	4.00	1.53e+08	5.26e+07
13	6.00	1.69e+08	5.33e+07
14	8.00	1.80e+08	5.28e+07
15	10.00	1.87e+08	5.15e+07

Table D.12 : Complex Modulus for Redwater Asphalt Sample @ 0°C

No.	Frequency, Hz	G', Pa	G", Pa
1	0.01	1.61E+06	2.69E+06
2	0.03	3.72E+06	4.72E+06
3	0.05	5.29E+06	5.62E+06
4	0.08	7.01E+06	6.45E+06
5	0.10	7.79E+06	6.86E+06
6	0.20	1.13E+07	8.76E+06
7	0.40	1.54E+07	9.96E+06
8	0.60	1.82E+07	1.08E+07
9	0.80	2.03E+07	1.12E+07
10	1.00	2.21E+07	1.13E+07
11	2.00	2.76E+07	1.24E+07
12	4.00	3.56E+07	1.28E+07
13	6.00	4.04E+07	1.29E+07
14	8.00	4.95E+07	1.28E+07
15	10.00	5.03E+07	1.13E+07

Table D.13 : Complex Modulus for Redwater Asphalt Sample @ 20°C

No.	Frequency, Hz	G', Pa	G", Pa
1	0.05	6.65e+03	3.65e+04
2	0.08	1.15e+04	5.53e+04
3	0.10	1.41e+04	6.57e+04
4	0.20	2.88e+04	1.20e+05
5	0.40	5.95e+04	2.16e+05
6	0.60	9.02e+04	3.03e+05
7	0.80	1.22e+05	3.82e+05
8	1.00	1.52e+05	4.58e+05
9	2.00	3.00e+05	7.81e+05
10	4.00	5.89e+05	1.30e+06
11	6.00	8.70e+05	1.73e+06
12	8.00	1.15e+06	2.11e+06
13	10.00	1.42e+06	2.43e+06
14	15.00	2.10e+06	3.23e+06
15	20.00	2.76e+06	3.79e+06

Table D.14 : Complex Modulus for Redwater Asphalt Sample @ 40°C

No.	Frequency, Hz	G', Pa	G", Pa
1	0.20	1.12e+02	1.04e+03
2	0.40	2.32e+02	2.13e+03
3	0.60	3.23e+02	2.96e+03
4	0.80	4.49e+02	3.96e+03
5	1.00	5.59e+02	4.74e+03
6	2.00	1.15e+03	9.00e+03
7	4.00	2.40e+03	1.71e+04
8	6.00	3.88e+03	2.47e+04
9	8.00	5.23e+03	3.20e+04
10	10.00	6.59e+03	3.89e+04
11	15.00	1.05e+04	5.58e+04
12	20.00	1.46e+04	7.17e+04

Table D.15 : Complex Modulus for Redwater Asphalt Sample @ 50°C

No.	Frequency, Hz	G', Pa	G", Pa
1	1.00	8.06e+01	9.42e+02
2	2.00	1.84e+02	1.95e+03
3	4.00	3.78e+02	3.79e+03
4	6.00	5.86e+02	5.57e+03
5	8.00	8.31e+02	7.31e+03
6	10.00	1.09e+03	9.01e+03
7	15.00	1.84e+03	1.30e+04
8	20.00	2.66e+03	1.67e+04

Table D.16 : Shifted G' and G" for Redwater Asphalt Sample (Reference Temp. 20°C)

Reduced Frequency, Hz	G', Pa	G", Pa	Reduced Frequency, Hz	G', Pa	G", Pa
0.001	8.06e+01	9.42e+02	2.15e+03	2.76e+07	1.24e+07
0.002	1.84e+02	1.95e+03	2.99e+03	3.17e+07	1.39e+07
0.004	3.78e+02	3.79e+03	3.22e+03	3.27e+07	1.45e+07
0.006	5.86e+02	5.57e+03	4.29e+03	3.65e+07	1.53e+07
0.007	8.31e+02	7.31e+03	5.00e+03	3.73e+07	1.47e+07
0.009	1.09e+03	9.01e+03	5.37e+03	3.85e+07	1.54e+07
0.020	2.40e+03	1.71e+04	7.99e+03	4.23e+07	1.57e+07
0.031	3.88e+03	2.47e+04	1.00e+04	4.49e+07	1.55e+07
0.051	6.59e+03	3.89e+04	1.62e+04	5.15e+07	1.67e+07
0.077	1.05e+04	5.58e+04	2.01e+04	5.21e+07	1.53e+07
0.103	1.46e+04	7.17e+04	2.15e+04	5.41e+07	1.73e+07
0.201	2.88e+04	1.20e+05	3.22e+04	6.12e+07	1.72e+07
0.400	5.95e+04	2.16e+05	4.00e+04	5.95e+07	1.56e+07
0.600	9.02e+04	3.03e+05	4.29e+04	6.66e+07	1.69e+07
0.799	1.22e+05	3.82e+05	4.86e+04	6.48e+07	1.54e+07
1.00	1.52e+05	4.58e+05	5.37e+04	6.97e+07	1.64e+07
2.01	3.00e+05	7.81e+05	6.00e+04	6.37e+07	1.54e+07
4.00	5.89e+05	1.30e+06	7.99e+04	6.70e+07	1.51e+07
6.00	8.70e+05	1.73e+06	8.11e+04	7.11e+07	1.48e+07
7.99	1.15e+06	2.11e+06	1.00e+05	6.98e+07	1.48e+07
10.00	1.42e+06	2.43e+06	1.30e+05	7.64e+07	1.42e+07
10.71	1.61e+06	2.69e+06	1.62e+05	7.89e+07	1.34e+07
15.00	2.10e+06	3.23e+06	2.01e+05	7.64e+07	1.43e+07
20.06	2.76e+06	3.79e+06	3.25e+05	8.57e+07	1.12e+07
32.07	3.72e+06	4.72e+06	4.00e+05	8.34e+07	1.28e+07
53.58	5.29e+06	5.62e+06	6.00e+05	8.74e+07	1.14e+07
85.65	7.01e+06	6.45e+06	6.48e+05	9.09e+07	9.72e+06
160.83	1.01e+07	7.68e+06	7.99e+05	8.92e+07	1.03e+07
268.47	1.30e+07	9.02e+06	9.74e+05	9.39e+07	8.69e+06
428.34	1.54e+07	9.96e+06	1.00e+06	9.10e+07	9.66e+06
429.30	1.60e+07	1.03e+07	1.30e+06	9.60e+07	7.81e+06
537.10	1.77e+07	1.07e+07	1.50e+06	9.36e+07	7.92e+06
643.31	1.82e+07	1.08e+07	1.62e+06	9.75e+07	7.18e+06
856.53	2.03e+07	1.12e+07	9.74e+06	1.08e+08	2.35e+06

APPENDIX - E

Results of Empirical and Performance-Based Tests

Table E.1: Cold Lake Asphalt Samples

Sample No.	CL1	CL2	CL3	CL4	CL5
STANDARD TESTS					
Penetration at 25 °C, dmm (100g/5s)	64	130	140	210	281
Kinematic Viscosity at 135 °C, CSt	459	296	253	208	167
Viscosity 60°C (S.Rate 0.05s^{-1}), Pa.s	315	118	97	58	37
TESTS After TFOT					
TFOT Mass Loss, %	0.01	0.12	0.18	0.35	0.72
Penetration at 25°C, dmm (100g/5s)	52	93	103	130	181
% Residual Penetration	74.0	64.5	64.0	56.0	55.6
Viscosity 60°C (S.Rate 0.05s^{-1}), Pa.s	580	245	220	142	92
Aging Index	1.84	2.08	2.27	2.45	2.49
Ductility	150+ @25°C	150+ @25°C	150+ @25°C	150+ @15.6°C	150+ @15.6°C
SHRP TESTS					
Original Binder Properties					
Flash Point, °C	288	286	278	270	250
Dynamic Viscosity at 135 °C, mPa.s	461	280	267	208	165
Dynamic Shear (G*/sinδ), kPa	1.07	1.09	1.11	1.14	1.09
Temperature, °C	68.0	58.9	58.0	55.0	51.0
RTFOT					
RTFOT Mass Loss, %	0.03	0.21	0.31	0.56	1.11
Dynamic Shear (G*/sinδ),					
(Min. 2.20 KPa), kPa	2.46	2.22	2.24	2.42	2.37
Temperature, °C	64.0	62.0	58.0	55.1	52.0
Pressure Aging Vessel Residue					
Weight Gain, %	0.59	0.64	0.66	0.64	0.61
PAV Aging Temperature, °C	100	100	100	90	90
Dynamic Shear [G*(sin δ)],					
(Max. 5000 KPa),kPa	4614	4897	4567	4545	4958
Temperature, °C	19.9	16.0	13.0	10.9	6.1
Creep Stiffness					
(S - max. 300 MPa) @ 60 s	298	276	285	284	278
(M value - min. 0.3) @ 60 s	0.335	0.343	0.329	0.345	0.361
Temperature, °C	-16.0	-21.0	-22.0	-24.1	-26.0
SHRP Grading	PG64-22	PG58-28	PG58-28	PG52-34	PG46-34

Table E.2 : Bow Valley Asphalt Samples

Sample No.	BV1	BV2	BV3	BV4	BV5	BV6
STANDARD TESTS						
Penetration at 25 °C, dmm	38	90	145	214	228	400
Kinematic Viscosity at 135 °C, CSt	573	334	241	198	177	122
Viscosity @ 60°C (S.Rate $0.05s^{-1}$), Pa.s	489.0	157.0	83.3	50.5	42.1	19.8
TESTS After TFOT						
TFOT Mass Loss %	(+0.08)	(+0.09)	(+0.09)	(+0.08)	(+0.05)	(+0.03)
Penetration at 25°C, dmm	37	69	107	139	157	314
% Residual Penetration	71.2	65.1	62.6	58.4	59.2	63.3
Viscosity @ 60°C (S.Rate $0.05s^{-1}$), Pa.s	1100.0	325.0	146.0	92.3	85.2	34.3
Aging Index	2.25	2.07	1.75	1.83	2.02	1.73
Ductility, cm	150+ @25°C	150+ @25°C	150+ @25°C	150+ @15.6°C	150+ @15.6°C	150+ @15.6°C
SHRP TESTS						
Original Binder Properties						
Flash Point, °C	361	332	321	317	307	301
Dynamic Viscosity at 135 °C, mPa.s	572	340	243	203	184	124
Dynamic Shear ($G^*/\sin\delta$),						
(Min. 1.0 KPa), kPa	1.12	1.04	1.01	1.06	1.12	1.16
Temperature, °C	73	63	58	54	54	46
RTFOT						
RTFOT Mass Loss, %	(+0.073)	(+0.109)	(+0.090)	(+0.040)	(+0.007)	0.030
Dynamic Shear ($G^*/\sin\delta$),						
(Min. 2.20 KPa), kPa	2.44	2.40	2.39	2.25	2.44	2.41
Temperature, °C	70	63	57	52	51	45
Pressure Aging Vessel Residue						
Weight Gain, %	0.60	0.58	0.45	0.46	0.45	0.45
PAV Aging Temperature, °C	100	100	90	90	90	90
Dynamic Shear [$G^*(\sin\delta)$],						
(Max. 5000 Kpa), kPa	4584	4946	4801	4494	4494	-
Temperature, °C	23	20	14	11	10	-
Creep Stiffness						
(S - max. 300 MPa) @ 60 s	268	269	271	278	257	248
(M value - min. 0.3) @ 60 s	0.334	0.338	0.360	0.354	0.376	0.382
Temperature, °C	-11.1	-16.1	-20.1	-21.9	-23.0	-27.0
SHRP Grading	PG70-16	PG58-22	PG52-28	PG52-28	PG46-28	PG40-34

Table E.3 : Redwater Asphalt Samples

Description of Material	Redwater Crude Oil Vacuum Distillation Residue				
Sample No.	RW1	RW2	RW3	RW4	RW5
STANDARD TESTS					
Penetration at 25 °C, dmm (100g/5s)	100	151	195	220	295
Kinematic Viscosity at 135 °C ,CSt	193.8	161.2	155.7	129.8	119.7
Viscosity @ 60°C (S.Rate 0.05s^{-1}), Pa.s	94.0	53.0	41.0	29.4	28.0
TESTS After TFOT (T179)					
TFOT Mass Loss ,%	(+0.12)	(+0.13)	(+0.14)	(+0.15)	(+0.12)
Penetration at 25°C, dmm (100g/5s)	65	91	110	125	169
% Residual Penetration	65.0	60.2	56.4	56.8	57.3
Viscosity @ 60°C (S.Rate 0.05s^{-1}), Pa.s	199.0	96.0	85.0	50.0	45.2
Aging Index	2.12	1.81	2.07	1.70	1.61
Ductility, mm	150+ @25°C	150+ @25°C	150+ @25°C	150+ @15.6°C	150+ @15.6°C
SHRP TESTS					
Original Binder Properties					
Flash Point, °C	338	334	322	321	318
Dynamic Viscosity at 135 °C, mPa.s	209.3	154.7	138.1	122.9	110.2
Dynamic Shear (G*/sin δ),					
(Min. 1.0 KPa), kPa	1.06	1.08	1.07	1.11	1.08
Temperature, °C	60.0	54.0	50.9	49.9	48.0
RTFOT (T240)					
RTFOT Mass Loss, %	(+0.13)	(+0.13)	(+0.13)	(+0.14)	(+0.15)
Dynamic Shear (G*/sin δ),					
(Min. 2.20 KPa), kPa	2.38	2.26	2.48	2.45	2.38
Temperature, °C	58.9	54.1	52.0	51.0	49.0
Pressure Aging Vessel Residue					
Weight Gain, %	0.72	0.50	0.47	0.49	0.49
PAV Aging Temperature, °C	100	90	90	90	90
Dynamic Shear [G*(sin δ)],					
(Max. 5000 Kpa), kPa	4950	4566	4419	4936	4617
Temperature, °C	18.0	16.1	14.0	14.0	10.1
Creep Stiffness					
(S - max. 300 MPa) @ 60 s	303	275	263	294	266
(M value - min. 0.3) @ 60 s	0.343	0.339	0.363	0.339	0.356
Temperature, °C	-16.0	-18.6	-19.4	-20.0	-22.0
SHRP Grading	PG58-22	PG52-28	PG52-28	PG46-28	PG46-28

Table E.4: Asphalt Samples from 75% Cold Lake and 25% Redwater Crude Oils

Sample No.	CL75-1	CL75-2	CL75-3	CL75-4	CL75-5
STANDARD TESTS					
Penetration at 25 °C, dmm (100g/5s)	73	114	149	217	262
Kinematic Viscosity at 135 °C, CSt	376	286	244	183	159
Viscosity @ 60°C (S.Rate 0.05s^{-1}), Pa.s	230	121	85.5	49.8	37.4
TESTS After TFOT					
TFOT Mass Loss, %	(+0.04)	(+0.01)	(+0.01)	0.08	0.13
Penetration at 25°C, dmm (100g/5s)	55	81	95	146	174
% Residual Penetration	67.1	62.3	55.9	56.6	54.2
Viscosity @ 60°C (S.Rate 0.05s^{-1}), Pa.s	457	283	193	101	81.5
Aging Index	1.99	2.34	2.26	2.03	2.18
Ductility	150+ @25°C	150+ @25°C	150+ @25°C	150+ @15.6°C	150+ @15.6°C
SHRP TESTS					
Original Binder Properties					
Flash Point, °C	318	295	289	280	276
Dynamic Viscosity at 135 °C, mPa.s	389	287	239	188	159
Dynamic Shear ($G^*/\sin\delta$),					
(Min. 1.0 KPa), kPa	1.05	1.06	1.00	1.06	1.01
Temperature, °C	66.0	61.0	58.0	53.0	51.0
RTFOT					
RTFOT Mass Loss, %	(+0.01)	0.03	0.08	0.28	0.31
Dynamic Shear ($G^*/\sin\delta$),					
(Min. 2.20 KPa), kPa	2.25	2.28	2.21	2.46	2.30
Temperature, °C	66.0	61.0	58.0	54.0	52.0
Pressure Aging Vessel Residue					
Weight Gain, %	0.63	0.62	0.65	0.48	0.48
PAV Aging Temperature, °C	100	100	100	90	90
Dynamic Shear [$G^*(\sin\delta)$],					
(Max. 5000 Kpa), kPa	4995	4527	4830	4396	4951
Temperature, °C	20.0	19.0	16.0	10.0	9.0
Creep Stiffness					
(S - max. 300 MPa) @ 60 s	293	306	278	301	303
(M value - min. 0.3) @ 60 s	0.324	0.312	0.307	0.335	0.345
Temperature, °C	-16.1	-20.2	-21.2	-24.8	-25.0
SHRP Grading	PG64-22	PG58-28	PG58-28	PG52-34	PG46-34

Table E.5: Asphalt Samples from 60% Cold Lake and 40% Redwater Crude Oils

Sample No.	CL60-1	CL60-2	CL60-3
STANDARD TESTS			
Penetration at 25 °C, dmm (100g/5s)	70	145	215
Kinematic Viscosity at 135 °C, CSt	373	233	172
Viscosity @ 60°C (S.Rate 0.05s^{-1}), Pa.s	201	83	50
TESTS After TFOT			
TFOT Mass Loss %	0.07	0.04	0.01
Penetration at 25°C, dmm (100g/5s)	55	100	137
% Residual Penetration	78.6	69.0	63.7
Viscosity @ 60°C (S.Rate 0.05s^{-1}), Pa.s	488	166	107
Aging Index	2.43	2.00	2.14
Ductility	150+ @25°C	150+ @25°C	150+ @15.6°C
SHRP TESTS			
Original Binder Properties			
Flash Point, °C	322	296	292
Dynamic Viscosity at 135 °C, mPa.s	356	230	172
Dynamic Shear (G*/sin δ),			
(Min. 1.0 KPa), kPa	1.03	1.01	1.07
Temperature, °C	65.0	58.0	52.0
RTFOT			
RTFOT Mass Loss, %	(+0.10)	0.02	0.05
Dynamic Shear (G*/sin δ),			
(Min. 2.20 KPa), kPa	2.36	2.22	2.26
Temperature, °C	65.0	60.0	53.0
Pressure Aging Vessel Residue			
Weight Gain, %	0.64	0.65	0.55
PAV Aging Temperature, °C	100	100	90
Dynamic Shear [G*(sinδ)],			
(Max. 5000 Kpa), kPa	4594	4548	4783
Temperature, °C	20.0	16.0	10.0
Creep Stiffness			
(S - max. 300 MPa) @ 60 s	274	286	261
(M value - min. 0.3) @ 60 s	0.306	0.310	0.313
Temperature, °C	-17.1	-22.8	-24.3
SHRP Grading	PG64-22	PG58-28	PG52-34

IMAGE EVALUATION
TEST TARGET (QA-3)

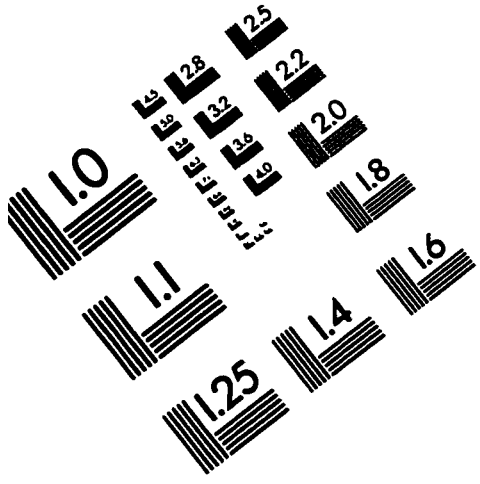

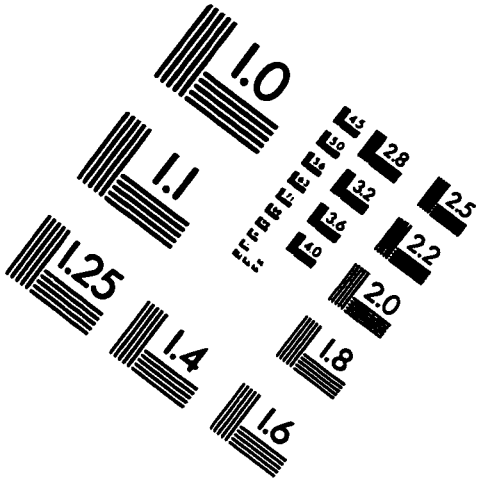

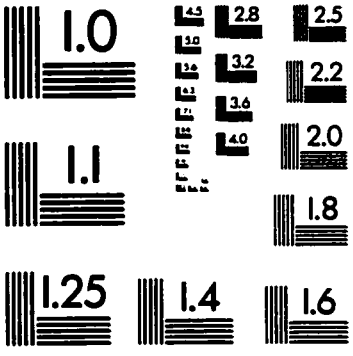

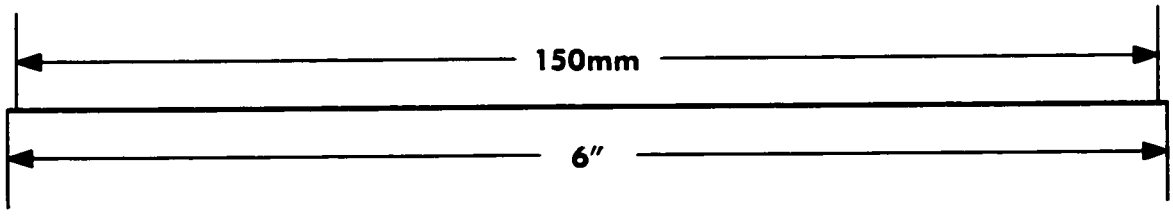

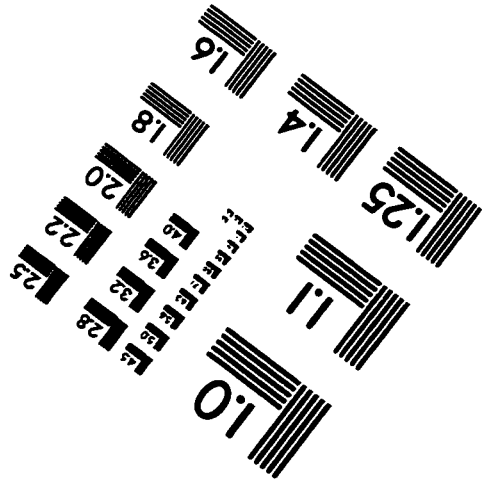

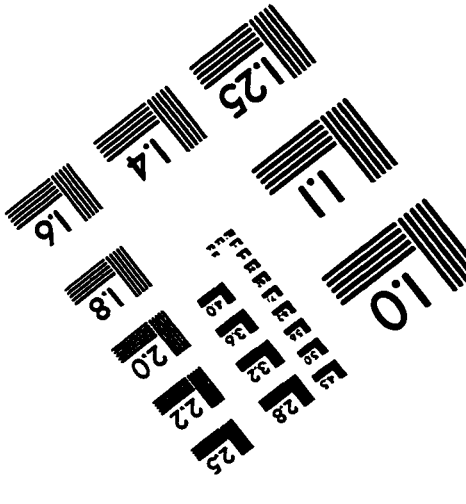

APPLIED IMAGE, Inc
1653 East Main Street
Rochester, NY 14609 USA
Phone: 716/482-0300
Fax: 716/288-5989